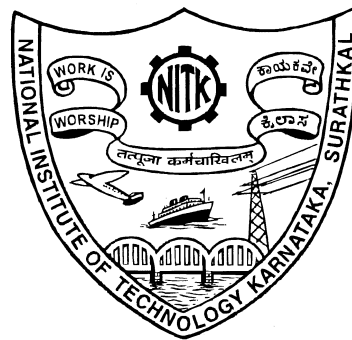


# **EFFICIENT TRACKING ALGORITHMS WITH PHASED ARRAY RADARS IN THE PRESENCE OF ELECTRONIC COUNTER MEASURES**

Thesis

Submitted in partial fulfillment of the requirements for the degree of  
**DOCTOR OF PHILOSOPHY**

by  
**GNANE SWARNADH SATAPATHI**



DEPARTMENT OF ELECTRONICS AND COMMUNICATION ENGINEERING,  
NATIONAL INSTITUTE OF TECHNOLOGY KARNATAKA,  
SURATHKAL, MANGALURU -575025

DECEMBER, 2017



## DECLARATION

I hereby *declare* that the Research Thesis entitled **EFFICIENT TRACKING ALGORITHMS WITH PHASED ARRAY RADARS IN THE PRESENCE OF ELECTRONIC COUNTER MEASURES** which is being submitted to the *National Institute of Technology Karnataka, Surathkal* in partial fulfillment of the requirements for the award of the Degree of *Doctor of Philosophy* in **Electronics and Communication Engineering** is a *bonafide report of the research work carried out by me*. The material contained in this thesis has not been submitted to any University or Institution for the award of any degree.

**Gnane Swarnadh Satapathi**  
Register No.: 135044EC13F02  
Department of Electronics and Communication Engineering

Place: NITK - Surathkal

Date:

## **CERTIFICATE**

This is to *certify* that the Research Thesis entitled **EFFICIENT TRACKING ALGORITHMS WITH PHASED ARRAY RADARS IN THE PRESENCE OF ELECTRONIC COUNTER MEASURES**, submitted by **Gnane Swarnadh Satapathi** (Register Number: 135044EC13F02) as the record of the research work carried out by him, is *accepted* as the *Research Thesis submission* in partial fulfillment of the requirements for the award of degree of *Doctor of Philosophy*.

**Dr. Pathipati Srihari**  
Research Guide  
Assistant Professor  
Dept. Electronics and Communication Engg.  
NITK Surathkal - 575025

**Chairman - DRPC**  
(Signature with Date and Seal)

## **ACKNOWLEDGEMENTS**

Firstly, I profusely thank my research supervisor Dr. Pathipati Srihari from bottom of my heart. His assistance and guidance throughout this research has been unending, and he has made my stay at NITK both pleasant and memorable. I would like to express my sincere gratitude to Prof. U. Shripathi Acharya and Prof. Muralidhar Kulkarni, Dept. of E&C Engg., NITK and Prof. Katta Venkataramana, Dean (Academics), NITK for their kind words, timely support and encouragement when I was begging for help and assistance.

I would also like to express my heartfelt thanks to Prof. T Kirubarajan, McMaster University, Canada for introducing estimation theory to our research group. In addition to him, I thank Mr. Rick Gentile, Product Manager, Phased Array System Toolbox and Signal Processing Toolbox, Mathworks for his appropriate help in implementing STAP and adaptive thresholding mechanisms. I express my gratitude to Prof. Ganapati Panda, Distinguished Professor, Indian Institute of Technology, Bhubaneswar for teaching me soft and evolutionary computing techniques. I thank Prof. G Ram Mohana Reddy, HOD-IT, NITK for providing inputs while publishing the research work.

I am also thank full to Dr. Ashvini Chaturvedi, Associate Professor for their constant support while writing the thesis. I would also express my sincere gratitude to Dr. Prashantha Kumar H, Assistant Professor, Dr. Shyam Lal, Assistant Professor, Dr. Aparna P., Assistant Professor, and Dr. A. V. Narasimhadhan, Assistant Professor, Dept of E&C Engineering for their invaluable support during my stay at NITK. Particularly thanks go to Mr. Y V Srinivasa Murthy, Mr. Santosh Kumar Gedela, Mr. Bethi Pardha Saradhi and Mr. Gunnery Srinadh for supporting me all the time and made my stay comfortable at NITK. I sincerely thank all teaching and non-teaching staff of the Department of E&C Engg., NITK who have helped me directly or indirectly during my research work. I also extend my thanks to Director, Dean and administrative staff of

NITK.

I would also like to thank Department of Science and Technology, Govt. of India for their support through Young Scientist Research Grant (No. SB/FTP/ETA-110/2014).

Lastly, and most importantly, I would like to thank Dr. Swarna Renu Devi (mother), Dr. Ramanatha Satapathi (father), Mr. Govindo Misro (grand father), Dr. Jagannadha Satapathi (Uncle), Mr. Ramakrishna Misro (Uncle) and Mr. Vivekanandh Nath Satapathi (brother) and all my teachers, to whom this thesis is dedicated. Their never ending support in all my endeavors has been invaluable.

(Gnane Swarnadh Satapathi)

## ABSTRACT

In this dissertation, the problem of target tracking in the presence of electronic counter measures (ECM) with phased array radars is studied. This work focuses mainly on tracking airborne targets in the presence of strong interference. Three major challenging problems of target tracking in the ECM scenario are considered. Primarily waveform agile sensing approach is used as electronic counter counter measure (ECCM) technique to tackle the ECM for tracking benchmark target trajectories. In addition to ECM, other attributes such as multi-path, clutter and false alarms (FA) are considered. Three different types of frequency coded waveforms (linear frequency, Gaussian frequency and stepped frequency) are considered in the waveform bank. The next waveform that is to be transmitted is selected so as to reduce the tracking error. In addition, the present investigation is aimed to optimize radar resources (average power, radar time and energy). Further, the work is extended to multidimensional filtering approach. In this context, waveform agile sensing with space time adaptive processing (STAP) is proposed to improve the track performance for benchmark trajectories.

This research also proposes novel data association techniques to improve the track performance in the presence of strong interference. The measurements obtained from sensors has to be allocated to a particular target precisely in the multi-target scenario, so as to track the targets accurately. Two soft and evolutionary computing based data association approaches (fuzzy particle swarm optimization (Fuzzy-PSO) and fuzzy genetic algorithm (Fuzzy-GA) ) are presented to enhance the performance. Fuzzy-GA based data association approach produced superior results as compared to joint probabilistic data association (JPDA), fuzzy clustering means (FCM) and Fuzzy-PSO in the presence of ECM. Further more, two computationally efficient fuzzy based data association algorithms ( all neighbor fuzzy relational and rough fuzzy) have been presented. Four different case studies are considered to validate these novel data association techniques.

This thesis further deals with tracking closely spaced targets in the presence of ECM. An investigation is carried out to resolve the closely spaced targets using Stockwell transform based multiple signal classification (MUSIC) direction of arrival algorithm. This method yields improved performance compared to that obtained from other existing methods.

This thesis is dedicated to

***My Parents and Research Supervisor***

# TABLE OF CONTENTS

<b>ACKNOWLEDGEMENTS</b>	<b>i</b>
<b>ABSTRACT</b>	<b>iii</b>
<b>LIST OF FIGURES</b>	<b>xiv</b>
<b>LIST OF TABLES</b>	<b>xvi</b>
<b>ABBREVIATIONS</b>	<b>xvii</b>
<b>1 INTRODUCTION</b>	<b>1</b>
1.1 Target tracking . . . . .	1
1.2 Track while scan (TWS) procedure . . . . .	2
1.3 Interferences . . . . .	3
1.3.1 Jammers . . . . .	3
1.3.2 Clutter model . . . . .	5
1.3.3 Multipath . . . . .	6
1.3.4 False alarms . . . . .	7
1.4 Motivation . . . . .	7
1.5 Objectives of the research work . . . . .	8
1.6 Thesis outline and contribution . . . . .	8
<b>2 WAVEFORM AGILE SENSING APPROACH FOR TRACKING BENCHMARK IN THE PRESENCE OF ECM USING IMMPDAF</b>	<b>11</b>
2.1 Introduction . . . . .	11
2.2 Literature survey . . . . .	11
2.3 Problem formulation . . . . .	13
2.3.1 Measurement model . . . . .	13

2.3.2	Performance Measures . . . . .	15
2.4	Neutralizing techniques for ECM, clutter and multipath effects . . . . .	15
2.4.1	Waveform agile sensing . . . . .	15
2.4.2	Adaptive beamforming . . . . .	18
2.4.3	Adaptive thresholding . . . . .	19
2.5	Interacting multiple model probability data association filter . . . . .	20
2.5.1	Probability data association filter (PDAF) . . . . .	21
2.5.2	Interacting multiple model estimator (IMM) . . . . .	23
2.6	Simulation results . . . . .	25
2.6.1	Benchmark trajectories . . . . .	26
2.6.2	Simulation results & discussion . . . . .	28
2.7	Conclusion . . . . .	34
<b>3</b>	<b>STAP BASED APPROACH FOR TARGET TRACKING USING WAVEFORM AGILE SENSING IN THE PRESENCE OF ECM</b>	<b>35</b>
3.1	Introduction . . . . .	35
3.2	Space time adaptive processing . . . . .	35
3.3	Problem formulation . . . . .	37
3.4	Results and discussion . . . . .	37
3.5	Conclusion . . . . .	44
<b>4</b>	<b>SOFT AND EVOLUTIONARY COMPUTATION BASED DATA ASSOCIATION APPROACHES FOR TRACKING MULTIPLE TARGETS IN THE PRESENCE OF ECM</b>	<b>45</b>
4.1	Introduction . . . . .	45
4.2	Literature survey . . . . .	46
4.3	Problem formulation . . . . .	48
4.4	Proposed data association approaches . . . . .	53
4.4.1	Calculating association weights . . . . .	53
4.4.2	Computing updated state estimate and covariance matrix. . . . .	61
4.5	Results and discussion . . . . .	62

4.5.1	Linear crossing targets . . . . .	64
4.5.2	Parallel targets . . . . .	65
4.5.3	Maneuvering and linear crossing targets . . . . .	71
4.5.4	Maneuvering crossing targets . . . . .	71
4.5.5	Computational complexity . . . . .	78
4.6	Conclusion . . . . .	82
<b>5</b>	<b>FUZZY BASED DATA ASSOCIATION APPROACHES FOR TRACKING MULTIPLE TARGETS IN THE PRESENCE OF ECM</b>	<b>83</b>
5.1	Introduction . . . . .	83
5.2	Proposed data association techniques . . . . .	83
5.2.1	Rough fuzzy data association . . . . .	84
5.2.2	All neighbor fuzzy relational data association(ANFRDA) . . . . .	87
5.3	Result and discussion . . . . .	89
5.3.1	Linear crossing targets . . . . .	90
5.3.2	Parallel targets . . . . .	91
5.3.3	Maneuvering and linear crossing targets . . . . .	96
5.3.4	Maneuvering crossing targets . . . . .	99
5.3.5	Computational Complexity . . . . .	105
5.4	Conclusion . . . . .	105
<b>6</b>	<b>DIRECTION OF ARRIVAL ESTIMATION FOR CLOSELY SPACED TARGETS USING STOCKWELL TRANSFORM BASED MUSIC ALGORITHM IN THE PRESENCE OF ECM</b>	<b>107</b>
6.1	Introduction . . . . .	107
6.2	Literature survey . . . . .	107
6.3	Proposed Stockwell transform based MUSIC DOA algorithm . . . . .	110
6.4	Rao-Blackwellized Monte Carlo data association based extended Kalman filter (EKF) . . . . .	112
6.4.1	Extended Kalman filter . . . . .	112
6.4.2	Rao-Blackwellized Monte Carlo data association . . . . .	113
6.5	Results and discussion . . . . .	116

6.5.1	Case 1 . . . . .	116
6.5.2	Case 2 . . . . .	117
6.6	Conclusion . . . . .	122
<b>7</b>	<b>CONCLUSIONS AND FUTURE WORK</b>	<b>125</b>
7.1	Conclusions . . . . .	125
7.2	Future work . . . . .	127
	<b>REFERENCES</b>	<b>129</b>
	<b>LIST OF PAPERS BASED ON THESIS</b>	<b>137</b>
	<b>CURRICULUM VITAE</b>	<b>139</b>

## LIST OF FIGURES

1.1	Block diagram of Track-While-Scan radar processing . . . . .	3
2.1	Flowchart of entire simulation process . . . . .	14
2.2	Received signal before adaptive beamforming . . . . .	18
2.3	Received signal after adaptive beamforming . . . . .	19
2.4	Illustrating adaptive thresholding mechanism . . . . .	21
2.5	Tracking of Benchmark target trajectory-2 in the presence of FA, SOJ, clutter and multipath . . . . .	27
2.6	Tracking of Benchmark target trajectory-4 in the presence of FA, SOJ, clutter and multipath . . . . .	28
2.7	Comparison of position RMSE for benchmark trajectories in the presence of SOJ, SSJ, clutter, false alarms and multipath . . . . .	29
2.8	Comparison of velocity RMSE for benchmark trajectories in the presence of SOJ, SSJ, clutter, false alarms and multipath . . . . .	29
2.9	Performance of position RMSE Vs number of waveforms for Benchmark Trajectories in the presence of SOJ, clutter, false alarm and multipath . . . . .	33
2.10	Performance of position RMSE Vs number of waveforms for Benchmark Trajectories in the presence of SSJ, clutter, false alarm and multipath . . . . .	33
3.1	Flowchart of entire simulation process . . . . .	38

3.2	Comparison of position RMSE for benchmark trajectories in the presence of SOJ, SSJ, clutter and false alarms . . . . .	41
3.3	Comparison of velocity RMSE for benchmark trajectories in the presence of SOJ, SSJ, clutter and false alarms . . . . .	42
3.4	Performance of position RMSE Vs number of waveforms for Benchmark Trajectories in the presence of SOJ, clutter, false alarm and multipath . . . . .	43
3.5	Performance of position RMSE Vs number of waveforms for Benchmark Trajectories in the presence of SSJ, clutter, false alarm and multipath . . . . .	43
4.1	Block diagram of a typical multitarget tracking scenario . . . . .	49
4.2	Flowchart of entire process . . . . .	50
4.3	Example of two targets and five validated measurements . . . . .	54
4.4	True and estimated trajectory by using JPDA . . . . .	65
4.5	True and estimated trajectory by using fuzzy data association . . . . .	65
4.6	True and estimated trajectory by using Fuzzy-PSO . . . . .	66
4.7	True and estimated trajectory by using Fuzzy-GA . . . . .	66
4.8	Comparison performance of position RMSE of two crossing targets $T1 \rightarrow Target - 1, T2 \rightarrow Target - 2$ . . . . .	67
4.9	Comparison performance of velocity RMSE of two crossing targets $T1 \rightarrow Target - 1, T2 \rightarrow Target - 2$ . . . . .	67
4.10	True and estimated trajectory by using JPDA . . . . .	68
4.11	True and estimated trajectory by using fuzzy data association . . . . .	69
4.12	True and estimated trajectory by using Fuzzy-PSO . . . . .	69

4.13	True and estimated trajectory by using Fuzzy-GA . . . . .	69
4.14	Comparison performance of Position RMSE of two Parallel targets $T1 \rightarrow$ $Target - 1, T2 \rightarrow Target - 2$ . . . . .	70
4.15	Comparison performance of velocity RMSE of two Parallel targets $T1 \rightarrow$ $Target - 1, T2 \rightarrow Target - 2$ . . . . .	70
4.16	True and estimated trajectory by using JPDA . . . . .	72
4.17	True and estimated trajectory by using fuzzy data association . . . . .	72
4.18	True and estimated trajectory by using Fuzzy-PSO data association . . . . .	72
4.19	True and estimated trajectory by using Fuzzy-GA data association . . . . .	73
4.20	Comparison performance of Position RMSE of two targets $T1 \rightarrow$ $Target - 1, T2 \rightarrow Target - 2$ . . . . .	73
4.21	Comparison performance of Velocity RMSE of two targets $T1 \rightarrow$ $Target - 1, T2 \rightarrow Target - 2$ . . . . .	74
4.22	True and estimated trajectory by using JPDA . . . . .	75
4.23	True and estimated trajectory by using fuzzy data association . . . . .	75
4.24	True and estimated trajectory by using Fuzzy-PSO data association . . . . .	75
4.25	True and estimated trajectory by using Fuzzy-GA data association . . . . .	76
4.26	Comparison performance of Position RMSE of two targets $T1 \rightarrow$ $Target - 1, T2 \rightarrow Target - 2$ . . . . .	76
4.27	Comparison performance of Velocity RMSE of two targets $T1 \rightarrow$ $Target - 1, T2 \rightarrow Target - 2$ . . . . .	77
5.1	Tracking linear crossing targets using RF-JPDA technique . . . . .	91
5.2	Tracking linear crossing targets using ANFRDA technique . . . . .	92

5.3	Comparison performance of position RMSE of two crossing targets $T1 \rightarrow Target - 1, T2 \rightarrow Target - 2$ . . . . .	92
5.4	Comparison performance of velocity RMSE of two crossing targets $T1 \rightarrow Target - 1, T2 \rightarrow Target - 2$ . . . . .	93
5.5	Tracking of parallel targets using RF-JPDA technique . . . . .	94
5.6	Tracking linear parallel targets using ANFRDA technique . . . . .	94
5.7	Comparison performance of position RMSE of two crossing targets $T1 \rightarrow Target - 1, T2 \rightarrow Target - 2$ . . . . .	95
5.8	Comparison performance of velocity RMSE of two crossing targets $T1 \rightarrow Target - 1, T2 \rightarrow Target - 2$ . . . . .	95
5.9	Tracking of maneuvering and linear crossing targets using RF-JPDA technique . . . . .	97
5.10	Tracking of maneuvering and linear crossing targets using ANFRDA technique . . . . .	97
5.11	Comparison performance of position RMSE of two crossing targets $T1 \rightarrow Target - 1, T2 \rightarrow Target - 2$ . . . . .	98
5.12	Comparison performance of velocity RMSE of two crossing targets $T1 \rightarrow Target - 1, T2 \rightarrow Target - 2$ . . . . .	98
5.13	Tracking maneuvering crossing targets using RF-JPDA technique . . . . .	100
5.14	Tracking maneuvering crossing targets using ANFRDA technique . . . . .	100
5.15	Comparison performance of position RMSE of two crossing targets $T1 \rightarrow Target - 1, T2 \rightarrow Target - 2$ . . . . .	101
5.16	Comparison performance of velocity RMSE of two crossing targets $T1 \rightarrow Target - 1, T2 \rightarrow Target - 2$ . . . . .	101

6.1	Block diagram of closely spaced tracking scenario using bi-static passive radars . . . . .	108
6.2	Flowchart of entire process . . . . .	114
6.3	Tracking of closely spaced benchmark scenario-1 . . . . .	117
6.4	Position RMSE of target-1 from closely spaced benchmark scenario-1	118
6.5	Position RMSE of target-2 from closely spaced benchmark scenario-1	118
6.6	Tracking of closely spaced benchmark scenario-2 using STFT based MUSIC . . . . .	119
6.7	Tracking of closely spaced benchmark scenario-2 using Stockwell transform based MUSIC . . . . .	119
6.8	Position RMSE of target-1 from closely spaced benchmark scenario-2	120
6.9	Position RMSE of target-2 from closely spaced benchmark scenario-2	120

## LIST OF TABLES

2.1	Performance measures . . . . .	16
2.2	Comparison results for benchmark targets in the presence of FA + SOJ+ clutter + multipath . . . . .	30
2.3	Comparison results for benchmark targets in the presence of FA + SSJ+ clutter + multipath . . . . .	31
3.1	Comparison results for Benchmark Targets in the presence of FA + SOJ+ Clutter + Multipath . . . . .	39
3.2	Comparison results for Benchmark Targets in the presence of FA + SSJ+ Clutter + Multipath . . . . .	40
4.1	Comparison of execution time in seconds . . . . .	79
4.2	Performance comparison in the presence of stand off jamming, clutter and false alarms . . . . .	80
4.3	Performance comparison in the presence of stand off jamming, clutter and false alarms . . . . .	81
5.1	Comparison of execution time in seconds . . . . .	102
5.2	Performance comparison in the presence of stand off jamming, clutter and false alarms . . . . .	103
5.3	Performance comparison in the presence of stand off jamming, clutter and false alarms . . . . .	104

6.1 Comparison of results for closely spaced benchmark target scenario	121
--	-----

## ABBREVIATIONS

<b>ANFRDA</b>	All neighbor fuzzy relational data association
<b>AML</b>	Asymptotic maximum likelihood
<b>CA-CFAR</b>	Cell averaging-constant false alarm rate
<b>CRLB</b>	Crammer-Rao lower bound
<b>CUT</b>	Cell under test
<b>DOA</b>	Direction of arrival
<b>ECM</b>	Electronic counter measures
<b>ECCM</b>	Electronic counter counter measures
<b>ERP</b>	Effective radiated power
<b>EKF</b>	Extended Kalman filter
<b>ESPRIT</b>	Estimation of signal parameters via rotational invariance technique
<b>FAs</b>	False alarms
<b>FCM</b>	Fuzzy clustering means
<b>Fuzzy-PSO</b>	Fuzzy particle swarm optimization
<b>Fuzzy-GA</b>	Fuzzy genetic algorithm
<b>GA</b>	Genetic algorithm
<b>GFM</b>	Gaussian frequency modulation
<b>GLRT</b>	Generalized likelihood ratio test
<b>GOCA-CFAR</b>	Greatest-of cell-averaging constant false alarm rate
<b>IMM</b>	Interacting multiple model
<b>IMM/MHT</b>	Interacting multiple model multi-hypothesis technique
<b>IMMJPDA</b>	Interacting multiple model joint probabilistic data association
<b>IMMPDAF</b>	Interacting multiple model probabilistic data association filter
<b>IR</b>	Infrared
<b>JPDA</b>	Joint probabilistic data association

<b>LFM</b>	Linear frequency modulation
<b>MIMO</b>	Multi-input and Multi-output
<b>MHT</b>	Multi-hypothesis tracker
<b>ML</b>	Maximum likelihood
<b>MOPSO</b>	Multi-objective particle swarm optimization
<b>MSE</b>	Mean square error
<b>MTT</b>	Multiple target tracking
<b>MUSIC</b>	Multiple signal classification
<b>MVDR</b>	Minimum variance distortion less response
<b>NNF</b>	Nearest neighbor filter
<b>PDAF</b>	Probabilistic data association filter
<b>PSO</b>	Particle swarm optimization
<b>RBMCDA</b>	Rao-Blackwellized Monte Carlo data association
<b>RF-JPDA</b>	Rough fuzzy joint probabilistic data association
<b>RGPO</b>	Range gate pull-off
<b>RMSE</b>	Root mean square error
<b>SCR</b>	Signal to clutter ratio
<b>SFM</b>	Stepped frequency modulation
<b>SNF</b>	Strongest neighbor filter
<b>SNR</b>	Signal to noise ratio
<b>SOJ</b>	Stand-off jammer
<b>SSJ</b>	Self-screening jammer
<b>STAP</b>	Space time adaptive processing
<b>STFT</b>	Short time Fourier transform
<b>TWS</b>	Track-While-Scan
<b>UCAs</b>	Uniform circular arrays
<b>ULAs</b>	Uniform linear arrays
<b>URA</b>	Uniform rectangular arrays
<b>VGPO</b>	Velocity gate pull-off
<b>WAS</b>	Waveform agile sensing



# CHAPTER 1

## INTRODUCTION

### 1.1 Target tracking

Target tracking is a vital operation in surveillance systems involving single/multiple sensors with computing machinery to depict the environment. Usually, radar, sonar or infrared (IR) are used as sensors to collect observations from various sources. The sources may be targets, background clutter, jammer, etc. The goal of target tracking is to collect the observations from the sensors and subsequently using it to estimate the future state of the target at regular intervals. The attributes of target state may be position, velocity or acceleration. Consecutive estimation of target states illustrates the target trajectory.

The globally accepted filtering technique with mathematical framework is Bayesian filtering. The posterior probability in Bayesian filter is iteratively estimated to compute the mean and covariance of the target state. In general, Kalman filter is used as basic filter for estimating Gaussian distributed single linear target (Kalman et al., 1960).

Typically multiple targets may present in the environment which leads to multiple target tracking (MTT) problem. The observations in MTT scenario can be more than the number of targets and these observations may arise due to missed detections, clutter or noise present in the environment. In such cases, a data association method is used to solve the issue. The data association in MTT scenario assigns the correct observation to the right target to estimate the future state of the target accurately. The following subsection describes about track-while-scan (TWS) algorithm which is used to acquire the observations and estimate the future state of target simultaneously.

## 1.2 Track while scan (TWS) procedure

Modern radars are developed in order to perform numerous operations such as detection, tracking and differentiating multiple targets. With the assistance of advanced computer systems, these radars are able to track number of targets simultaneously. The measurements (range, azimuthal and elevation angles) of a particular target are obtained for a single scan. Smoothing and prediction mechanisms are performed on the obtained measurements to estimate the future position of the target. The radar systems that can accomplish multi-target tracking and multi-tasking simultaneously are known as Track-While-Scan (TWS) radars.

If radar detects a new target, a new track file is allocated for the target and successive scans are performed on the target to predict future parameters. The parameters in track file includes position, velocity and acceleration. Usually, two simultaneous successful detections are required to create a new track file. AS soon as a target is detected in a scan, TWS radar decides weather the target is a new or old target and the decision is taken by using correlation and association techniques. The correlation technique correlates the newly detected target measurements with the earlier ones so as to avoid unnecessary tracks. If the newly detected target correlated with more than one tracks, then association mechanism will assign to the proper track based on probabilistic association methods. The basic block diagram of TWS radar processing is shown in Figure 1.1.

In general, TWS radar places a validation gate around the target position and tries to track target inside the gate. Initially, as the target position is not known exactly, a large gate area is taken so that the target position doesn't change in consecutive scans. After detecting the target successfully for multiple scans, the gate area is reduced. An error distance is calculated between new and estimated measurement. If this value is less than the predefined threshold for a target, then the measurement is assigned to the particular target. If the error distance is less than the threshold for multiple targets, then association rules determines the assigning appropriate mapping existing targets, then a

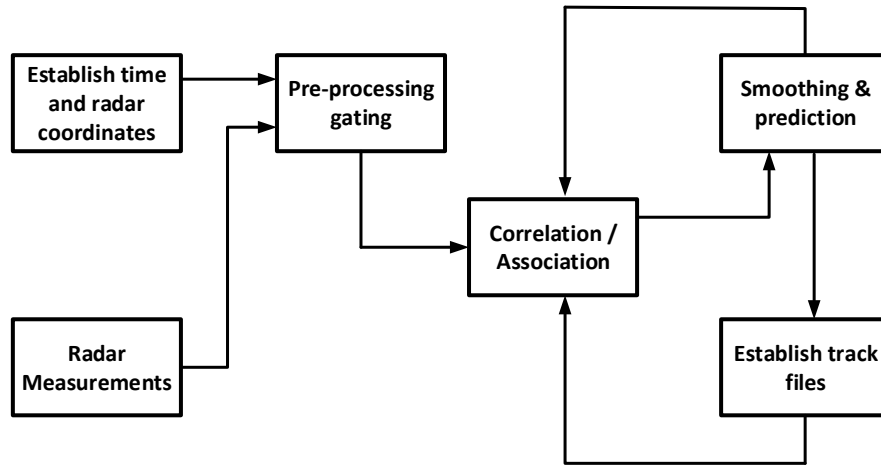


Figure 1.1: Block diagram of Track-While-Scan radar processing

new track file is created.

## 1.3 Interferences

The combinations of interferences are considered to be present in the environment and are briefly described as follows:

### 1.3.1 Jammers

The chief function of jammer is to restrict the radar functionality by illuminating intentional interference (Mahafza, 2008). Jammers transmits high power radio frequency signals to deceive the radar all over its operating bandwidth. These jammers can be on-board or with an escort to the enemy target. Mainly, there are two types of jammers viz self-screening jammer (SSJ) and stand-off jammer (SOJ). The noise generated by jammer is computed in terms of effective radiated power (ERP) and is defined as:

$$ERP = \frac{P_J G_J}{L_J} \quad (1.1)$$

Where,  $P_J$  is jammer transmitted power,  $G_J$  is gain in jammer antenna and  $L_J$  is total loss in jammer.

The subsequent subsections narrates concisely about SSJ and SOJ.

### 1.3.1.1 Self-Screening Jammer

Self screening jammers (SSJs) are commonly known as self-protection jammers and are situated on-board the enemy target. They utilize the benefit in the radar surveillance sector and transmits noise echoes towards the radar main beam so as to break the lock of radar. Signal to Jamming ratio ( $S/J$ ) for self screening jammer case (Mahafza, 2008) is stated as

$$\frac{S}{J} = \frac{\tau P_t \sigma B_J G}{(ERP) 4\pi L R^2} \quad (1.2)$$

Where,  $\tau$  is radar pulse width,  $P_t$  is peak transmit power,  $\sigma$  is radar cross section,  $B_J$  is Jammer bandwidth,  $G$  is antenna gain,  $L$  is receiver loss,  $R$  is range,  $ERP$  represents effective radiated power and  $B_r$  is receiver bandwidth. Usually, jammer power is considered to be greater than signal power dissipated by the radar ( $S/J < 1$ ). However, when a target move towards the radar, at a specific range signal power of radar will become equivalent to the jamming power and this range is known as cross-over range. Above this cross-over range the jammer power will be lame and is described as

$$(R_{co})_{SSJ} = \left[ \frac{B_J G \sigma P_t}{4\pi (ERP) L B_r} \right]^{1/2} \quad (1.3)$$

### 1.3.1.2 Stand-Off Jammer

Stand off jammers (SOJs) emits noisy signals from outside the radar range and tries to jam the radar so that the radar cannot detect the enemy targets which will enter into the surveillance area.

Signal to Jamming ratio for stand-off jammer is given by

$$\frac{S}{J} = \frac{P_t B_J G^2 \tau \sigma R_J^2}{4\pi (ERP) L R^4} \quad (1.4)$$

and cross-over range where signal power is equivalent to jammer power is

$$(R_{co})_{SOJ} = \left[ \frac{P_t G^2 G_{pc} \sigma B_J R_J^2}{4\pi L B_r G' (ERP)} \right]^{1/4} \quad (1.5)$$

Where,  $G_{pc}$  is time bandwidth product and  $R_J$  represents range of jammer from the radar. The target should stay behind this  $(R_{co})_{SOJ}$  range, and try to transmit spurious signals towards the radar for improper detection of the targets.

### 1.3.2 Clutter model

Two types of clutter models are considered in this thesis which are discussed below:

#### 1.3.2.1 Poisson clutter

Let  $Z_{k,1}, Z_{k,2} \dots Z_{k,n}$  be the  $n$  observations received from radar at  $k^{th}$  time instant. In general due to the presence of clutter the received observations may contain false alarms with real measurements. If  $V_k$  as validation gate volume (Bar-Shalom and Fortmann, 1988) and  $\rho$  represents clutter density then false alarms are assumed to be Poisson distributed with mean  $V_k \rho$ . The observations from radar, which will fall within the validation gate region are only considered for tracking. Poisson probability for achieving  $n$  false alarms is given as

$$\mu(n) = \frac{e^{-V_k \rho} (V_k \rho)^n}{n!} \quad (1.6)$$

In the above mentioned expression,  $V_k$  represents to clutter volume and is presume to follow uniform distribution.

### 1.3.2.2 Gamma clutter

Clutter is due to the reflections of radar waveform from buildings, sea, surface, etc. The clutter returns may be considered as a target by mistake. In this chapter, we considered constant gamma clutter whose clutter characteristics depend on the value of normalized reflectivity ( $\gamma$ ) (Barton, 1985). The normalized reflectivity of constant gamma model is given as

$$\gamma = \gamma_0 + 5 \log \left( \frac{f}{f_0} \right) \quad (1.7)$$

The value of  $\gamma$  depends upon the radar operating frequency ( $f$ ) and type of terrain.  $\gamma_0$  is a particular value for a specific frequency  $f_0$  (Barton, 1985).

### 1.3.3 Multipath

The echoes from the target return to the receiver other than the direct path is known as multipath. Multipath generates false targets to appear and misleads the radar receiver. These multipath creates false targets, which are very difficult to distinguish from actual targets. If the echo is reflected from the rough surface, then error occurs in both azimuth and elevation angles due to diffuse scattering. Further, if the echo is reflected from building or non-flat land then error occurs significantly in azimuth angle. The major problem in tracking targets due to multipath effect is that, the false targets and actual targets seems to be coherent. The envelop sum of signals that are received at the receiver is considered as Rayleigh distributed. The signals arriving at the receiver may have destructive or constructive interference. Let  $R_n$  and  $\phi_n$  be electric field and relative phase of  $N$  multipath signals. Then, the total electric field at the receiver is given by

$$\tilde{R} = \sum_{n=1}^N R_n e^{j\phi_n} \quad (1.8)$$

It is assumed that  $R_n$  and  $\phi_n$  are independent and identically distributed. The prob-

ability density function of Rayleigh distribution is given by

$$f_R(r) = \frac{r}{\sigma^2} e^{-\frac{r^2}{2\sigma^2}} \quad (1.9)$$

Equation (1.9) is for slow fading and is valid  $\forall r \geq 0$ .

### **1.3.4 False alarms**

False alarms are erroneous targets that are detected due to the presence of noise in the environment or in the internal radar receiver. An elaborated discussion about false alarms is presented in (Skolnik, 1970).

## **1.4 Motivation**

Radar target tracking algorithms have been one of the significant research areas in radar systems. The benchmark for radar allocation and tracking in the presence of electronic counter measures (ECM) was presented in the past. However, in the earlier studies radar clutter and multipath effects were ignored. Radar waveform plays a key role in detecting and tracking of a particular target. Traditionally, fixed waveforms have been applied to track the benchmark targets. These fixed waveforms have the limited capability in the presence of ECM, clutter and multipath effects.

Comprehensive literature review in this area revealed potential research problems to be addressed in future. Also, varying waveforms adaptively has been enlisted as an important research problem to be explored. This motivated us to present tracking benchmark in the presence of ECM using waveform agile sensing approach. Further, tracking multiple targets in the presence of ECM is also envisaged as significant research problem to be carried out in future with improved performance in terms of root mean square error (RMSE) and computational complexity. Besides this, tracking closely spaced benchmark targets has also been listed to be carried out as a future research work. Hence, there is a strong need to address these research issues. This further motivated

us to take up multiple target tracking and closely spaced target tracking as key research investigation.

## **1.5 Objectives of the research work**

This research work intends to focus on tracking targets in the presence of electronic counter measures (ECM). This work has fulfilled the following objectives and the obtained significant research outcomes are analyzed.

- To enhance the performance of benchmark target tracking using waveform agile sensing technique in the presence of ECM, clutter, false alarms and multipath.
- To analyze the performance of target tracking by combining space time adaptive processing with waveform agile sensing technique in the presence of ECM, clutter and false alarms.
- To address the problem of data association with hybrid soft and evolutionary computing techniques (Fuzzy Genetic Algorithm and Fuzzy Particle Swarm Optimization) to overcome the problem of local minima.
- To investigate further more into data association problem to reduce the execution time with comparable results in terms of position and velocity root mean square error (RMSE) by applying all neighbor fuzzy relational and rough fuzzy clustering approaches.
- To explore the problem of detecting the closely spaced targets in the presence of ECM by using Stockwell transform based MUSIC direction of arrival techniques.

## **1.6 Thesis outline and contribution**

The objective of this work is to investigate and develop novel algorithms for efficiently track targets with phased array radars in the presence of electronic counter measures (ECM). The ultimate aim is to improve the performance of target tracking algorithms with comparable computational complexity.

Chapter 1 describes a brief introduction of the problem, research objectives and chapter wise contribution of the thesis.

Chapter 2 introduces an efficient approach based on waveform agile sensing to enhance the performance of benchmark target tracking in the presence of strong interference. In addition to it, a brief description of problem formulation, different types of ECM techniques, clutter, multipath, false alarm and benchmark target trajectories are incorporated. The effect of root mean square values (position and velocity) along with radar resources (radar energy, time and average power) are studied on considering 5 to 50 varieties of waveforms from the waveform bank for stand-off and self-screening jamming conditions. Simulation results reveal that there is a reduction in radar average power, time and energy. However, there is an increase in root mean square error (position and velocity) values. To further decrease the root mean square error values a multidimensional approach of space time adaptive processing (STAP) with waveform agile sensing to mitigate the clutter and jamming effect for the benchmark trajectories is proposed in chapter 3. In both the chapters, the waveform that needs to be transmitted in next scan is selected based on posterior Crammer-Rao Lower Bound (CRLB). Interacting multiple model probability data association filter is employed for tracking targets.

Chapter 4 and chapter 5 deals with data association techniques for multi-target tracking algorithms. In Chapter 4, two novel soft and evolutionary computing based hybrid data association approaches are discussed to track multiple targets in the presence of ECM, clutter and FAs. Joint probabilistic data association (JPDA) technique is employed for tracking multiple targets (Bar-Shalom, 2000). Fuzzy clustering means (FCM) technique was suggested earlier as an efficient method for data association, but its cluster centers may fall to local minima (Aziz et al., 1999; Aziz, 2007, 2011, 2013, 2014, 2015). Hence, new hybrid data association techniques based on fuzzy particle swarm optimization (Fuzzy-PSO) and fuzzy genetic algorithm (Fuzzy-GA) clustering techniques have been proposed as robust methods to overcome local minima problem. The data association matrix is computed for all tracks using validated measurements received by phased array radar for four different cases using four data association methods (JPDA, FCM, Fuzzy-PSO, and Fuzzy-GA).

Chapter 5 presents two fuzzy based (all neighbor fuzzy relational and rough fuzzy)

data association approaches. A concise investigation is made by considering four different cases for various jammer powers. The results were comparable with Fuzzy-PSO and Fuzzy-GA with less computational complexity. Rough fuzzy joint probabilistic data association algorithm (RF-JPDA) and all neighbor data association approaches are proposed to improve the performance of multitarget tracking in the presence of clutter, ECM and FAs. In RF-JPDA, possibility data association matrix is computed by applying upper and lower approximations of validated measurements which are obtained from the radar. While in all neighbor data association likelihood values and similarity index are determined for each measurement obtained from radar, expectation maximization method (Molnar and Modestino, 1998) is utilized to acquire possibility association matrix. Experimental study is carried out for linear crossing targets, nonlinear crossing targets, and parallel targets. The aim of this chapter is to decrease the computational complexity w.r.t soft and evolutionary computing based hybrid data association techniques while achieving comparable performance in terms of root mean square error.

Chapter 6 presents a hybrid combination of MUSIC based direction of arrival algorithm with Stockwell transform for detecting closely spaced targets in the presence of ECM. The results are compared with MUSIC and short time Fourier transform (STFT) based MUSIC approaches. This chapter investigates detection and tracking of the closely spaced multiple targets in the presence of ECM. Stockwell transform based multiple signal classification (MUSIC) direction of arrival (DOA) estimator for closely spaced targets in the presence of electronic counter measure (ECM), clutter and false alarms (FAs) is presented. Rao-Blackwellized Monte Carlo data association (RBM-CDA) (Särkkä et al., 2004; Hartikainen and Särkkä, 2008) based extended Kalman filter (EKF) is utilized to track closely spaced benchmark target trajectories. The Stockwell based MUSIC DOA is compared with MUSIC (Bruckstein et al., 1985; Baig and Malik, 2013) and STFT based MUSIC DOA methods.

Finally, Chapter 7 concludes the thesis with a summary of the contributions of research work along with some suggestions in a form of future work to be carried out.

## **CHAPTER 2**

# **WAVEFORM AGILE SENSING APPROACH FOR TRACKING BENCHMARK IN THE PRESENCE OF ECM USING IMMPPDAF**

### **2.1 Introduction**

This chapter proposes an electronic counter counter measure (ECCM) based on waveform agile sensing (WAS) in the presence of intense interference. The intense interference include ECM like SOJ/ SSJ with the combination of multipath, clutter and FAs. The WAS library contains waveforms like Gaussian frequency modulation (GFM), linear frequency modulation (LFM) and stepped frequency modulation (SFM). The aim of this chapter is to choose a suitable waveform from waveform bank based on CRLB so as to minimize the mean square error. IMMPPDAF is used to track the benchmark target trajectories.

### **2.2 Literature survey**

Target tracking problem with six benchmark trajectories has been suggested in (Blair et al., 1994). Interacting Multiple Model (IMM) track filter was proposed as an alternative target tracking method for highly non linear trajectories (Daeipour et al., 1994). Further contributions were carried out on tracking standard trajectories in the presence of ECM (Blair et al., 1995; Kirubarajan et al., 1995; Slocumb et al., 1995; Rago and Mahra, 1997). In all the above cases, SOJ and range gate pull off (RGPO) were considered as major intentional interference sources. Further, benchmark trajectories has been reported (Kirubarajan et al., 1998; Blair et al., 1998) and deployed IMMPPDAF as

an estimation algorithm. Future research problems pertaining to benchmark problem were suggested in (Blair et al., 1998). Significant among them are adaptive waveform selection using different radar signals, estimating closely spaced target trajectories, including on-board jammer, incorporating background clutter and considering multipath effects.

Besides, IMM/MHT algorithms to the benchmark tracking was suggested in (Blackman et al., 1999), using optimum radar resources compared to (Blair et al., 1998). But IMM/MHT was computationally expensive to be deployed for practical scenarios. Benchmark tracking with IMMPDAF was further enhanced by incorporating clutter using LFM waveform (Angelova et al., 1999). Alternative techniques for radar resource management were presented in (Behar et al., 2001; Behar and Kabakchiev, 2002), describes post detection integration methods for benchmark tracking to further improve the radar resources in the presence of counter measures. In all these techniques, single LFM radar signal was applied for benchmark tracking.

WAS approach was suggested to select a suitable waveform from a waveform bank, which maximize the radar detection and improve the state estimation accuracy. A new technique was suggested using adaptive radar signal selection for linear target tracking using Kalman filter without using clutter and it was further extended to incorporate clutter (Kershaw and Evans, 1994, 1997). Various optimization methods for radar signal design were presented in (Rago et al., 1998; Niu et al., 2002; Hong et al., 2005). Enhanced non-linear model for target tracking based on dynamic radar signal selection was proposed in (Sira et al., 2006). Generalized frequency modulated radar signals for non-linear framework were explored in (Sira and Morrell, 2007; Sira et al., 2009). Both these methods yielded improved results for different scenarios. Adaptive waveform selection was applied for multi-static radars using IMMPDAF model in (Nguyen et al., 2015).

## 2.3 Problem formulation

In the proposed WAS technique, an active phased array radar (operating at 10 GHz frequency and a rectangular array with 900 elements) with minimum variance distortionless response (MVDR) adaptive beamformer is applied to extract the observations. The radar signal that is to be transmitted is chosen based on CRLB of updated measurement errors. The aim is to increase the tracking performance by constructing a multiple waveform library and choose a particular radar waveform based on future state of the target. Cell Averaging-Constant False Alarm Rate (CA-CFAR) adaptive thresholding approach is engaged for target detection. In addition to ECM (SSJ/SOJ), background clutter, FA and multipath effects are included in the environment. IMMPDAF estimator is used to estimate all the benchmark target trajectories in the presence of intense interference. The overall work flow is briefly represented in Figure 2.1.

### 2.3.1 Measurement model

The observations obtained from radar will be in spherical coordinates (range, elevation angle and azimuthal angle). The radar searches the entire area in both angular directions (azimuth and elevation). The observations from spherical coordinates are transformed into Cartesian coordinates with respect to position of the radar. The radar observations are determined as

$$Z_i = [Z_{ix}, Z_{iy}, Z_{iz}] \quad (2.1)$$

Where,  $Z_{ix}$ ,  $Z_{iy}$  and  $Z_{iz}$  are the radar observations in  $x$ ,  $y$  &  $z$  directions respectively at  $i^{th}$  scan. The environment is considered to be degraded by the presence of intense interference (ECM, multipath, clutter and FAs). It is also assumed that the environment also contains clutter, ECM, false alarm and multipath. So, the observations obtained from radar is a combination of target and interference which is given as

$$Z = Z_{target} + Z_{multipath} + Z_{jammer} + Z_{clutter} + Z_{falsealarm} \quad (2.2)$$

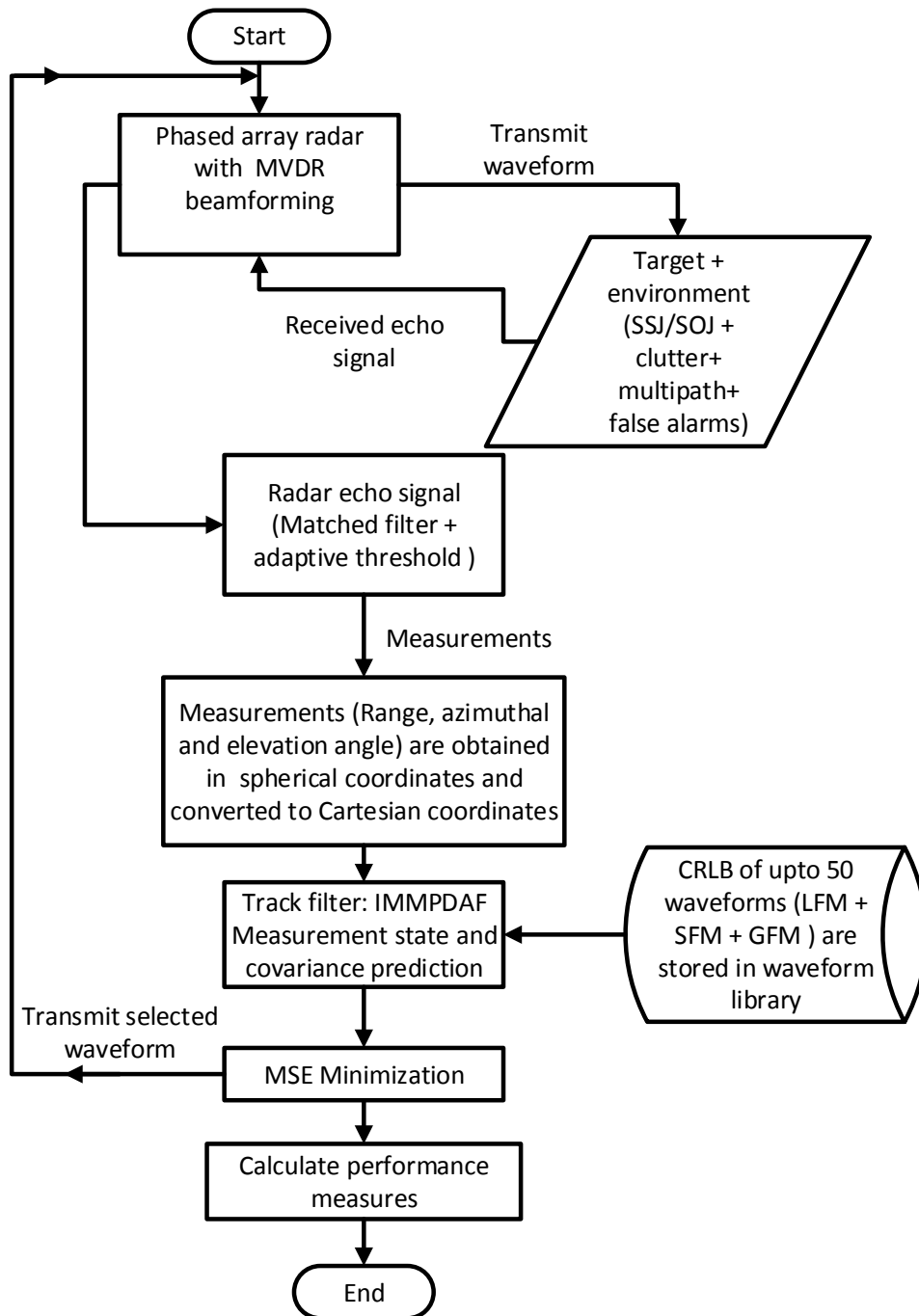


Figure 2.1: Flowchart of entire simulation process

where  $Z_{target}$ ,  $Z_{multipath}$ ,  $Z_{jammer}$ ,  $Z_{clutter}$ , and  $Z_{falsealarm}$  are observations due to target, multipath jamming, clutter and false alarm at the radar receiver respectively.

### 2.3.2 Performance Measures

In the target tracking literature, different performance measures have been suggested in (Gorji et al., 2011). The performance measures listed in Table 2.4.1 are considered for analyzing the track performance of benchmark targets in the presence of intense interference.

## 2.4 Neutralizing techniques for ECM, clutter and multipath effects

Neutralizing techniques for ECM, multipath and clutter are briefly described in this section. Waveform agile sensing, adaptive beamforming and adaptive thresholding techniques are applied successfully to nullify the unwanted interferences. The subsequent subsections concisely narrate these techniques.

### 2.4.1 Waveform agile sensing

The principal aim of adaptive waveform selection is to reduce the estimation mean square error (MSE). Selecting the waveform from waveform bank is based on signal to clutter ratio (SCR), signal to noise ratio (SNR) and type of estimator algorithm. The constraint ( $\Omega_j$ ) of the radar waveform is chosen so as to reduce the estimator MSE which is described as

$$J(\Omega_j) = E_{X_j, Z_j | Z_{1:j}} \left[ (X_j - \hat{X}_j)^T (X_j - \hat{X}_j) \right] \quad (2.3)$$

Where,  $E(\cdot)$  is represented as expectation function over real and predicted state of observations.  $\hat{X}_j$  depicts the state estimate of  $X_j$  for  $j$  observations. Equation (2.3) is

considered as the cost function and objective is to choose the radar signal parameter which gives minimum MSE at a certain scan  $j$ .

Table 2.1: Performance measures

Sl.No	Performance metrics	Description	Reference
1	Root Mean Square Error (RMSE)	<p>It measures the difference between actual value and estimated value.</p> $RMSE = \sqrt{\frac{1}{K} \sum_{i=1}^k (x_i - \hat{x}_i)^2}$ <p>Where, <math>x_i</math>=Actual value;  <math>\hat{x}_i</math>=Predicted value; <math>K</math>=No of observations.</p>	(Gorji et al., 2011)
2	Track Loss	<p>The track is declared to be lost if the error in the estimated value of the target is greater than 1.5 range gates in range. It measures the percentage of tracks that are lost during simulation.</p>	(Gorji et al., 2011; Blair et al., 1998)
3	Cost functions ( $C_1$ & $C_2$ )	<p><math>C_1</math>: It corresponds to period of operation when radar energy is critical.</p> $C_1 = \bar{E}_{ave} + 10^3 \bar{T}_{ave}$ <p><math>C_2</math>: It corresponds to period of operation when radar time is critical.</p> $C_2 = \bar{E}_{ave} + 10^5 \bar{T}_{ave}$ <p>Where, <math>\bar{E}_{ave}</math>= Average energy per second; <math>\bar{T}_{ave}</math> = Average radar time per second.</p>	(Blair et al., 1998)
4	Average Power	<p>Rate of energy flow averaged over one full period.</p> $P_{avg} = \frac{PulseWidth (\tau)}{PRT (T)} * PeakPower$	(Blair et al., 1998)

In real time scenario, single transition model may not represent the target motion

model since the targets may make maneuvers. Due to this reason IMM filter is used with three different transition models. Each PDAF algorithm in IMM filter will be executed in parallel and each transition model in PDAF refers to a specific motion of the target. The state vector and covariance matrix is updated by the weighted amalgamation of individual PDAF state vector and covariance matrix respectively. The detailed derivation of IMM algorithm is described in (Bar-Shalom et al., 2004).

The MSE of a particular track can be minimized by choosing a radar waveform adaptively and this is achieved by minimizing the trace of updated covariance matrix. The updated covariance matrix is represented as

$$P_{j+1|j+1}(\Omega_{j+1}) = P_{j+1|j} - [1 - \beta_{j+1}^0] W_{j+1}(\Omega_{j+1}) S_{j+1}(\Omega_{j+1}) W_{j+1}^T(\Omega_{j+1}) + \tilde{P}_{j+1}(\Omega_{j+1}) \quad (2.4)$$

It is noticeable from Equation (2.4) that updated covariance matrix is a function of radar signal  $\Omega_{j+1}$ . Then, it is also evident that the updated covariance matrix in each  $P_{j+1|j+1}^{IMM}$  is also a function of  $\Omega_{j+1}$ . The radar waveform bank include multiple radar waveforms with different amalgamation of parameters.

$$\Omega_{j+1} = \min (Trace(P_{j+1|j+1}^{i*})) , \quad (2.5)$$

where,  $i^* = \arg \max_i \mu_{j+1|j+1}^i$

The cost function for choosing radar waveform is illustrated briefly in (Kershaw and Evans, 1994). The cost function is evaluated by computing the trace of updated covariance matrix of Kalman filter. Similar technique was implemented to IMM estimator in (Nguyen et al., 2015; Savage and Moran, 2007) and Equation 2.5 is selected as one of the cost function. The radar waveform parameter which achieves minimum covariance cost and high model probability of  $i^{th}$  PDAF model is chosen to transmit in the next scan. This method is used for LFM, SFM and GFM waveforms so as to nullify the interferences.

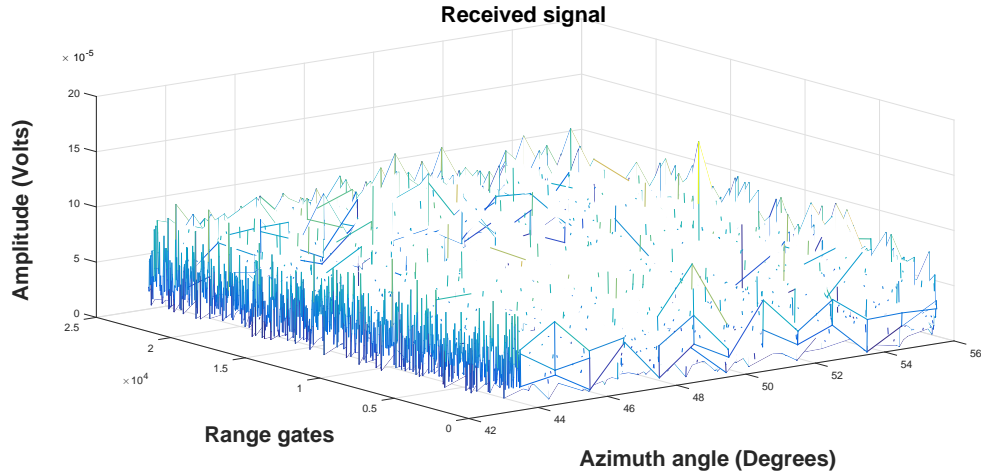


Figure 2.2: Received signal before adaptive beamforming

## 2.4.2 Adaptive beamforming

The main principle of beamforming is to emphasize the radar main beam in a desired direction and to fix a null in the unintended direction. Conventional beamforming fails in the practical scenario since the target is non-stationary and the radar echo may arrive in any direction. Whereas in adaptive beamforming the array weights are continuously adapted with change in the environment. In this work, Minimum variance distortion less response (MVDR) beamformer is used to adapt the array weights. The beamformer weights are computed by using direction of arrival (DOA) of the radar echo.

$$W = \frac{R^{-1}S(\theta)}{S(\theta)^H R S(\theta)} \quad (2.6)$$

Where  $R$  is termed as spatial covariance matrix and  $S(\theta)$  is labeled as steering vector related to a particular DOA. By continuously adapting the array weights, the MVDR beamformer tries to minimize the total output noise power by fixing unity gain in a specific direction.

Figure 2.2 illustrates the received radar echo with jamming, clutter, FAs and multipath before applying adaptive beamforming. It is very tough to detect the target as it is submerged in strong interference. Figure 2.3 depicts the radar echo with MVDR beamforming. It can be envisioned that target can be detected with multipath when noise

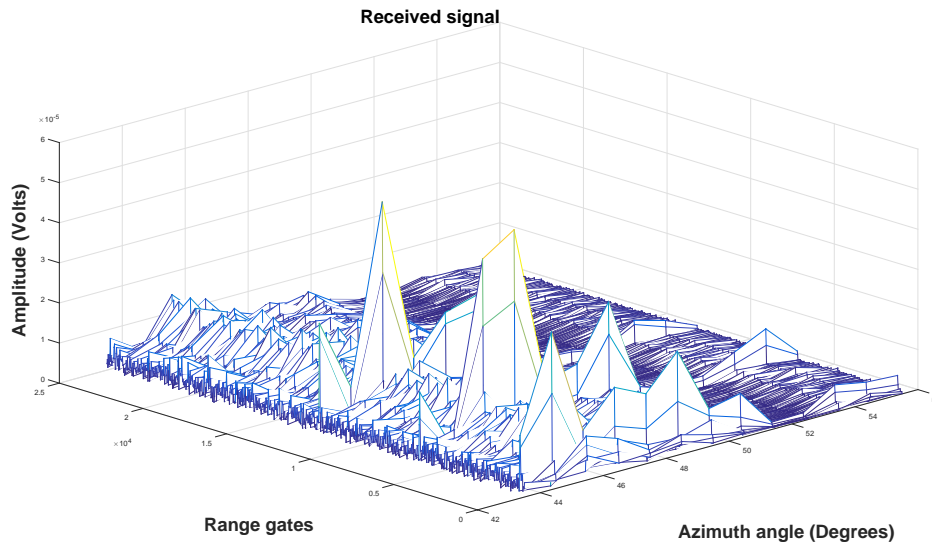


Figure 2.3: Received signal after adaptive beamforming

floor is suppressed.

### 2.4.3 Adaptive thresholding

This subsection deals with adaptive threshold mechanism which is used as counter measure to clutter, ECM and multipath. Generally a fixed threshold is used at the output of the matched filter so as to detect the target. The target declared to be present if the output of matched filter exceeds the threshold. But, for calculation of fixed threshold complete statistical data of the radar echo signal is required. However, in real time scenario complete statistical data of radar echo may not be possible as the environment may be influenced by intense interferences. Hence, there is a need for adaptive thresholding mechanism which is altered according to the environmental interferences.

The chief function of radar detector is to minimize the probability of false alarm and maximize the detection probability. Cell averaging constant false alarm rate (CA-CFAR) is selected as adaptive thresholding mechanism. In CA-CFAR, the cell under detection is labeled as cell under test (CUT). The cells neighboring to CUT are utilized to calculate the noise power. A few of neighboring CUT cells (leading and lagging) are known as guard cells. The leading and lagging cells of CUT are neglected while

calculating noise power so as to circumvent the leakage of signal energy towards the training cells. The noise power is computed from training cells which is described as

$$U_1 = \frac{1}{N_1} \sum_{i=1}^{N_1} x_i \quad (2.7a)$$

$$U_2 = \frac{1}{N_2} \sum_{j=1}^{N_2} x_j \quad (2.7b)$$

The training cell samples are represented as  $x_i$  and  $x_j$  respectively and the number of training cells are rendered as  $N_1$  and  $N_2$ . The total noise power ( $P_n$ ) is computed by adding  $U_1$  and  $U_2$  respectively. The noise power is scaled by a factor  $\alpha$  to maintain constant false alarm probability. The threshold detection ( $T$ ) is represented as

$$T = \alpha P_n \quad (2.8)$$

The decision on target presence is decided when the value of CUT is exceeds the threshold. Figure 2.4 depicts target detection using CA-CFAR. It clearly illustrates the target is been detected along with false alarms and multipath. CA-CFAR is employed to suppress clutter, FAs, ECM and multipath.

The radar echo signal from the target is degraded by clutter, ECM, multipath effects and false alarms. Amalgamation of the aforementioned techniques such as; WAS, adaptive thresholding and adaptive beamforming have been successfully employed to reduce the impact of these intense interferences.

## **2.5 Interacting multiple model probability data association filter**

This subsection briefly narrates about IMMPDFAF estimator. For tracking single maneuvering targets effectively, the probability data association filter (PDFAF) is integrated

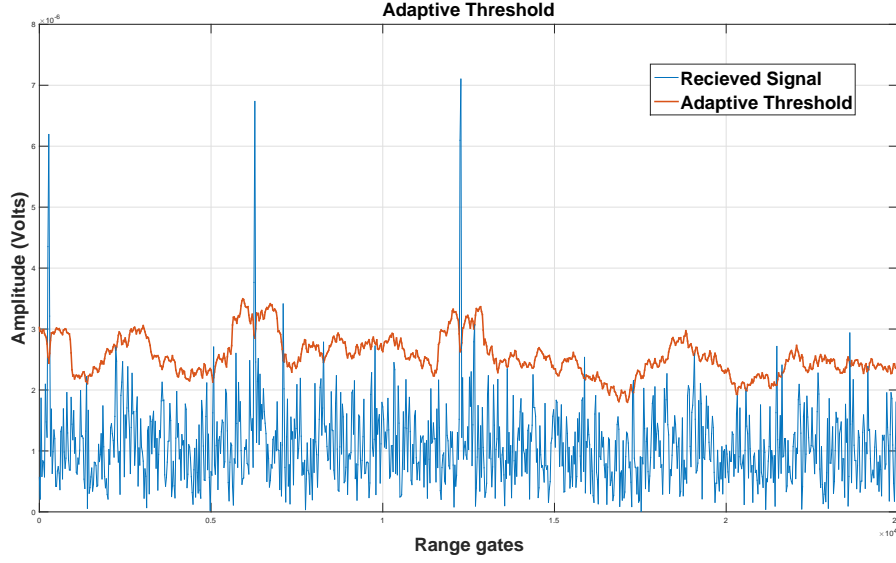


Figure 2.4: Illustrating adaptive thresholding mechanism

with interacting multiple model (IMM) (Blair et al., 1998).

### 2.5.1 Probability data association filter (PDAF)

The PDAF computes the association probability for each validated observation. It is assumed that the number of validated observations obtained from radar at a specific scan is  $m$ . The equations to update state vector and covariance matrix are describes as

State predicted equation is described as

$$\hat{x}_{j+1|j} = F\hat{x}_{j|j} \quad (2.9)$$

Observation vector is represented as

$$\hat{z}_{j+1|j} = H\hat{x}_{j+1|j} \quad (2.10)$$

Covariance of the predicted state

$$P_{j+1|j} = FP_{j|j}F' + Q \quad (2.11)$$

Covariance wrt observation

$$S_{j+1}(\Omega_{j+1}) = HP_{j+1|j}H + C_{j+1}(\Omega_{j+1}) \quad (2.12)$$

Where,  $C_{j+1}$  is the observation error covariance matrix corresponding to  $\Omega_{j+1}$  waveform. The validation region (gate)-the ellipsoid can be written as

$$\mathcal{V}_{j+1} = \left\{ z : [z - \hat{z}_{j+1|j}]^T S_{j+1}(\Omega_{j+1})^{-1} [z - \hat{z}_{j+1|j}] \leq \gamma \right\} \quad (2.13)$$

Where  $\gamma$  is the gate threshold determined by the chosen gate probability  $P_G$ . Innovation corresponding to the  $i$ -th validated measurement

$$v_{j+1}^i = z_{j+1}^i - \hat{z}_{j+1|j} \quad i = 1, \dots, m_{j+1} \quad (2.14)$$

Volume of the validation region is given as

$$V_{j+1}(\Omega_{j+1}) = c_{n_z} |\gamma S_{j+1}(\Omega_{j+1})|^{1/2} \quad (2.15)$$

Where  $c_{n_z}$  represents unit hypersphere volume with dimension  $n_z$  (i.e.  $[c_1, c_2, c_3] = [2, \pi, 4\pi/3]$ ) Probability of the  $i$ -th validated measurement is

$$\beta_{j+1}^i(\Omega_{j+1}) = \begin{cases} \frac{e^i(\Omega_{j+1})}{b + \sum_{l=1}^{m(j+1)} e_l(\Omega_{j+1})} & i = 1, \dots, m(j+1) \\ \frac{b}{b + \sum_{l=1}^{m(j+1)} e_l(\Omega_{j+1})} & i = 0 \end{cases} \quad (2.16)$$

$\beta_0(k+1)$  is association probability which represents that none of the measurement is correct,

$$e^i(\Omega_{j+1}) \triangleq e^{-\frac{1}{2} v_{j+1}^i T S_{j+1}(\Omega_{j+1})^{-1} v_{j+1}^i} \quad (2.17)$$

$$b \triangleq \left( \frac{2\pi}{\gamma} \right)^{\frac{n_z}{2}} m(j+1) c_{n_z}^{-1} \frac{1 - P_D P_G}{P_D} \quad (2.18)$$

State update

$$\hat{x}_{j+1|j+1}(\Omega_{j+1}) = \hat{x}_{j+1|j} + W_{j+1}(\Omega_{j+1})v_{j+1}(\Omega_{j+1}) \quad (2.19)$$

Where,  $W_{j+1}(\Omega_{j+1})$  is filter gain and  $v_{j+1}(\Omega_{j+1})$  is known as combined innovation which is calculated as

$$v_{j+1} \triangleq \sum_{i=1}^{m(j+1)} \beta_{j+1}^i v_{j+1}^i \quad (2.20a)$$

$$W_{j+1}(\Omega_{j+1}) \triangleq P_{j+1|j} H' S_{j+1}(\Omega_{j+1}) \quad (2.20b)$$

Covariance associated to update state is given as

$$P_{j+1|j+1}(\Omega_{j+1}) = P_{j+1|j} - [1 - \beta_{j+1}^0] W_{j+1}(\Omega_{j+1}) S_{j+1}(\Omega_{j+1}) W_{j+1}^T(\Omega_{j+1}) + \tilde{P}_{j+1}(\Omega_{j+1}) \quad (2.21a)$$

$$\tilde{P}_{j+1}(\Omega_{j+1}) \triangleq \left[ \sum_{i=1}^{m(j+1)} \beta_{j+1}^i(\Omega_{j+1}) v_{j+1}^i v_{j+1}^{i T} - v_{j+1} v_{j+1}^T \right] \times W_{k+1}^T(\Omega_{j+1}) \quad (2.21b)$$

Equations 2.19 and 2.21 illustrates the final update equation for state vector and covariance matrix of PDAF respectively.

## 2.5.2 Interacting multiple model estimator (IMM)

This subsection demonstrate the framework of IMM estimator. PDAF is employed to track single target effectively. But, in real time environment the target may maneuver with high acceleration values. So, PDAF is integrated in to the IMM filters and each PDAF has different state transition models depending on the motion of the target. The final state vector and covariance matrix is updated by using weighted sum of each PDA

filters. Detailed explanation and derivation of IMM estimator is described in (Bar-Shalom et al., 2004).

Updated state vector  $\hat{x}_{j|j}^l$ , model probability value  $\mu_{j|j}^l$  and updated covariance matrix  $\hat{P}_{j|j}^l$  of particular filter data is present for updating next  $(j + 1)^{th}$  iteration with observation value  $z_{j+1}$ . A brief derivation of IMM estimator is described as:

- Computing mixed input to tracking filter

Predicted model probability is calculated by

$$\mu_{j+1|j}^r = \sum_{l=1}^n p_{lr} \mu_{j|j}^l \quad (2.22)$$

Where, the model probability conditioned on  $j$  is

$$\mu_{j|j}^{l|r} = (1/\mu_{j+1|j}^r) p_{lr} \mu_{j|j}^l \quad (2.23)$$

The mixed state estimate and covariance which is given as input to the PDAF filter is computed by

$$\hat{x}_{j|j}^{0r} = \sum_l^n \mu_{j|j}^{l|r} \hat{x}_{j|j}^l \quad (2.24a)$$

$$P_{j|j}^{0r} = \sum_{l=1}^n \mu_{j|j}^{l|r} \{P_{j|j}^l + [\hat{x}_{j|j}^l - \hat{x}_{j|j}^{0r}][\hat{x}_{j|j}^l - \hat{x}_{j|j}^{0r}]^T\} \quad (2.24b)$$

- Updating mixed state estimate and covariance

The state estimate and covariance of each  $r^{th}$  filter is updated from the input (2.24a) and (2.24b) to obtain updated state estimate ( $\hat{x}_{j+1|j+1}^r$ ) and covariance ( $\hat{P}_{j+1|j+1}^r$ ).

- Calculating model likelihood function

$$\Lambda_{j+1}^m = \frac{1}{\sqrt{|2\pi S_{j+1}^r|}} e^{-\frac{1}{2}[\tilde{z}_{j+1}]^T [S_{j+1}^r]^{-1} [\tilde{z}_{j+1}]} \quad (2.25)$$

- Updating model probability of each filter

$$\mu_{j+1|j+1}^r = \frac{1}{b} \mu_{j+1|j}^r \Lambda_{j+1}^r \quad (2.26)$$

Where  $b$  is a normalization factor

$$b = \sum_{l=1}^r \mu_{j+1|j}^l \Lambda_{j+1}^l \quad (2.27)$$

- Combining state estimate

$$\hat{x}_{j+1|j+1}^{IMM} = \sum_{r=1}^n \mu_{j+1|j+1}^r \hat{x}_{j+1|j+1}^r \quad (2.28a)$$

$$\begin{aligned} P_{j+1|j+1}^{IMM} &= \sum_{r=1}^n \mu_{j+1|j+1}^r \\ &\times \{ P_{j+1|j+1}^r + [\hat{x}_{j+1|j+1}^r - \hat{x}_{j+1|j+1}^{IMM}] \\ &[\hat{x}_{j+1|j+1}^r - \hat{x}_{j+1|j+1}^{IMM}]^T \} \end{aligned} \quad (2.28b)$$

Equations 2.28a and 2.28b illustrates the final update equations for state vector and covariance matrix of IMM estimator. At any point of time the target trajectory will be approximated to any one of the transition model in IMM estimator and the corresponding transition model is switched on automatically. This process is performed by computing the model probability.

## 2.6 Simulation results

This subsection describes about simulation results and related discussion. Six benchmark target trajectories used for conducting the simulation experiments are illustrated in the following subsection.

## 2.6.1 Benchmark trajectories

Six benchmark target trajectories from (Blair et al., 1998) have been utilized for testing WAS approach in combined ECM (SSJ and SOJ), multipath and clutter scenario by employing IMMPDFAF. Each trajectory simulated time, trajectory turn rates, target type and velocity is described below:

### 2.6.1.1 Benchmark trajectory-1

Initial and final positions of the target from the radar are at  $[75, 30, 1.26]$  km and  $[73.54, 4.7, 1.26]$  km respectively. The target makes  $2g$  and  $3g$  maneuvers. The speed is maintained constant at  $290m/s$  and the flight time of the target is  $165s$ . The trajectory represents a large aircraft.

### 2.6.1.2 Benchmark trajectory-2

Initial and final positions of the target from the radar are at  $[47, -45, 4.57]$  km and  $[34, -36.54, 3.760]$  km respectively. The target makes  $2.5g$  and  $4g$  maneuvers. The total flight time of the target is  $150s$ . The trajectory depicts small maneuverable commercial jet. Figure 2.5 illustrates the estimated and original target trajectory of benchmark trajectory-2.

### 2.6.1.3 Benchmark trajectory-3

The target turns  $45^\circ$  and  $90^\circ$  with  $4g$  acceleration at  $30s$  and  $60s$  respectively. The total flight time of the target is  $145s$ . The maximum speed limit is maintained up to  $457 m/s$ , while the minimum speed is maintained  $274 m/s$ . The trajectory represents medium bomber.

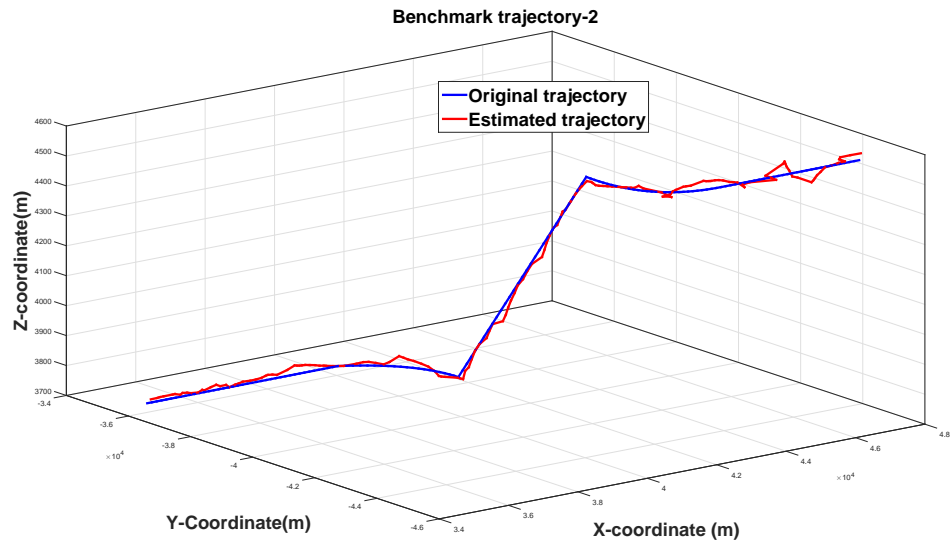


Figure 2.5: Tracking of Benchmark target trajectory-2 in the presence of FA, SOJ, clutter and multipath

#### 2.6.1.4 Benchmark trajectory-4

The target maneuvers  $45^\circ$  with  $4g$  and  $6g$  acceleration rate. The minimum speed of the target is maintained at  $251\text{ m/s}$ . The total flight time of the target is  $184s$ . The trajectory represents medium bomber. Figure 2.6 illustrates the estimated and original target trajectory of benchmark trajectory-4.

#### 2.6.1.5 Benchmark trajectory-5

The target makes complicated maneuvering turns with acceleration rates  $5g$ ,  $6g$  and  $7g$ . The total flight time of the target is  $182s$ . The trajectory represents a fighter aircraft.

#### 2.6.1.6 Benchmark trajectory-6

The target maneuvers two  $6g$  and two  $7g$  acceleration turns. The constant speed of the target is maintained at  $426\text{ m/s}$ . The total flight time of the target is  $188s$ . The trajectory represents a fighter aircraft.

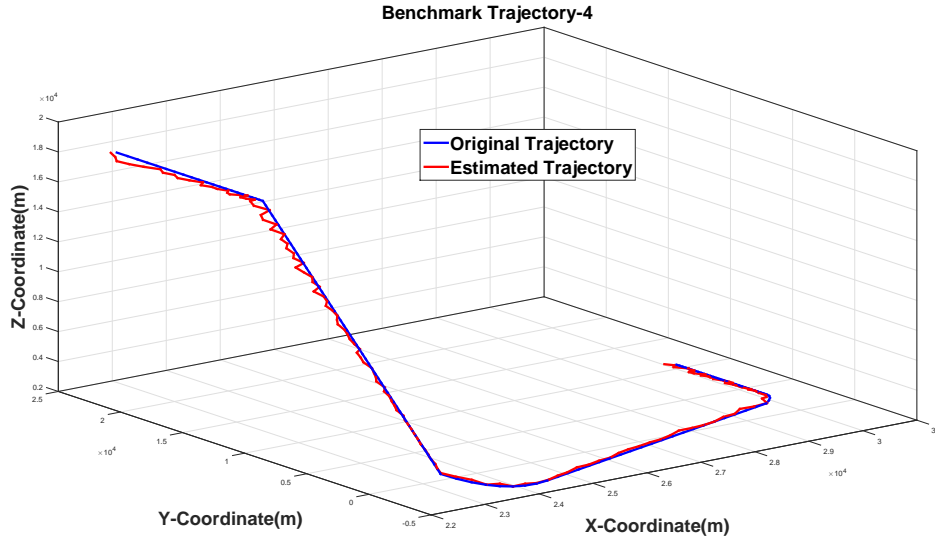


Figure 2.6: Tracking of Benchmark target trajectory-4 in the presence of FA, SOJ, clutter and multipath

## 2.6.2 Simulation results & discussion

Simulation results for the six benchmark target trajectories in the complicated scenario is tabulated in Table 2.2 and Table 2.3 respectively. The results obtained for the scenario 1: clutter, SOJ, FAs and multipath is illustrated in Table 2.2. The results are compared with earlier research work (Angelova et al., 1999) which neglected multipath effects. Furthermore, the results obtained for the scenario 2: clutter, SSJ, FAs and multipath is tabulated in Table 2.3. Since the earlier studies did not consider jammer on board the target, therefore the obtained results are not compared with any of the studies.

From the Table 2.2 it is evident that the average power in the present study is reduced significantly for all benchmark target trajectories excluding benchmark trajectory-4. Furthermore, it is noticeable from the simulation results that the proposed WAS approach needs only 39.98% lower mean average power when compared to earlier studies (Angelova et al., 1999). Moreover, the cost function ( $C_1$ ) related to radar energy is lowered significantly. But, the cost function ( $C_2$ ) related to radar time is increased by a small amount. The track loss for benchmark target trajectories -3, 4, 5, and 6 are

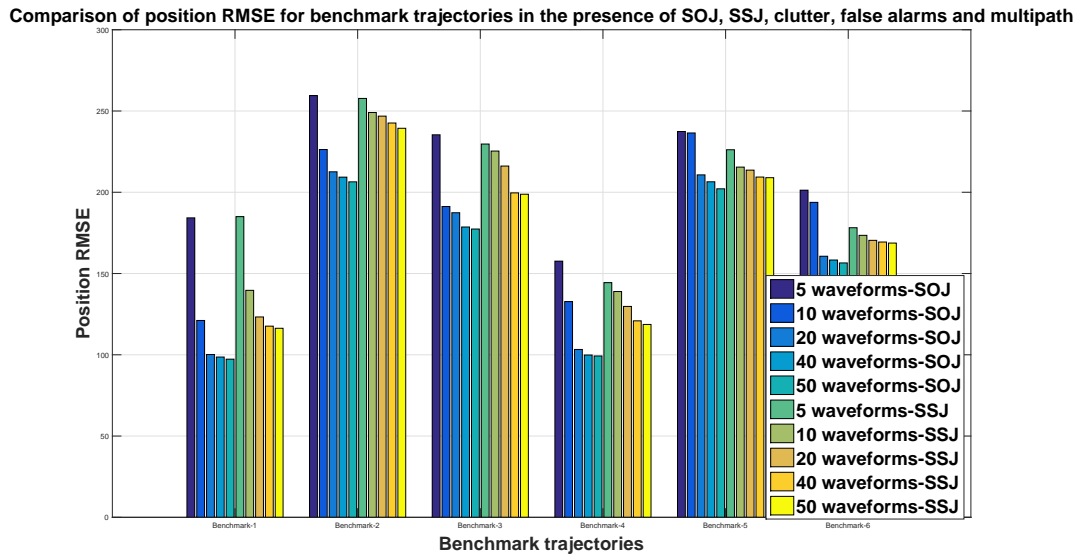


Figure 2.7: Comparison of position RMSE for benchmark trajectories in the presence of SOJ, SSJ, clutter, false alarms and multipath

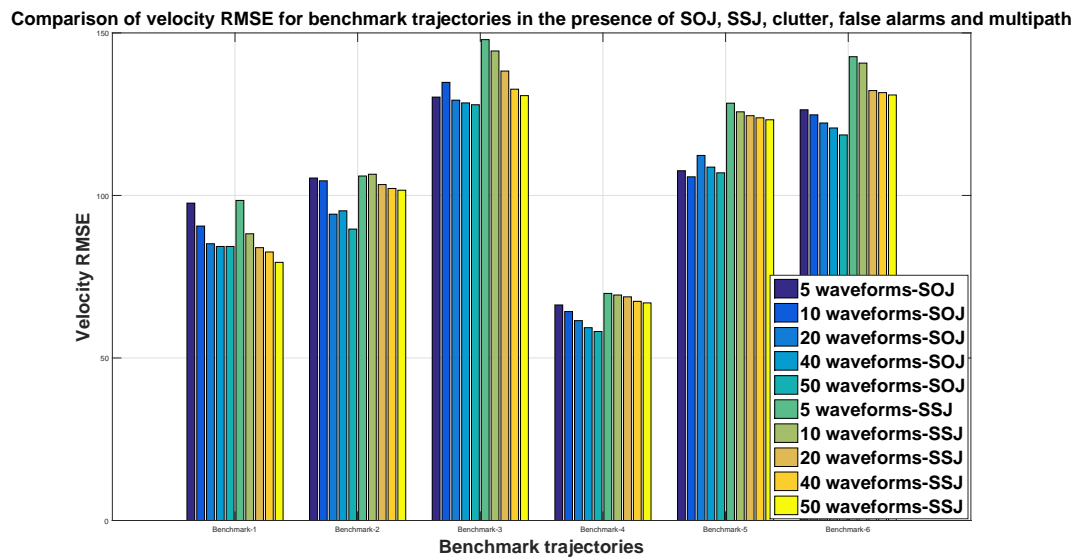


Figure 2.8: Comparison of velocity RMSE for benchmark trajectories in the presence of SOJ, SSJ, clutter, false alarms and multipath

Table 2.2: Comparison results for benchmark targets in the presence of FA + SOJ+ clutter + multipath

SINo	Track Length (s)	Max. Acc. ( $m/s^2$ )	Man. Density (%)	Number of Waveforms	Ave.Power (W)	Pos.RMSE (m)	Vel.RMSE ( $m/s$ )	Cost $C_1$	Cost $C_2$	Track loss (%)
Benchmark Trajectory -1										
1				5	3.14	184.26	97.64	3.61	50.15	0
2	165	29.4	24.24	10	2.85	121.12	90.58	3.31	48.53	0
3				20	2.60	100.17	85.15	3.04	47.31	0
4				40	2.55	98.62	84.31	2.78	46.89	0
5				50	2.52	97.31	84.31	2.78	46.83	0
Benchmark Trajectory -2										
6				5	3.09	259.48	105.36	3.56	50.52	0
7	150	39.2	34.66	10	3.42	226.29	104.51	3.91	52.03	0
8				20	2.96	212.60	94.24	3.43	49.77	0
9				40	2.88	209.31	95.28	3.37	48.64	0
10				50	2.79	206.42	89.65	3.31	48.59	0
Benchmark Trajectory -3										
11				5	7.34	235.37	130.26	7.93	66.13	2
12	145	39.2	20.83	10	7.16	191.24	134.79	7.82	66.02	1.5
13				20	7.03	187.41	129.32	7.78	65.67	1.5
14				40	6.93	178.63	128.47	7.32	65.21	1.5
15				50	6.72	177.38	127.91	7.01	65.07	1.5
Benchmark Trajectory -4										
16				5	7.29	157.62	66.31	7.89	65.72	0.8
17	184	58.8	9.92	10	7.19	132.73	64.28	7.75	65.61	0
18				20	7.13	103.28	61.49	7.71	65.47	0
19				40	7.10	99.86	59.32	7.68	65.39	0
20				50	7.06	99.27	58.14	7.63	65.30	0
Benchmark Trajectory -5										
21				5	7.41	237.38	107.61	7.92	66.01	1.8
22	182	68.6	17.5	10	7.30	236.49	105.74	7.84	65.92	1.3
23				20	7.26	210.71	112.31	7.79	65.49	0.8
24				40	7.19	206.46	108.72	7.74	65.37	0.8
25				50	7.12	202.13	106.97	7.68	65.22	0.8
Benchmark Trajectory -6										
26				5	4.47	201.28	126.37	4.78	57	2.3
27	188	68.6	18	10	4.36	193.79	124.81	4.63	56.24	2.1
28				20	4.29	160.64	122.29	4.57	56.08	2.1
29				40	4.16	158.31	120.76	4.46	55.91	1.6
30				50	4.01	156.52	118.62	4.39	55.71	1.6

<sup>1</sup>-Authors (Angelova et al., 1999) ignored multipath effects.

Table 2.3: Comparison results for benchmark targets in the presence of FA + SSJ+ clutter + multipath

SINo	Track Length (s)	Max. Acc. ( $m/s^2$ )	Man. Density (%)	Number of Waveforms	Ave.Power (W)	Pos.RMSE (m)	Vel.RMSE ( $m/s$ )	Cost $C_1$	Cost $C_2$	Track loss (%)
<b>Benchmark Trajectory -1</b>										
1				5	3.03	185	98.47	3.49	49.47	0
2	165	29.4	24.24	10	2.71	139.66	88.21	3.16	47.65	0
3				20	2.63	123.28	83.94	3.08	47.45	0
4				40	2.58	117.62	82.61	2.93	46.28	0
5				50	2.51	116.31	79.42	2.82	46.21	0
<b>Benchmark Trajectory -2</b>										
6				5	3.13	257.74	105.98	3.61	50.62	0
7	150	39.2	34.66	10	3.06	249.07	106.53	3.53	50.28	0
8				20	3	246.85	103.35	3.47	49.98	0
9				40	2.98	242.61	102.15	3.36	47.32	0
10				50	2.73	239.37	101.61	3.32	45.23	0
<b>Benchmark Trajectory -3</b>										
11				5	7.43	229.67	147.94	8.76	68.01	2.6
12	145	39.2	20.83	10	7.39	225.36	144.45	8.41	67.82	2.4
13				20	7.35	138.27	138.27	8.32	67.39	2.0
14				40	7.16	199.62	132.69	7.83	66.97	1.7
15				50	7.12	198.79	130.71	7.78	66.83	1.7
<b>Benchmark Trajectory -4</b>										
16				5	7.32	144.38	69.86	7.92	65.87	1.2
17	184	58.8	9.92	10	7.28	138.92	69.37	7.86	65.70	0
18				20	7.21	129.76	68.81	7.74	65.59	0
19				40	7.07	120.89	67.43	7.43	65.06	0
20				50	7.04	118.67	66.94	7.39	64.93	0
<b>Benchmark Trajectory -5</b>										
21				5	7.32	226.17	128.39	7.91	66.03	0
22	182	68.6	17.5	10	7.26	215.48	125.73	7.88	65.95	0
23				20	7.19	213.62	124.54	7.76	65.82	0
24				40	7.09	209.36	123.89	7.69	65.62	0
25				50	7.03	208.97	123.28	7.42	65.54	0
<b>Benchmark Trajectory -6</b>										
26				5	4.79	178.19	142.69	5.06	55.86	3.1
27	188	68.6	18	10	4.63	173.50	140.72	5.01	55.29	2.2
28				20	4.54	170.42	132.26	4.82	55.07	2.2
29				40	4.46	169.38	131.63	4.78	54.91	2.2
30				50	4.32	168.74	130.91	4.71	54.86	2.2

1.6%, 0.8% , 1.1% and 1.94% respectively. While the track loss for benchmark target trajectories -1, 2 is zero. It can also be noticed from Table 2.2 is that the position and velocity RMSEs are higher when compared to (Angelova et al., 1999). This obviously suggests that the multipath effect has increased the observation error along with clutter.

Figure 2.7 and Figure 2.8 clearly depicts that the position and velocity RMSEs decreases as the number of waveforms increase from 5 to 50 (Miao et al., 2011). It can also be noticed that position RMSE for all benchmark target trajectories has a mean difference of  $52.124m$  for 50 waveforms excluding benchmark target trajectory-1. From Table 2.2, it is evident that the velocity RMSE in present study is high with mean difference of  $40.56m/s$  when compared to previous work. The previous studies (Angelova et al., 1999) neglected the multipath effect in the environment. In the present study along with jammer and clutter, multipath effects are also considered which is the reason for reduced performance in terms of velocity RMSE.

The performance evaluation of IMM-PDAF in the presence of clutter, SSJ, false alarm and multipath is listed in Table 2.3. For this case, it can be noticed that the position and velocity RMSEs for all six benchmark target trajectories reduces as the waveforms increased from 5 to 50. However, the average power for benchmark target trajectories -3, 4 and 5 is higher than benchmark target trajectories -1, 2 and 6. The average track loss for benchmark target trajectories -3, 4, and 6 is 1.86%. On the other hand the track loss for benchmark target trajectories -1, 2 and 5 is zero. Besides, it is also observed that, the cost function values ( $C_1$  &  $C_2$  ) are lower for benchmark target trajectories 1, 2 and 6 when compared to benchmark target trajectories 3, 4 and 5.

From Figure 2.7 and Figure 2.8, it can be noticed that the position RMSE and velocity RMSE of SOJ is significantly lower than SSJ for all six benchmark target trajectories. Figures 2.9 to 2.10 illustrates reduction in position RMSE, when the number of waveforms are increasing in waveform bank. Moreover, the dotted line in Figures 2.9 to 2.10 depicts the optimal number of waveforms required for both SOJ and SSJ cases respectively. In case of SOJ, the optimal number of waveforms for benchmark target trajectories is 20 except for benchmark target trajectory -3. While the optimality

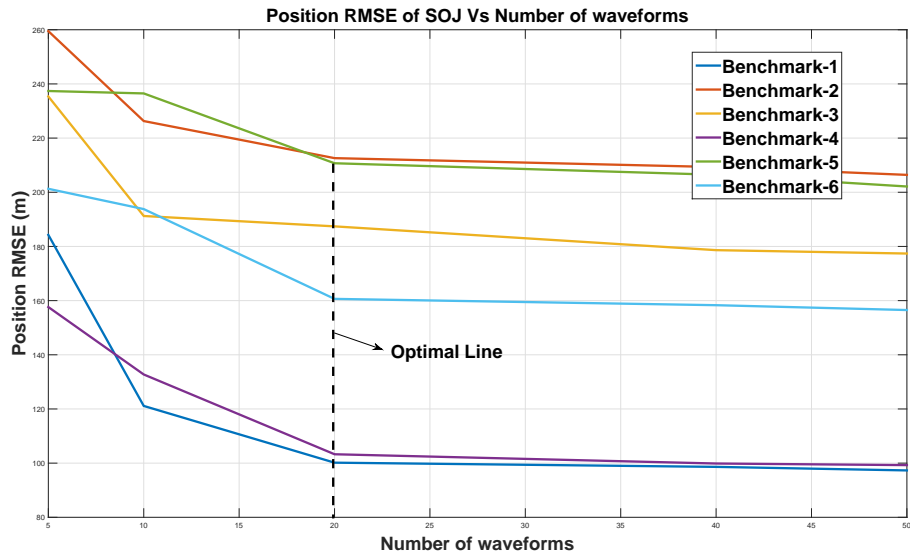


Figure 2.9: Performance of position RMSE Vs number of waveforms for Benchmark Trajectories in the presence of SOJ, clutter, false alarm and multipath

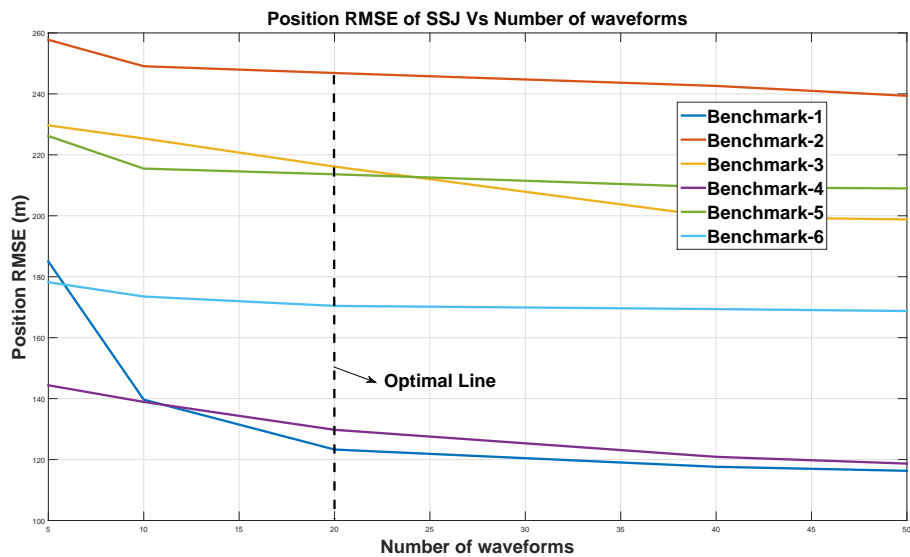


Figure 2.10: Performance of position RMSE Vs number of waveforms for Benchmark Trajectories in the presence of SSJ, clutter, false alarm and multipath

for benchmark target trajectory -3 for SOJ case is achieved at 10 waveforms. Whereas in case of SSJ, the optimal number of waveforms for benchmark target trajectory -2, 5 and 6 is 20. For benchmark target trajectory -1 and 4 the optimality is attained at 20 waveforms. However, for benchmark target trajectory -3, in case of SSJ the optimality is obtained for 40 waveforms. For both cases, the average optimality is attained at 20 waveforms.

The experimental results reveals that there is an improvement in performance by using WAS technique in the presence of clutter, ECM, multipath and FAs. Therefore, highly maneuvering targets can be tracked by using this approach in the presence of intense interference.

## **2.7 Conclusion**

In this chapter enhanced performance for tracking benchmark target trajectories has been exhibited using WAS approach in the presence of intense interference. The track performance is improved by applying 5 to 50 frequency coded waveforms (GFM, LFM and SFM) from the waveform bank. IMMPPDAF estimator is employed to track highly maneuvering benchmark target trajectories with ECM (SSJ/SOJ), multipath and background clutter. The simulation results reveals that the proposed WAS technique needs 39.98% lower mean average power when compared to earlier studies (Angelova et al., 1999). It can also be noticeable that there is decrease in both position and velocity RMSE with increase in number of waveforms in waveform bank from 5 to 50. However, there is an increase in position and velocity RMSEs when compared to earlier fixed waveform studies. To further improve the performance space-time adaptive processing (STAP) based WAS approach is presented, which is described in the next chapter.

## CHAPTER 3

# STAP BASED APPROACH FOR TARGET TRACKING USING WAVEFORM AGILE SENSING IN THE PRESENCE OF ECM

### 3.1 Introduction

This chapter proposes WAS approach to track single targets in the presence of intense interference (ECM, false alarms and clutter) by employing space time adaptive processing (STAP) at the receiver end. STAP based approach effectively suppresses the intense interference (jamming and clutter) by applying the filtering operations in multidimensional aspect (in terms of range and Doppler) (Rabideau, 2000). Based on CRLB, a particular waveform that has to be transmitted for next scan is chosen from the waveform bank. SOJ and SSJ are considered as major ECM technique. IMM-PDAF is employed to track the targets. The literature survey related to these approaches have been described in section 2.2. The following subsections briefly describes this method.

### 3.2 Space time adaptive processing

Space time adaptive processing (STAP) is associated with two-dimensional filtering in both time and spatial domain to detect the targets by effectively suppressing both jamming and clutter. Let,  $N$  be the number of sensors in linear phased array radar and  $M$  be the number of delayed echo pulses obtained at the receiver. The pulses with time delay depicts the signal in time domain and the array sensor collects the signal in spatial domain. Following equations illustrate the STAP approach in two dimensions.

If the transmitted radar waveform is  $x(t)$ , then the waveform echo obtained at sensor  $k$  with angle of arrival ( $\theta$ ) at time instant ( $i$ ) is described as

$$Y_k(t_i) = x(t_i)e^{-j\delta\theta_k} \quad (3.1)$$

where,  $\delta\theta_k = \frac{2\pi d(k-1)}{\lambda} \sin(\theta)$ ;  $k = 1, 2, \dots, N$ ;  $\lambda$  is the wavelength and  $d$  represents distance between two sensors.

Let the spatial steering vector corresponding to angle of arrival ( $\theta$ ) be  $L_s(\theta)$ , then the received radar echo is represented as

$$\mathbf{Y}_i = x(t_i)L_s(\theta) \quad (3.2)$$

where,  $L_s(\theta) = e^{\frac{-j2\pi d(k-1)\sin(\theta)}{\lambda}}$ ;  $k = 1, 2, \dots, N$ .

Let, the temporal steering vector with Doppler shift ( $f_D$ ) be  $L_t(f_D)$ , then the waveform echo at  $k^{th}$  sensor due to  $M$  pulses is given as

$$\mathbf{Y}_k(t - (j - 1)T) = x(t)L_t(f_D) \quad (3.3)$$

where,  $j = 1, 2, \dots, M$  and  $k = 1, 2, \dots, N$ .

From Equations 3.2 and 3.3, the compounded echo waveform at  $i^{th}$  time instant from a target with angle of arrival ( $\theta$ ) and Doppler frequency ( $f_D$ ) is represented as

$$\mathbf{Y}_i = x(t_i) [L_s(\theta) \otimes L_t(f_D)] \quad (3.4)$$

where,  $\otimes$  is the Kronecker product.

After applying two-dimensional beamformer, the output signal is described as

$$C = W\mathbf{Y}_i \quad (3.5)$$

where,  $W$  is the weight matrix which is computed by using adaptive algorithm so as to maximize the signal to interference ratio.

### 3.3 Problem formulation

In the proposed WAS technique, an active phased array radar (operating at  $X$ -band and a linear phased array with 900 elements) with adaptive displaced phase center antenna is applied to extract the observations. The radar waveform that is to be transmitted is chosen based on CRLB of updated measurement errors. The radar waveforms are varied from 5 to 50 in the waveform bank and linear frequency modulated (LFM) waveforms with different pulse repetition frequency's (PRFs) and pulse widths are collected to be present in the waveform bank. In addition to ECM (SSJ/SOJ), background clutter and FAs are included in the environment. Greatest-of cell-averaging constant false alarm rate (GOCA-CFAR) adaptive thresholding approach is engaged for target detection (Skolnik, 1970). IMMPDAF estimator is used to estimate all the benchmark target trajectories in the presence of intense interference. Benchmark target trajectories which are discussed in subsection 2.6.1 are used in the present investigation. An elaborated discussion of problem formulation is described in chapter 2.3. The overall work flow is briefly represented in Figure 3.1.

### 3.4 Results and discussion

Simulation results for the aforementioned six benchmark target trajectories in the complicated scenario is tabulated in Table 3.1 and Table 3.2 respectively. The results obtained for the scenario-1: clutter, SOJ and FAs is illustrated in Table 3.1. Furthermore, the results obtained for the scenario-2: clutter, SSJ and FAs is tabulated in Table 3.2. These results are compared with results obtained in chapter-2 (Satapathi and Pathipati, 2017).

From the Table 3.1 it is evident that the average power in the present study is increased significantly for all benchmark target trajectories. Furthermore, it is noticeable from the simulation results that the proposed STAP based WAS approach needs

---

<sup>1</sup> in Table 3.1 and Table 3.2 refers that the values are calculated using the algorithm in (Satapathi and Pathipati, 2017)

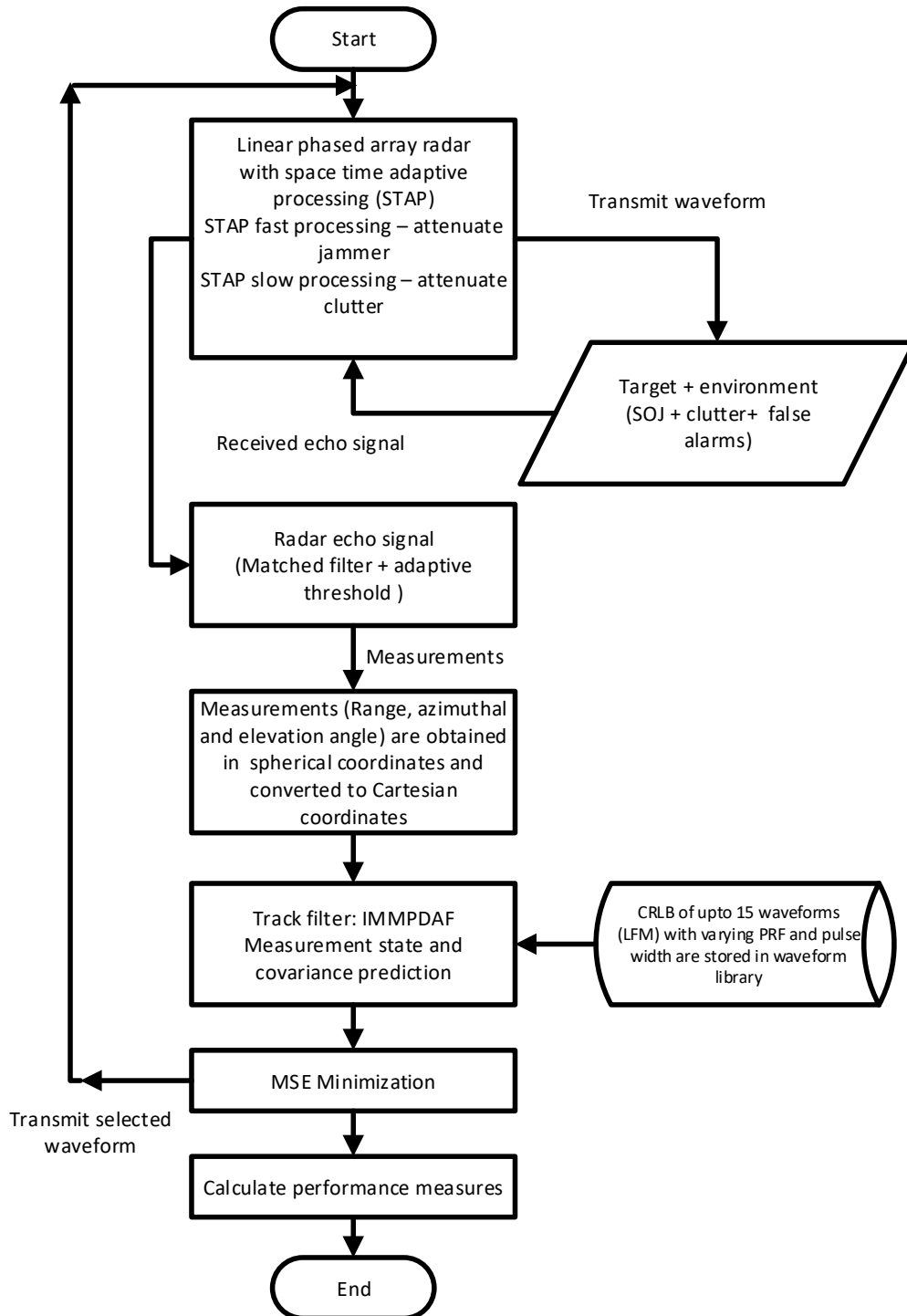


Figure 3.1: Flowchart of entire simulation process

Table 3.1: Comparison results for Benchmark Targets in the presence of FA + SOJ+ Clutter + Multipath

SINo	Track Length (s)	Max. Acc. ( $m/s^2$ )	Man. Density (%)	Number of Waveforms	Ave.Power (W)	Pos.RMSE (m)	Vel.RMSE (m/s)	Cost $C_1$	Cost $C_2$	Track loss (%)						
Benchmark Trajectory -1																
1				5	5.67	3.14 <sup>1</sup>	74.37	184.26 <sup>1</sup>	58.51	97.64 <sup>1</sup>	6.31	3.61 <sup>1</sup>	54.66	50.15 <sup>1</sup>	0	0 <sup>1</sup>
2	165	29.4	24.24	10	5.64	2.85 <sup>1</sup>	74.28	121.12 <sup>1</sup>	58.46	90.58 <sup>1</sup>	6.28	3.31 <sup>1</sup>	54.61	48.53 <sup>1</sup>	0	0 <sup>1</sup>
3				20	5.58	2.60 <sup>1</sup>	74.21	100.17 <sup>1</sup>	58.43	85.15 <sup>1</sup>	6.28	3.04 <sup>1</sup>	54.57	47.31 <sup>1</sup>	0	0 <sup>1</sup>
4				40	5.55	2.55 <sup>1</sup>	74.17	98.62 <sup>1</sup>	58.34	84.31 <sup>1</sup>	6.21	2.78 <sup>1</sup>	54.53	46.89 <sup>1</sup>	0	0 <sup>1</sup>
5				50	5.53	2.52 <sup>1</sup>	74.24	97.31 <sup>1</sup>	58.44	84.31 <sup>1</sup>	6.17	2.78 <sup>1</sup>	54.49	46.83 <sup>1</sup>	0	0 <sup>1</sup>
Benchmark Trajectory -2																
6				5	5.27	3.09 <sup>1</sup>	96.24	259.48 <sup>1</sup>	72.17	105.36 <sup>1</sup>	6.34	3.56 <sup>1</sup>	51.36	50.52 <sup>1</sup>	0	0 <sup>1</sup>
7	150	39.2	34.66	10	5.25	3.42 <sup>1</sup>	96.07	226.29 <sup>1</sup>	71.83	104.51 <sup>1</sup>	6.28	3.91 <sup>1</sup>	49.50	52.03 <sup>1</sup>	0	0 <sup>1</sup>
8				20	5.23	2.96 <sup>1</sup>	95.84	212.60 <sup>1</sup>	71.78	94.24 <sup>1</sup>	5.49	3.43 <sup>1</sup>	48.98	49.77 <sup>1</sup>	0	0 <sup>1</sup>
9				40	5.19	2.88 <sup>1</sup>	95.78	209.31 <sup>1</sup>	71.74	95.28 <sup>1</sup>	5.27	3.37 <sup>1</sup>	48.71	48.64 <sup>1</sup>	0	0 <sup>1</sup>
10				50	5.17	2.79 <sup>1</sup>	95.75	206.42 <sup>1</sup>	71.75	89.65 <sup>1</sup>	5.22	3.31 <sup>1</sup>	48.46	48.59 <sup>1</sup>	0	0 <sup>1</sup>
Benchmark Trajectory -3																
11				5	9.48	7.34 <sup>1</sup>	95.63	235.37 <sup>1</sup>	67.64	130.26 <sup>1</sup>	11.72	7.93 <sup>1</sup>	76.53	66.13 <sup>1</sup>	1	2 <sup>1</sup>
12	145	39.2	20.83	10	9.45	7.16 <sup>1</sup>	95.78	191.24 <sup>1</sup>	67.60	134.79 <sup>1</sup>	11.68	7.82 <sup>1</sup>	76.50	66.02 <sup>1</sup>	1	1.5 <sup>1</sup>
13				20	9.41	7.03 <sup>1</sup>	95.52	187.41 <sup>1</sup>	67.56	129.32 <sup>1</sup>	11.65	7.78 <sup>1</sup>	76.46	65.67 <sup>1</sup>	0	1.5 <sup>1</sup>
14				40	9.37	6.93 <sup>1</sup>	95.48	178.63 <sup>1</sup>	67.56	128.47 <sup>1</sup>	11.65	7.32 <sup>1</sup>	76.46	65.21 <sup>1</sup>	0	1.5 <sup>1</sup>
15				50	9.37	6.72 <sup>1</sup>	95.48	177.38 <sup>1</sup>	67.54	127.913 <sup>1</sup>	11.59	7.01 <sup>1</sup>	76.42	65.07 <sup>1</sup>	0	1.5 <sup>1</sup>
Benchmark Trajectory -4																
16				5	8.16	7.29 <sup>1</sup>	67.82	157.62 <sup>1</sup>	58.42	66.31 <sup>1</sup>	8.47	7.89 <sup>1</sup>	71.38	65.72 <sup>1</sup>	0	0.8 <sup>1</sup>
17	184	58.8	9.92	10	8.12	7.19 <sup>1</sup>	67.77	132.73 <sup>1</sup>	58.38	64.28 <sup>1</sup>	8.45	7.75 <sup>1</sup>	71.29	65.61 <sup>1</sup>	0	0 <sup>1</sup>
18				20	8.07	7.13 <sup>1</sup>	67.74	103.28 <sup>1</sup>	58.35	61.49 <sup>1</sup>	8.32	7.71 <sup>1</sup>	71.25	65.47 <sup>1</sup>	0	0 <sup>1</sup>
19				40	8.05	7.10 <sup>1</sup>	67.69	99.86 <sup>1</sup>	58.29	59.32 <sup>1</sup>	8.26	7.68 <sup>1</sup>	71.23	65.39 <sup>1</sup>	0	0 <sup>1</sup>
20				50	8.01	7.06 <sup>1</sup>	67.65	99.27 <sup>1</sup>	57.54	58.14 <sup>1</sup>	8.21	7.63 <sup>1</sup>	71.19	65.30 <sup>1</sup>	0	0 <sup>1</sup>
Benchmark Trajectory -5																
21				5	8.43	7.41 <sup>1</sup>	123.12	237.38 <sup>1</sup>	74.44	107.61 <sup>1</sup>	8.98	7.92 <sup>1</sup>	73.19	66.01 <sup>1</sup>	0	1.8 <sup>1</sup>
22	182	68.6	17.5	10	8.36	7.30 <sup>1</sup>	123.08	236.49 <sup>1</sup>	74.39	105.74 <sup>1</sup>	8.94	7.84 <sup>1</sup>	73.15	65.92 <sup>1</sup>	0	0.8 <sup>1</sup>
23				20	8.32	7.26 <sup>1</sup>	123.01	210.71 <sup>1</sup>	74.37	112.31 <sup>1</sup>	8.91	7.79 <sup>1</sup>	73.11	65.49 <sup>1</sup>	0	0.8 <sup>1</sup>
24				40	8.27	7.19 <sup>1</sup>	122.86	206.46 <sup>1</sup>	74.32	108.72 <sup>1</sup>	8.83	7.74 <sup>1</sup>	73.05	65.37 <sup>1</sup>	0	0.8 <sup>1</sup>
25				50	8.21	7.12 <sup>1</sup>	122.82	202.13 <sup>1</sup>	74.29	106.97 <sup>1</sup>	8.81	7.68 <sup>1</sup>	72.83	65.22 <sup>1</sup>	0	0.8 <sup>1</sup>
Benchmark Trajectory -6																
26				5	6.14	4.47 <sup>1</sup>	98.07	201.28 <sup>1</sup>	64.33	126.37 <sup>1</sup>	6.41	4.78 <sup>1</sup>	63.71	57 <sup>1</sup>	0	2.3 <sup>1</sup>
27	188	68.6	18	10	6.09	4.36 <sup>1</sup>	98.01	193.79 <sup>1</sup>	64.27	124.81 <sup>1</sup>	6.38	4.63 <sup>1</sup>	62.84	56.24 <sup>1</sup>	0	2.1 <sup>1</sup>
28				20	6.03	4.29 <sup>1</sup>	97.86	160.64 <sup>1</sup>	64.24	122.29 <sup>1</sup>	6.37	4.57 <sup>1</sup>	62.83	56.08 <sup>1</sup>	0	2.1 <sup>1</sup>
29				40	5.93	4.16 <sup>1</sup>	97.85	158.31 <sup>1</sup>	64.24	120.76 <sup>1</sup>	6.29	4.46 <sup>1</sup>	62.71	55.91 <sup>1</sup>	0	1.6 <sup>1</sup>
30				50	5.91	4.01 <sup>1</sup>	97.85	156.52 <sup>1</sup>	64.19	118.62 <sup>1</sup>	6.27	4.39 <sup>1</sup>	62.78	55.71 <sup>1</sup>	0	1.6 <sup>1</sup>

Table 3.2: Comparison results for Benchmark Targets in the presence of FA + SSJ+ Clutter + Multipath

SINo	Track Length (s)	Max. Acc. ( $m/s^2$ )	Man. Density (%)	Number of Waveforms	Ave.Power (W)	Pos.RMSE (m)	Vel.RMSE (m/s)	Cost		Track loss (%)						
								$C_1$	$C_2$							
Benchmark Trajectory -1																
1				5	5.48	3.03 <sup>1</sup>	110.56	185 <sup>1</sup>	86.15	98.47 <sup>1</sup>	6.54	3.49 <sup>1</sup>	52.42	49.47 <sup>1</sup>	0	0 <sup>1</sup>
2	165	29.4	24.24	10	5.37	2.71 <sup>1</sup>	109.71	139.66 <sup>1</sup>	85.88	88.21 <sup>1</sup>	6.51	3.16 <sup>1</sup>	52.36	47.65 <sup>1</sup>	0	0 <sup>1</sup>
3				20	5.31	2.63 <sup>1</sup>	108.36	123.28 <sup>1</sup>	85.64	83.94 <sup>1</sup>	6.47	3.08 <sup>1</sup>	52.31	47.45 <sup>1</sup>	0	0 <sup>1</sup>
4				40	5.26	2.58 <sup>1</sup>	108.29	117.62 <sup>1</sup>	85.61	82.61 <sup>1</sup>	6.39	2.93 <sup>1</sup>	52.24	46.28 <sup>1</sup>	0	0 <sup>1</sup>
5				50	5.22	2.51 <sup>1</sup>	107.92	116.31 <sup>1</sup>	85.59	79.42 <sup>1</sup>	6.38	2.82 <sup>1</sup>	52.23	46.21 <sup>1</sup>	0	0 <sup>1</sup>
Benchmark Trajectory -2																
6				5	5.42	3.13 <sup>1</sup>	105.21	257.74 <sup>1</sup>	71.74	105.98 <sup>1</sup>	6.48	3.61 <sup>1</sup>	52.13	50.62 <sup>1</sup>	0	0 <sup>1</sup>
7	150	39.2	34.66	10	5.39	3.06 <sup>1</sup>	104.74	249.07 <sup>1</sup>	71.71	106.53 <sup>1</sup>	6.45	3.53 <sup>1</sup>	52.07	50.28 <sup>1</sup>	0	0 <sup>1</sup>
8				20	5.35	3 <sup>1</sup>	104.81	246.85 <sup>1</sup>	70.92	103.35 <sup>1</sup>	6.39	3.47 <sup>1</sup>	52.04	49.98 <sup>1</sup>	0	0 <sup>1</sup>
9				40	5.36	2.98 <sup>1</sup>	103.97	242.61 <sup>1</sup>	70.87	102.15 <sup>1</sup>	6.36	3.36 <sup>1</sup>	51.98	47.32 <sup>1</sup>	0	0 <sup>1</sup>
10				50	5.29	2.73 <sup>1</sup>	103.91	239.37 <sup>1</sup>	70.85	101.61 <sup>1</sup>	6.34	3.32 <sup>1</sup>	51.96	45.23 <sup>1</sup>	0	0 <sup>1</sup>
Benchmark Trajectory -3																
11				5	9.68	7.43 <sup>1</sup>	112.58	229.67 <sup>1</sup>	62.74	147.94 <sup>1</sup>	9.72	8.76 <sup>1</sup>	70.38	68.01 <sup>1</sup>	0	2.6 <sup>1</sup>
12	145	39.2	20.83	10	9.63	7.39 <sup>1</sup>	112.32	225.36 <sup>1</sup>	62.63	114.45 <sup>1</sup>	9.71	8.41 <sup>1</sup>	68.94	67.82 <sup>1</sup>	1	2.4 <sup>1</sup>
13				20	9.61	7.35 <sup>1</sup>	110.76	216.13 <sup>1</sup>	58.98	138.27 <sup>1</sup>	9.71	8.32 <sup>1</sup>	68.72	67.39 <sup>1</sup>	1	2 <sup>1</sup>
14				40	9.57	7.16 <sup>1</sup>	110.46	199.62 <sup>1</sup>	58.95	132.69 <sup>1</sup>	9.68	7.83 <sup>1</sup>	68.70	66.97 <sup>1</sup>	1	1.7 <sup>1</sup>
15				50	9.55	7.12 <sup>1</sup>	110.40	198.79 <sup>1</sup>	58.87	130.71 <sup>1</sup>	9.68	7.78 <sup>1</sup>	68.65	66.83 <sup>1</sup>	1	1.7 <sup>1</sup>
Benchmark Trajectory -4																
16				5	9.93	7.32 <sup>1</sup>	86.19	144.38 <sup>1</sup>	42.51	69.86 <sup>1</sup>	10.01	7.92 <sup>1</sup>	67.65	65.87 <sup>1</sup>	0	1.2 <sup>1</sup>
17	184	58.8	9.92	10	9.90	7.28 <sup>1</sup>	86.16	138.92 <sup>1</sup>	42.68	69.37 <sup>1</sup>	9.97	7.86 <sup>1</sup>	67.63	65.70 <sup>1</sup>	0	0 <sup>1</sup>
18				20	9.87	7.21 <sup>1</sup>	86.13	129.76 <sup>1</sup>	42.49	68.81 <sup>1</sup>	9.95	7.74 <sup>1</sup>	67.52	65.59 <sup>1</sup>	0	0 <sup>1</sup>
19				40	9.71	7.07 <sup>1</sup>	86.14	120.89 <sup>1</sup>	42.48	67.43 <sup>1</sup>	9.90	7.43 <sup>1</sup>	67.48	65.06 <sup>1</sup>	0	0 <sup>1</sup>
20				50	9.84	7.04 <sup>1</sup>	86.13	118.67 <sup>1</sup>	42.48	66.94 <sup>1</sup>	9.94	7.39 <sup>1</sup>	67.54	64.93 <sup>1</sup>	0	0 <sup>1</sup>
Benchmark Trajectory -5																
21				5	8.78	7.32 <sup>1</sup>	133.37	2226.17 <sup>1</sup>	76.26	128.39 <sup>1</sup>	8.94	7.91 <sup>1</sup>	74.48	66.03 <sup>1</sup>	0	0 <sup>1</sup>
22	182	68.6	17.5	10	8.74	7.26 <sup>1</sup>	133.34	215.48 <sup>1</sup>	76.25	125.73 <sup>1</sup>	8.93	7.88 <sup>1</sup>	74.44	65.95 <sup>1</sup>	0	0 <sup>1</sup>
23				20	8.73	7.19 <sup>1</sup>	133.32	213.62 <sup>1</sup>	76.01	124.54 <sup>1</sup>	8.90	7.76 <sup>1</sup>	74.39	65.82 <sup>1</sup>	0	0 <sup>1</sup>
24				40	8.65	7.09 <sup>1</sup>	133.28	209.36 <sup>1</sup>	75.95	123.89 <sup>1</sup>	8.82	7.69 <sup>1</sup>	74.35	65.62 <sup>1</sup>	0	0 <sup>1</sup>
25				50	8.61	7.03 <sup>1</sup>	133.36	208.97 <sup>1</sup>	76.25	123.28 <sup>1</sup>	8.76	7.42 <sup>1</sup>	74.35	65.54 <sup>1</sup>	0	0 <sup>1</sup>
Benchmark Trajectory -6																
26				5	6.75	4.79 <sup>1</sup>	102.59	178.19 <sup>1</sup>	71.09	142.69 <sup>1</sup>	7.23	5.06 <sup>1</sup>	67.28	55.86 <sup>1</sup>	0	3.1 <sup>1</sup>
27	188	68.6	18	10	6.70	4.63 <sup>1</sup>	102.53	173.50 <sup>1</sup>	71.06	140.72 <sup>1</sup>	7.19	5.01 <sup>1</sup>	67.26	55.29 <sup>1</sup>	0	2.2 <sup>1</sup>
28				20	6.68	4.54 <sup>1</sup>	102.48	170.42 <sup>1</sup>	69.88	132.26 <sup>1</sup>	7.18	4.82 <sup>1</sup>	67.17	55.07 <sup>1</sup>	0	2.2 <sup>1</sup>
29				40	6.63	4.46 <sup>1</sup>	102.45	169.38 <sup>1</sup>	69.83	131.63 <sup>1</sup>	7.05	4.78 <sup>1</sup>	67.13	54.91 <sup>1</sup>	0	2.2 <sup>1</sup>
30				50	6.61	4.32 <sup>1</sup>	102.43	168.74 <sup>1</sup>	69.82	130.91 <sup>1</sup>	7.01	4.71 <sup>1</sup>	67.12	54.86 <sup>1</sup>	0	2.2 <sup>1</sup>

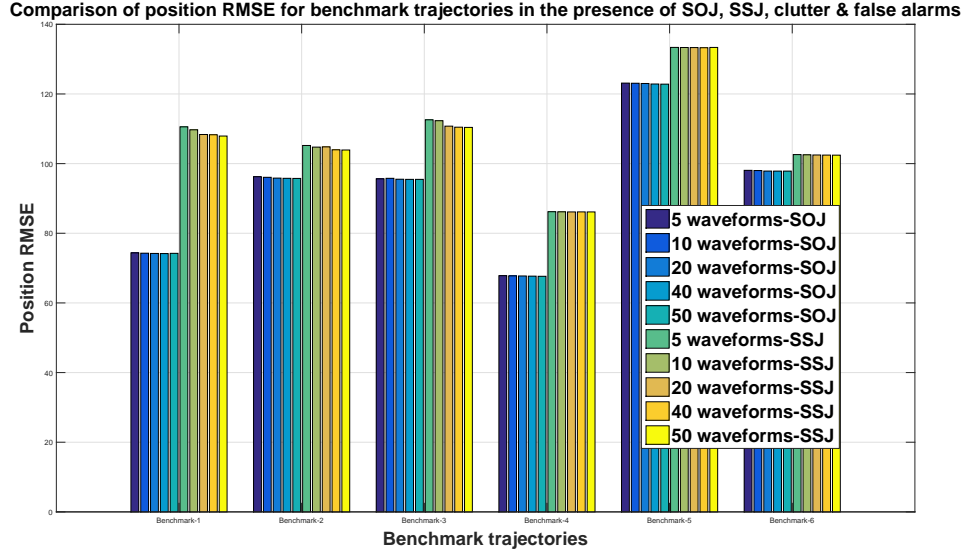


Figure 3.2: Comparison of position RMSE for benchmark trajectories in the presence of SOJ, SSJ, clutter and false alarms

28.11% higher mean average power when compared to results in chapter-2 (Satapathi and Pathipati, 2017). Moreover, the cost function ( $C_1$  &  $C_2$ ) related to radar energy and radar time is higher in a small proportion respectively. However, the track loss for all six benchmark target trajectories are reduced to lower extent except benchmark target trajectory-3 for both scenario-1 and scenario-2. It can also be noticed from Table 3.1 that the position and velocity RMSEs are lower when compared to results in chapter-2 (Satapathi and Pathipati, 2017). This obviously demonstrates that the multidimensional filtering STAP approach has suppressed the clutter and jamming effectively.

Figure 3.2 and Figure 3.3 clearly depicts that the position and velocity RMSEs decreases as the number of waveforms increase from 5 to 50 (Miao et al., 2011). It can also be noticed that position RMSE for all benchmark target trajectories has a mean difference of  $66.01m$  lower for 50 number of waveforms. From Table 3.1, it is evident that the velocity RMSE in present study is lower with a mean difference of  $35.74m/s$  when compared to results obtained in chapter-2 (Satapathi and Pathipati, 2017).

The performance evaluation of IMM-PDAF in the presence of clutter, SSJ and FAs is listed in Table 3.2. For this case (scenario-2) also it can be noticed that the position

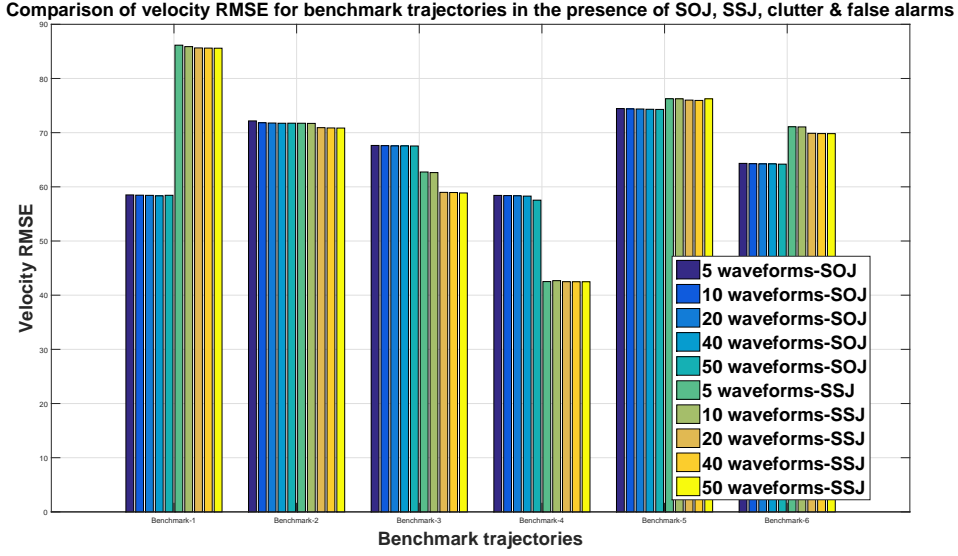


Figure 3.3: Comparison of velocity RMSE for benchmark trajectories in the presence of SOJ, SSJ, clutter and false alarms

and velocity RMSEs for all six benchmark target trajectories reduces with increase in number of waveforms from 5 to 50. The average power for all benchmark target trajectories is higher when compared to results obtained in chapter-2 (Satapathi and Pathipati, 2017). The average track loss for benchmark target trajectories is zero except for benchmark target trajectory-3. Both the cost functions ( $C_1$  &  $C_2$ ) are higher for all benchmark target trajectories compared to results in chapter-2 (Satapathi and Pathipati, 2017).

From Figure 3.2 and Figure 3.3, it can be noticed that the position RMSE and velocity RMSE of SOJ is significantly lower than SSJ for all six benchmark target trajectories. Figures 3.4 to 3.5 illustrates decrease in position RMSE when the number of waveforms are increasing in waveform bank. Moreover, the dotted line in Figures 3.4 to 3.5 depicts the optimal number of waveforms required for both SOJ and SSJ cases respectively. In case of SOJ (scenario-1), the optimal number of waveforms for benchmark target trajectories-2, 3 and 6 is 20. While the optimality for benchmark target trajectories - 1, 4 and 5 for SOJ case is achieved at 5 waveforms. Whereas in case of SSJ (scenario-2), the optimal number of waveforms for benchmark target trajectory -1 and 3 is 20. For benchmark target trajectory -4, 5 and 6 the optimality is attained at 5

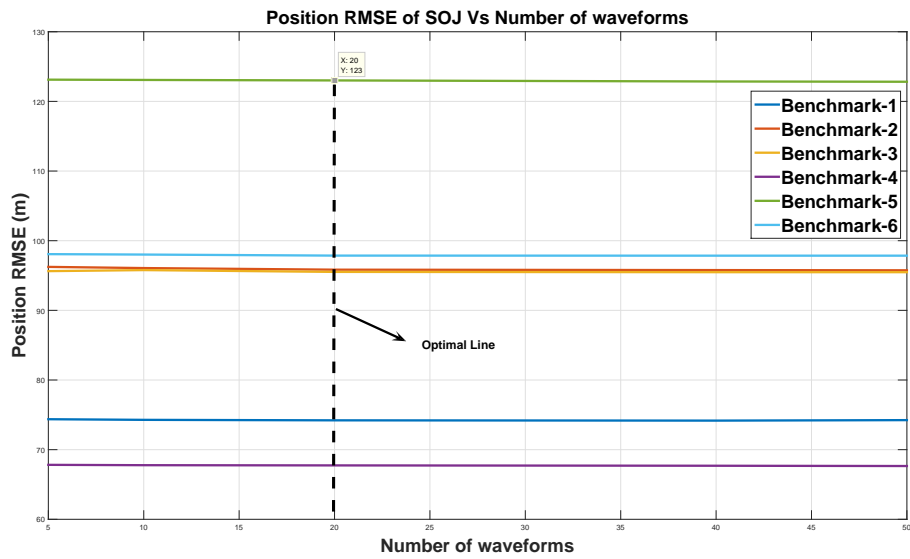


Figure 3.4: Performance of position RMSE Vs number of waveforms for Benchmark Trajectories in the presence of SOJ, clutter, false alarm and multipath

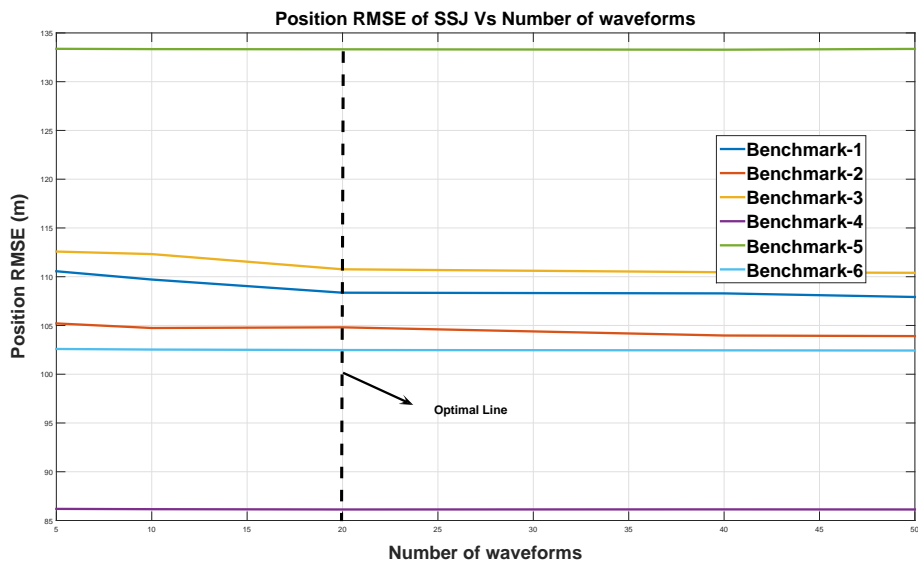


Figure 3.5: Performance of position RMSE Vs number of waveforms for Benchmark Trajectories in the presence of SSJ, clutter, false alarm and multipath

waveforms. However, for benchmark target trajectory -2, in case of SSJ the optimality is obtained for 40 waveforms. For both the scenario-1 and scenario-2 the average optimality is attained at 20 waveforms.

The experimental results reveals that, there is an improvement in radar performance by using STAP based WAS technique in the presence of clutter, ECM and FAs with significant increase in radar cost functions. Hence, there exists a trade off between radar track performance and radar cost functions. Therefore, STAP based approach is an alternative and efficient technique to track highly maneuvering targets in the presence of intense interference.

### **3.5 Conclusion**

This chapter demonstrates alternative and efficient technique for tracking benchmark target trajectories using STAP based WAS approach in the presence of intense interference. The track performance is improved by applying 5 to 50 frequency coded waveforms (LFM) from the waveform bank. IMMPDAF estimator is employed to track highly maneuvering benchmark target trajectories with ECM (SSJ/SOJ), background clutter and FAs. The simulation results reveals that the proposed STAP based WAS technique needs 28.11% higher mean average power when compared to earlier studies (Satapathi and Pathipati, 2017). It can also be noticeable that there is a decrease in both position and velocity RMSE with increase in number of waveforms in waveform bank from 5 to 50 with a significant increase in radar resources. Hence, a novel and alternative algorithm is accomplished to track benchmark target trajectories in the presence of strong interference.

## **CHAPTER 4**

# **SOFT AND EVOLUTIONARY COMPUTATION BASED DATA ASSOCIATION APPROACHES FOR TRACKING MULTIPLE TARGETS IN THE PRESENCE OF ECM**

### **4.1 Introduction**

Previous two chapters dealt with single target tracking problem in the presence of strong interference. In practice there may be multiple targets present in the environment. Hence, to address this problem, two novel soft and evolutionary based data association techniques have been presented. New hybrid data association approaches based on fuzzy particle swarm optimization (Fuzzy-PSO) and fuzzy genetic algorithm (Fuzzy-GA) clustering techniques have been presented as robust methods to overcome local minima problem. The data association matrix is evaluated for all tracks using validated measurements obtained by phased array radar for four different cases applying four data association methods (JPDA, FCM, Fuzzy-PSO, and Fuzzy-GA). The following subsections give detailed explanation of these data association methods.

The proposed data association approaches (Fuzzy-PSO and Fuzzy-GA) are based on stochastic optimized techniques with randomization and local search. The randomization process results in generating arbitrary solutions which helps the local search to find a global solution. Whereas, the global solution in a specific region is achieved by employing metaheuristic approach which is responsible for making convergence. The performance of the proposed approaches is higher when compared to JPDA and FCM with additional computational cost.

## 4.2 Literature survey

The data association problems are classified into two categories: all neighbor and nearest-neighbor data association approaches. Nearest neighbor filter (NNF) and strongest neighbor filter (SNF) techniques are two solutions for nearest neighbor data association approach (Bar-Shalom and Fortmann, 1988; Aziz et al., 1999). Only one valid measurement is used to predict the target track in SNF and NNF. The measurement which is nearest to the predicted target is selected in NNF and the valid measurement with the highest probability is selected in SNF. A brief explanation of nearest neighbor data association technique has been described in (Blackman, 1986; Aziz, 2013).

In all neighbor data association method, all the valid measurements are used to predict next state of the target. Multi-hypothesis, probability data association, joint probability data association etc., uses all neighbor data association technique to update the target state. Multi-hypothesis tracker (MHT) provides an optimal solution for multi-target tracking. The posterior probability in MHT is determined by using Bayes rule under model assumptions in order to obtain optimal solution (Bar-Shalom and Fortmann, 1988; Blackman, 1986). But, implementation of MHT in practical scenario is difficult due to its computational complexity and also information on noise should be known in priori. Due to these reasons, many suboptimal tracking algorithms like probabilistic data association (PDA) and joint probabilistic data association (JPDA) were implemented with less computational complexity (Bar-Shalom and Fortmann, 1988; Bar-Shalom, 1990).

Probabilistic data association technique is used to assign multiple measurements to a single target. Joint probabilistic data association is used to assign multiple measurements to multiple targets (Bar-Shalom and Fortmann, 1988). Both these methods (PDA and JPDA) compute association probability between latest scan validated measurements and target tracks. Further, the estimates are combined based on respective association techniques (Blackman, 1986; Fisher and Casasent, 1989; Zhou and Bose, 1993, 1995). Implementation of JPDA tracking algorithm is simple when compared

to MHT and also it uses all valid measurements to update the next state of the target. Besides, a modified approach using JPDA was suggested to reduce computational complexity in (Zhou and Bose, 1993, 1995). The procedure for calculating association probability for JPDA is briefly explained in (Aziz, 2007; Bar-Shalom and Fortmann, 1988; Bar-Shalom, 2000) assuming the measurements as Gaussian distributed. Interacting multiple model joint probabilistic data association (IMMJPDA) assigns multiple observations to multiple targets and are also capable of tracking targets with maneuvers (Aziz, 2007, 2008; Bar-Shalom et al., 1989). In addition, the performance results of IMMJPDA were comparable to MHT. In another communication, authors reported that expectation maximization technique gave better results when compared to JPDA, but with additional computations (Molnar and Modestino, 1998). The Kalman-levy filter (Sinha et al., 2007), the probability hypothesis density (PHD) filter (Clark and Bell, 2007; Panta et al., 2007), and the inverse gamma distributed texture (Balleri et al., 2007) are among other techniques reported in the literature for multi-target tracking.

Neural network based methods are also used as suboptimal approaches for data association of multi-target tracking (Chung et al., 2007; Perlovsky and Deming, 2007). However, these approaches require a large number of neurons and the training was tedious (Kosko, 1992; Sengupta and Iltis, 1989). Probabilistic weights were replaced by possibility weights by using fuzzy logic for data association for attaining better results. Preliminarily, the possibilistic weights were computed by using fuzzy IF-THEN rules to associate observations to tracks (Osman et al., 1996; Smith III, 1997; Tumala and Midwood, 1998; Singh and Bailey, 1997). A huge number of IF-THEN rules are required for better performance (Singh and Bailey, 1997; Aziz et al., 1999; Aziz, 2007). Many modified fuzzy data association techniques with fuzzy IF-THEN and fuzzy clustering were proposed in (Aziz et al., 1999; Dubois et al., 2005; Gad et al., 2001; Stubberud and Kramer, 2006). The solutions obtained by fuzzy data association were approximate and were further extended to complicated scenarios (Mazor et al., 1998). Simplified fuzzy data association based on fuzzy clustering means (FCM) were presented in (Aziz, 2011, 2013, 2014; Liang-Qun and Wei-Xin, 2014; Aziz, 2015). The number of computations are less when compared to other fuzzy data association tech-

niques (Fisher and Casasent, 1989; Zhou and Bose, 1993). Incorporating clutter and clutter free environment was considered for the above-proposed data association techniques. However, the solutions obtained by fuzzy clustering may fall into local minima.

Soft and evolutionary computing based techniques have been proposed to optimize the distance between cluster center and the data (Izakian and Abraham, 2011). PSO is a stochastic optimization tool designed and inspired by bird flocking (Poli et al., 2007). It is very easy to implement and also used for optimizing numerous optimization problems (Pang et al., 2004; Kennedy et al., 2001). The genetic algorithm is also used extensively for searching and optimizing functions in various engineering domains (Golberg, 1989) and it is based on Darwin's evolution principle. Both, hybrid Fuzzy-PSO and Fuzzy-GA has been applicable to various fields and the results achieved were promising and found to be the best (Yang et al., 2009; Magdalena and Monasterio, 1995; Silva Filho et al., 2015; Izakian and Abraham, 2011).

This chapter presents two novel hybrid evolutionary computing algorithms (PSO and GA) with FCM for data association to track multiple targets in the presence of strong interference. It considers all the validated gate measurements to estimate the next state of the target. The association matrix is determined by using Fuzzy-PSO and Fuzzy-GA clustering algorithms. The approach requires little prior information about the probability distribution of observations, and clutter density. Further, It does not require to calculate all possible data association probabilities like JPDA. On the other hand, FCM based data association techniques are not robust in the presence of high clutter and jamming scenario which results to fall the cluster center in local minima, in turn, produce counterintuitive results.

### **4.3 Problem formulation**

The main objective of this subsection is to describe briefly about the proposed measurement association problem formulation for multi-target tracking. The primary purpose of target tracking is to estimate next state of the target with high accuracy in the pres-

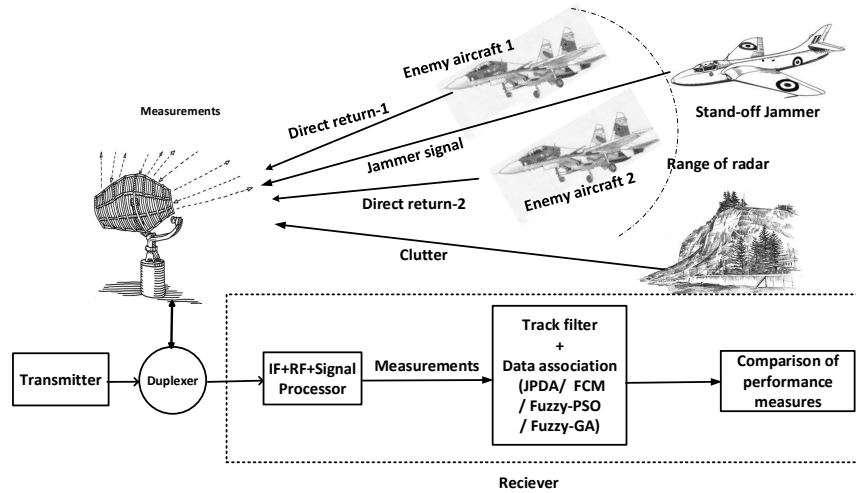


Figure 4.1: Block diagram of a typical multitarget tracking scenario

ence of strong interference. Estimation is correctly done if the measurements from radar echo waveform are associated properly to each individual target. Assuming that the number of targets is known to be  $N_T$  at each scan and number of valid observations that are received from the radar be  $N_V$ . The measurements  $Z_k = \{z_{1,k}, z_{2,k}, \dots, z_{N_V,k}\}$  received at the radar generally includes target return, clutter, false alarms and ECM for  $k^{th}$  scan.

A typical multi-target tracking scenario in the presence of stand of jammer is given in Figure 4.1. A waveform is transmitted through phased array radar with minimum variance distortionless response (MVDR) beamformer to hit the target. The echo which is received at radar receiver is a combination of target returns, jamming signals, and clutter. Intermediate frequency (IF), radio frequency (RF) signal processing techniques are performed to obtain the measurements. An important assumption made in this study is that the closely spaced targets have been ignored. Further, the entire process of multi-target tracking with 900 elements rectangular phased array radar with 10GHz frequency is illustrated in the flowchart of Figure 4.2.

The measurements received at each scan is more likely be greater than the number of targets, if the environment is affected by strong interference (clutter and ECM). There is no prior information related to the tracks associated with measurements that emerge from potential targets and also due to other sources. It is hence, essential to estimate

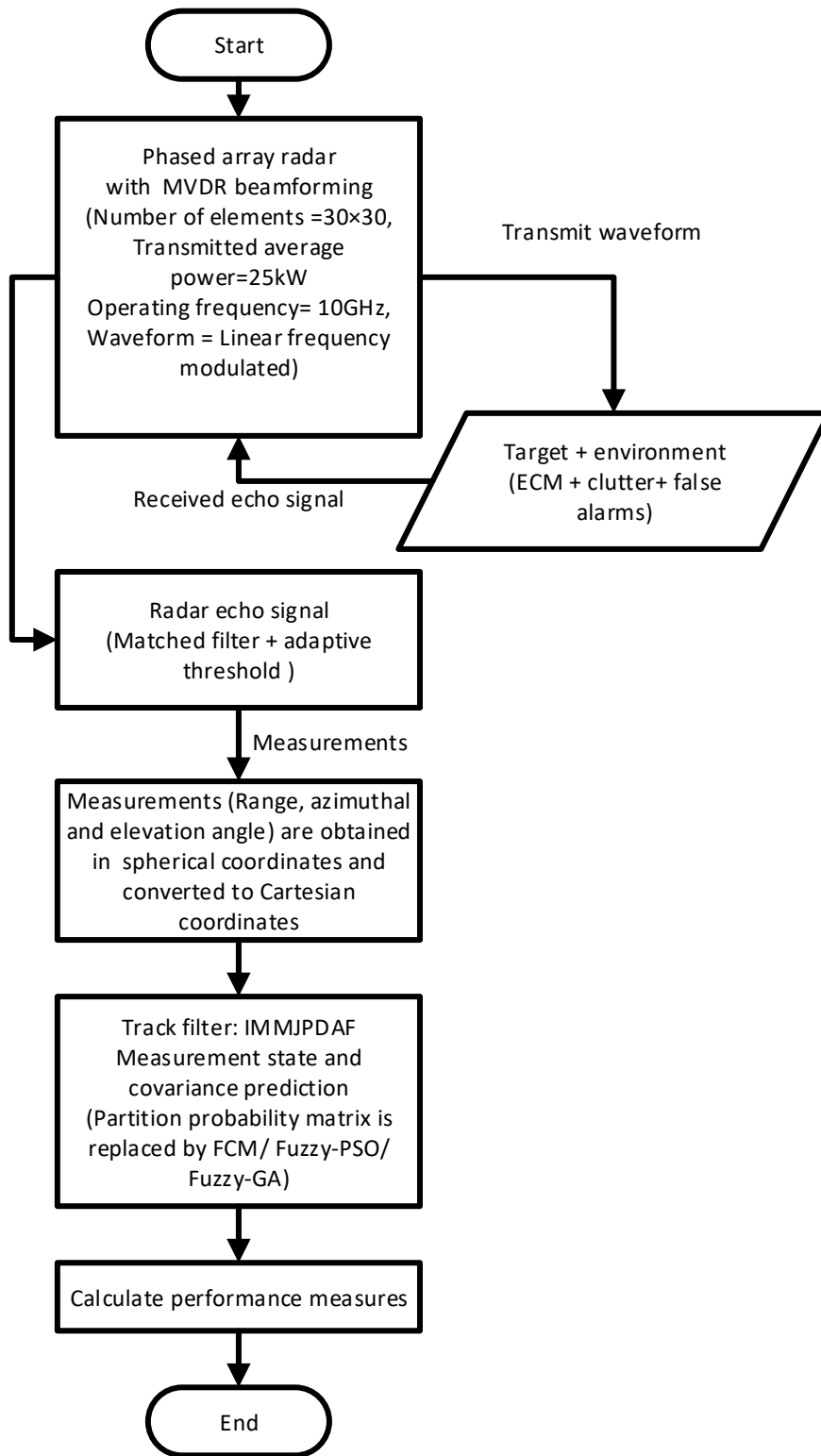


Figure 4.2: Flowchart of entire process

tracks for the targets that are under surveillance, using received measurements. It is a tough task to associate the closely spaced measurements corresponding to two or more targets. The main problem is to estimate the next state of the targets by using received measurements which are highly uncertain.

The dynamic model of  $i^{th}$  target is represented as

$$x_k^i = F^i x_{k-1}^i + v_{k-1}^i, \quad i = 1, 2, \dots, N_T \quad (4.1)$$

Where,  $x_k^i$  is the state vector of  $i^{th}$  target at  $k^{th}$  scan,  $v^i$  is process input noise for  $i^{th}$  target and  $F^i$  is defined as state transition matrix of  $i^{th}$  target.

If the environment is not effected by any clutter or ECM, then the estimation is done by using a simple Kalman filter based on true measurements. The following equations briefly provides the necessary procedure.

Let,  $x_k^i, P_k^i$  be the state vector and covariance matrix for  $i^{th}$  target at  $k^{th}$  scan respectively, then below mentioned Kalman filter equations are used to predict and update the next state of the target (Bar-Shalom, 1987; Blackman, 1986).

$$\hat{x}_{k|k-1}^i = F^i \hat{x}_{k-1|k-1}^i \quad (4.2)$$

$$P_{k|k-1}^i = F^i P_k^i F'^i + Q_k \quad (4.3)$$

$$\hat{x}_{k|k}^i = \hat{x}_{k|k-1}^i + K_k^i \tilde{z}_k^i \quad (4.4)$$

$$P_{k|k}^i = [I - K_k^i H_k^i] P_{k|k-1}^i \quad (4.5)$$

where,  $K$  is the filter gain of the Kalman filter and  $\tilde{z}$  is innovation covariance which is given by

$$K_k^i = P_{k|k-1}^i H_k'^i \left[ H_k^i P_{k|k-1}^i H_k'^i + R_k^i \right]^{-1} \quad (4.6)$$

$$\tilde{z}_k^i = Z_k^i - H_k^i \hat{x}_{k|k-1}^i \quad (4.7)$$

The innovation covariance matrix is given by

$$S_k^i = H_k^i P_{k|k-1}^i H_k^{i'} + R_k^i \quad (4.8)$$

where,  $F$  is state transition matrix with dimension  $n \times n$ ,  $H$  is measurement matrix with dimension  $m \times n$ . The process and measurement noise covariance matrices are represented as  $Q$  and  $R$  respectively. It is assumed that both  $Q$  and  $R$  are Gaussian distributed with zero mean and uncorrelated.

Only a few measurements which are validated from the received observations are used to update the target state. The measurements are validated by using a validation gate, assuming that the measurement is generated from the target source but not due to the clutter of ECM. The joint probability is calculated for the measurements associated with the target tracks in joint probability data association (JPDA) filter. There is a possibility for associating multiple measurements for a single track or a single measurement for multiple tracks. The comprehensive derivation of JPDA filter is described in (Bar-Shalom, 1987; Blackman, 1986). There is a change in only two equations in JPDA when compared to Kalman filter equations, which is presented as follows:

- i. The updated state estimate of target  $i$  is given as:

$$\hat{x}_{k|k}^i = \hat{x}_{k|k-1}^i + K_k^i \sum_{j=1}^{N_V} \beta^{ij} \tilde{z}_k^{ij}, \quad i = 1, 2, \dots, N_T \quad (4.9)$$

Where,  $\tilde{z}^{ij}$  represents residual value of target  $i$  and measurement  $j$ ,  $\beta^{ij}$  represents posterior probability of  $j^{th}$  validated measurement of  $i^{th}$  target.

- ii. The updated covariance matrix is determined as

$$P_{k|k}^i = P_{k|k}^{i0} + dP_{k|k}^i \quad (4.10)$$

where,

$$P_{k|k}^{i0} = \beta^{i0} P_{k|k-1}^i + (1 - \beta^{i0}) [I - K_k^i H_k^i P_{k|k-1}^i] \quad (4.11a)$$

$$dP_{k|k}^i = K_k^i \left[ \sum_{j=1}^{N_V} \beta^{ij} \tilde{z}_k^{ij} \tilde{z}_k^{i'j} - \tilde{z}_k^i \tilde{z}_k^{i'} \right] K_k^{i'} \quad (4.11b)$$

The posterior probability  $\beta^{i0}$  illustrates that zero measurement has been origi-

nated from  $i^{th}$  target. The equations of posterior probability is derived by assuming the observations that follows Gaussian distribution (Bar-Shalom, 1987, 1990; Blackman, 1986).

If the number of targets and validated measurements increase, there is an exponential increase in time to evaluate joint probabilities. Instead of calculating joint probability, techniques were proposed in the literature to use possibility weights (fuzzy clustering) to reduce the processor execution time (Aziz, 2011, 2013). But, the major drawback of FCM is that they may fall in to local minima. Further, results are largely dependent on selecting initial center of clusters.

The primary objective of this chapter is to apply soft and evolutionary computing techniques with FCM to associate uncertain validated measurements to the target tracks to provide enhanced performance. The validated measurements are obtained in the presence of strong interference (ECM, FA, and clutter).

## **4.4 Proposed data association approaches**

This subsection briefly explains about the proposed novel data association approaches Fuzzy-PSO and Fuzzy-GA. The two main steps involved in the proposed methods are given below:

- i. Calculating association weights.
- ii. Computing updated state estimate and covariance matrix.

The following subsections provide a detailed explanation of these two main steps:

### **4.4.1 Calculating association weights**

Let  $N_T$  be the number of targets to be tracked in the presence of ECM, clutter, and false alarms. The number of validated measurements is  $N_V$ , that are obtained by applying validation gate criterion. The valid measurements contain true measurements with more

probability as well as false measurements that occur due to clutter and ECM. Let  $P_{Gi}$  and  $P_{di}$  be the gate probability and detection probability of  $i^{th}$  target respectively. The validation gate of the target denotes the joint event. Validation matrix is obtained by using validation gate criterion (Aziz, 2013, 2011) and is defined as

$$\Omega = [\Omega_{ij}], \quad i = 1, 2, \dots, N_T, j = 0, 1, 2, \dots, N_V \quad (4.12)$$

and

$$\Omega_{ij} = \begin{cases} 1 & \text{If } j^{th} \text{ measurement lies within gate of target } i \\ 0 & \text{otherwise} \end{cases}$$

Case  $j = 0$  depict that none of the measurement is validated. There may be a case that even a single measurement may not lie in validation gate region, so the first column in validation matrix is considered as "1", i.e.  $\Omega_{ij} = 1, i = 1, 2, 3, \dots, N_T, j = 0$ . For example, consider two targets ( $N_T=2$ ) and five measurements ( $N_V=5$ ) that fall in validation gates as shown in Figure 4.3.

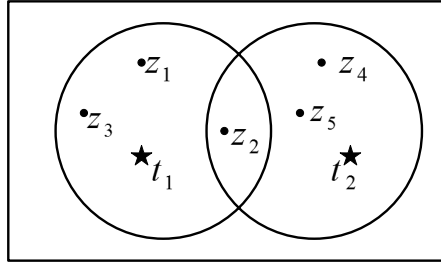


Figure 4.3: Example of two targets and five validated measurements

From Figure 4.3, the measurements  $z_1, z_3$  falls in the validation gate of target-1, i.e. ( $\Omega_{11} = 1, \Omega_{13} = 1$ ) and  $z_4, z_5$  falls in the validation gate of target-2 ( $\Omega_{24} = 1, \Omega_{25} = 1$ ). The measurement  $z_2$  falls in validation gates of both target-1 and target-2 ( $\Omega_{12} = \Omega_{22} = 1$ ).  $\Omega_{10} = 1$  and  $\Omega_{20} = 1$  depicts the case that no measurement is validated for either of the two targets respectively. The validation matrix for Figure 4.3 is given as

$$\Omega_{ij} = \begin{bmatrix} 1 & 1 & 1 & 1 & 0 & 0 \\ 1 & 0 & 1 & 0 & 1 & 1 \end{bmatrix}; i = 1, 2; j = 0, 1, \dots, 5 \quad (4.13)$$

The distance metric  $\delta^{ij}$  between  $j^{th}$  measurement and  $i^{th}$  target is considered as association measure in this approach. The weighted inner product of the innovation vector between  $j^{th}$  measurement and  $i^{th}$  target is considered as association measure which is mentioned as:

$$(d^{ij})^2 = (\tilde{z}^{ij})'(S^i)^{-1}(\tilde{z}^{ij}) = [z^j - \hat{z}^i]'(S^i)^{-1}[z^j - \hat{z}^i] \quad (4.14)$$

Where,  $\tilde{z}^{ij}$  is the difference between observed and predicted measurements and  $S^i$  is innovation covariance calculated by Equation 4.8.

The following rules are defined to calculate distance metric  $\delta^{ij}$  on the basis of validation matrix ( $\Omega$ ):

- i. Considering the fact that validated measurements are more likely to come from target rather than from other unnecessary sources and these valid measurements are directly related to detection probability. The probability of detection ( $P_{di}$ ) and gate probability ( $P_{Gi}$ ) are included in distance metric as shown in Equation 4.15. If ( $P_{di} = P_{Gi} = 1$ ), hence all the measurements from the target echo belongs to the target.
- ii. If  $j \neq 0$ ,  $\Omega_{ij} = 1$ , then  $j^{th}$  measurement belongs to  $i^{th}$  target and distance metric ( $\delta^{ij}$ ) is directly proportional to weighted inner product of the innovation vector between  $j^{th}$  measurement and  $i^{th}$  target. The value  $\lambda^{n_i-1}$  is included in the distance metric ( $\delta^{ij}$ ).  $\lambda^{n_i-1}$  represents that at least one measurement is originated due to target and remaining measurements ( $n_i - 1$ ) are originated due to noise. Where  $n_i$  is the number of validated measurements in gate and  $\lambda$  represents spatial density due to noise.
- iii. if  $j = 0$ ,  $\lambda^{n_i}$  is considered in distance metric which represents that no measurements are validated and all the measurements ( $n_i$ ) are originated due to noise.

Based on the above rules, the distance metric ( $\delta^{ij}$ ) between  $j^{th}$  measurement and  $i^{th}$  target is given as

$$\delta^{ij} = \begin{cases} P_{Gi}P_{di}\lambda^{n_i-1}(d^{ij})^2, & \forall j \neq 0, \Omega_{ij} = 1, i = 1, 2, \dots, N_T \\ \lambda^{n_i}(1 - P_{Gi}P_{di}), & \forall \Omega_{ij} = 0, j = 0, i = 1, 2, \dots, N_T \end{cases} \quad (4.15)$$

The condition  $\Omega_{ij} = 0$  and  $j \neq 0$ , represents that the  $j^{th}$  measurement does not

belong to  $i^{th}$  target. The correlation matrix ( $\psi$ ) which depicts possibility of  $j^{th}$  valid measurements for  $i^{th}$  target is given as:

$$\psi^{ij} = \delta^{ij} = \lambda^{n_i}(1 - P_{Gi}P_{di}), \quad i = 1, 2, \dots, N_T; j = 0 \quad (4.16)$$

and

$$\psi \in [0, 1], 1 \leq i \leq N_T, 1 \leq j \leq N_V \quad (4.17)$$

$$\sum_{i=1}^{N_T} \psi^{ij} = 1, \forall j \neq 0 \quad (4.18)$$

$$0 \leq \sum_{j=1}^{N_V} \psi^{ij} \leq N_T, i = 1, 2, \dots, N_T \quad (4.19)$$

The correlation matrix should satisfy conditions in Equation 4.17, 4.18 and 4.19 respectively.

#### 4.4.1.1 Fuzzy PSO data association

Let the number of particles be  $\kappa$ . Then position of  $\kappa^{th}$  particle is represented as  $X_\kappa$ . The particle position describes the fuzzy relation between validated measurements and number of targets which is given as

$$X = \psi^{ij} = \begin{bmatrix} \psi^{1,1} & \psi^{1,2} & \dots & \psi^{1,N_V} \\ \vdots & \vdots & \ddots & \vdots \\ \psi^{N_T,1} & \psi^{N_T,2} & \dots & \psi^{N_T,N_V} \end{bmatrix}, i = 1, 2, \dots, N_T; j = 1, 2, \dots, N_V \quad (4.20)$$

Where  $\psi^{ij}$  represents the possibility association matrix between  $i^{th}$  target and  $j^{th}$  measurement. The particle velocity ( $V_\kappa$ ) is of size  $N_T \times N_V$ . The velocity and position of  $\kappa^{th}$  are updated using the Equations 4.21a and 4.21b respectively.

$$V_\kappa(t) = \omega V_\kappa(t-1) + C_1 r_1 \otimes (pbest_\kappa(t-1) - X_\kappa(t-1)) + C_2 r_2 \otimes (gbest(t-1) - X_\kappa(t-1)) \quad (4.21a)$$

$$X_\kappa(t) = X_\kappa(t-1) \oplus V_\kappa(t-1) \quad (4.21b)$$

---

**Algorithm 1** Fuzzy-PSO data association

---

- 1: Load the parameters (population size,  $C_1$ ,  $C_2$ ,  $\omega$  and maximum iterative count).
  - 2: Generate swarm with  $\kappa$  particles.
  - 3: Compute partition matrix  $\psi$  (Equation 4.20) by using validation matrix  $\Omega$  (Equation 4.12) for the validated measurements that are obtained from radar. Initialize  $V$ ,  $pbest$  for each particle and  $gbest$  for each swarm.
  - 4: **for all** termination criterion **do**
  - 5:   Calculate the fitness value using Equation 4.23.
  - 6:   Determine  $pbest$  of each particle and  $gbest$  of each swarm.
  - 7:   Update the velocity and position matrix of each particle using Equations 4.21a, 4.21b respectively.
  - 8:   Compute the new fitness value.
  - 9: **end for**
  - 10: The position matrix which gives the best fitness value is considered as the partition matrix and it is normalized according to Equation 4.22.
  - 11: Estimate the next state of the target by using Equation 4.9.
- 

Where  $pbest_\kappa$  represents the best solution obtained by  $\kappa^{th}$  particle and  $gbest$  represents best solution obtained by all the particles.

The position matrix may not follow the rules in Equation 4.17,4.18 and 4.19 after updating. So, the updated position matrix is normalized. All the negative values in updates position matrix are made zero. In a row, if all the elements are zero, then random numbers are generated between interval  $[0,1]$  .

The position matrix is normalized as in (Silva Filho et al., 2015), so as to make the contributions of valid measurements equal to one.

$$\sum_{j=0}^{N_v} \psi_{normalize}^{ij} = 1, \quad i = 1, 2, \dots, N_T \quad (4.22)$$

$\psi_{normalize_k}^{ij}$  represents possibility association of  $j^{th}$  measurement to  $i^{th}$  matrix of particle  $k$ .

The fitness function which is used to calculate generalized solution is given in Equation 4.23:

$$F(x_k) = \frac{K}{J_m} \quad (4.23)$$

The correlation measure is given as:

$$\psi^{ij} = \frac{(1/\delta^{ij})}{\sum_{i=1}^{N_T} (1/\delta^{ij})}; \quad i = 1, 2, \dots, N_T; j = 1, 2, \dots, N_V \quad (4.24)$$

Where ,  $J_m = \sum_{i=1}^{N_T} \sum_{j=1}^{N_V} (\psi^{ij})^2 \delta^{ij}$  is the objective function of FCM and represents sum of squared errors,  $K$  is constant. For good clustering, the value of  $J_m$  should be small and the value of fitness function will be high. The entire Fuzzy-PSO association is as shown in the algorithm 1:

The condition is terminated if there is no further improvement in gbest value.

#### 4.4.1.2 Fuzzy-GA data association

The valid measurements ( $N_V$ ) can be associated to  $N_T$  tracks effectively by using Fuzzy-GA clustering due to its potential in searching. In this method, the following tasks are performed for associating the measurements to tracks.

##### 4.4.1.2.1 Initialization

The sequence of chromosome represents  $N_T$  cluster centers. The length of the chromosome is considered as  $N_T \times N$ . Where,  $N$  represents the dimension of the cluster center. If  $T$  is the population size of the genetic algorithm, then  $T$  chromosomes are generated by applying fuzzy clustering means (FCM) algorithm as described in (Aziz, 2011). The centers which are determined by FCM may fall in local minima. The convergence criterion can be easily detected by comparing the difference in cluster center or membership function at two consecutive iterations.

##### 4.4.1.2.2 Fitness computation

The process of fitness computation includes two steps. In the first step, the validated measurements ( $N_V$ ) are assigned to  $N_T$  cluster tracks according to the information encoded in each chromosome. The assignment of valid measurements ( $z_k$ ),  $k = 1, 2, \dots, N_V$  for each cluster ( $C_j$ ) is done by using the following condition

if  $\|z_k - b_j\| < \|z_k - b_\rho\|$ ;  $j = \rho = 1, 2, \dots, N_T$  and  $\rho \neq j$

In the second step, the cluster centers in each chromosome is updated by the mean value of the individual clusters. The new cluster center ( $b_i^*$ ) for cluster center  $C_i$  is given as

$$b_i^* = \frac{1}{N_{V_i}} \sum_{z_j \in C_i} z_j; \quad i = 1, 2, \dots, N_T \quad (4.25)$$

The new clustering metric ( $D$ ) is calculated as the sum of euclidean distance of each validated measurement from the individual cluster center. Which is given by:

$$D = \sum_{i=1}^{N_T} D_i \quad (4.26)$$

where,

$$D_i = \sum_{z_j \in C_i} \|z_j - b_i\|; \quad j = 1, 2, \dots, N_V \quad (4.27)$$

The fitness function is given as:

$$F = \frac{1}{D} \quad (4.28)$$

In the Equation 4.28, if the fitness value is maximized, then the result leads to minimization of intra clutter distance which is our main objective.

#### 4.4.1.2.3 Selection

Reproduction of new population is done by selecting chromosomes from population  $T$  using roulette wheel selection procedure (Gan et al., 2009) . Each chromosome in the population is assigned a probability based on fitness value. Two chromosomes are selected to produce children by applying roulette wheel selection. For  $T$  chromosomes, the selection probability of each chromosome is assigned as

$$p_j = \frac{F_j}{\sum_{i=1}^T F_i}; \quad j = 1, 2, \dots, T. \quad (4.29)$$

The least probability chromosomes are not considered for producing children.

#### 4.4.1.2.4 Crossover

In the crossover, two parent chromosomes exchange information to produce two new chromosomes (children). In this paper, single point crossover with a fixed crossover probability ( $P_c$ ) is used. If the length of the chromosome is  $L$ , then a random value in the range  $[1, L - 1]$  is generated which is known as a crossover point. The values right to the crossover points are exchanged to produce two children.

#### 4.4.1.2.5 Mutation

Each individual chromosome goes through mutation with a fixed probability ( $P_M$ ). Mutation is performed by just flipping the value from 0 to 1 and vice versa. As we are considering floating point value in this paper, a random number  $r$  is generated within the range  $[0, 1]$  with uniform distribution. If the value of the integer is  $v$  at the gene position. Then, after mutation the values becomes

$$\begin{aligned} v &= v \pm r * v, & v &\neq 0 \\ v &= v \pm r, & v &= 0; \end{aligned} \quad (4.30)$$

The signs (+ & -) are considered with equal probability. If a specific location in all chromosomes become positive or negative then we cannot generate new chromosome with negative or positive value at that specified location. So, we have included a factor ( $\xi$ ) while performing mutation.

$$v = v \pm (r \pm \xi) * v \quad (4.31)$$

where,  $\xi \in (0, 1)$ .

#### 4.4.1.2.6 Termination criterion

Crossover and mutation are performed in a systematic procedure for 100 iterations. The chromosome which gives the best fitness value is considered as the solution. At each iteration, the chromosome that gives the best value is stored i.e, we have applied the process of elitism. Thus, the process of termination of the chromosome gives the best solution. The algorithm has two steps in the individual iteration process. In step-1, the population is generated by using FCM algorithm and in step-2, the Genetic algorithm is applied on the population to do better clustering.

The entire process of Fuzzy-GA data association is briefly described in algorithm 2.

---

**Algorithm 2** Fuzzy-GA data association

---

- 1: Initialize the parameters for crossover rate, initial population, mutation rate and the maximum number of iterations.
  - 2: Compute partition matrix  $\psi$  (Equation 4.20) by using validation matrix  $\Omega$  (Equation 4.12) for the validated measurements that are obtained from radar.
  - 3: **for all** termination criterion **do**
  - 4:   Calculate fitness value using Equation 4.28.
  - 5:   Reproduce new population by using roulette wheel selection procedure.
  - 6:   Perform crossover to produce new chromosome.
  - 7:   Implement mutation.
  - 8:   Calculate the new fitness value.
  - 9: **end for**
  - 10: The chromosome which gives the best fitness value is considered as the partition matrix and it is normalized according to Equation 4.22.
  - 11: Estimate the next state of the target by using Equation 4.9.
- 

#### 4.4.2 Computing updated state estimate and covariance matrix.

After evaluating the association weights, the next important task is to estimate the next state of the target with high accuracy. JPDA is used only for tracking targets which follow a linear path. But, in the case maneuvering targets, interacting multiple model joint data association filter (IMMJPDAF) is applied to track the targets. In IMMJPDAF, multiple Kalman filters are placed in parallel and the state estimate is updated by model probability. IMMJPDAF is briefly elaborated in (Bar-Shalom, 1990; Bar-Shalom et al.,

2004). The partition probability matrix in IMMJPDA is replaced by the possibility matrix which is obtained by FCM, Fuzzy-PSO, Fuzzy-GA and the results have been compared. The following section describes the experimental results in detail for four different cases.

## 4.5 Results and discussion

This section furnishes results and discussions obtained by considering four case studies (linear crossing targets, parallel targets, linear and non-linear crossing targets, and non-linear crossing targets) to evaluate the performance of the proposed hybrid data association techniques. The results achieved in each case study are compared with existing techniques, such as JPDA and FCM. The measurements are obtained by using rectangular phased array radar with 900 elements. where, Linear frequency modulated (LFM) waveform is considered for transmission by the radar at operating frequency of 10 GHz. Assuming a barrage jammer is present beyond cross over range of the radar and emits jammer power towards the radar main lobe (Mahafza and Elsherbeni, 2003). Here, clutter is induced in the environment by a constant gamma clutter model (Barton, 1985). The target returns that are obtained from radar are affected with ECM, clutter and false alarms (strong interference). Signal processing techniques like adaptive beamforming (minimum variance distortionless response (MVDR)) and adaptive thresholding (cell averaging constant false alarm rate (CA-CFAR)) are applied to reduce the jamming effect, clutter and false alarms (FA).

The state vector ( $x_k$ ) is taken as two-dimensional (position and velocity) vector with respect to x and y directions i.e.

$$x_k = [X_k; V_{x,k}; Y_k; V_{y,k}] \quad (4.32)$$

where  $X_k, Y_k$  represents position with given velocities  $V_{x,k}, V_{y,k}$  in x and y directions at  $k^{th}$  scan, respectively. The observations are received from radar and are validated by using validation gate criterion (Bar-Shalom, 1990; Aziz, 2013, 2011). The validated

observations at  $k^{th}$  scan are represented as

$$Z_k = \{z_{1,k}, z_{2,k}, \dots, z_{N_V,k}\} \quad (4.33)$$

The three state transition matrices which are used in IMM model are given by

$$F^1 = \begin{bmatrix} 1 & \Delta T & 0 & 0 \\ 0 & 1 & 0 & 0 \\ 0 & 0 & 1 & \Delta T \\ 0 & 0 & 0 & 1 \end{bmatrix} \quad (4.34a)$$

$$F^2 = \begin{bmatrix} 1 & \sin(w_2 * \Delta T)/w_2 & 0 & (\cos(w_2 * \Delta T) - 1)/w_2 \\ 0 & \cos(w_2 * \Delta T) & 0 & \sin(w_2 * \Delta T) \\ 0 & (1 - \cos(w_2 * \Delta T))/w_2 & 1 & \sin(w_2 * \Delta T)/w_2 \\ 0 & -\sin(w_2 * \Delta T) & 0 & \cos(w_2 * \Delta T) \end{bmatrix} \quad (4.34b)$$

$$F^3 = \begin{bmatrix} 1 & \sin(w_3 * \Delta T)/w_3 & 0 & (\cos(w_3 * \Delta T) - 1)/w_3 \\ 0 & \cos(w_3 * \Delta T) & 0 & \sin(w_3 * \Delta T) \\ 0 & (1 - \cos(w_3 * \Delta T))/w_3 & 1 & \sin(w_3 * \Delta T)/w_3 \\ 0 & -\sin(w_3 * \Delta T) & 0 & \cos(w_3 * \Delta T) \end{bmatrix} \quad (4.34c)$$

Where,  $\Delta T$  is the sampling interval. The measurement matrix (H) is given by

$$H = \begin{bmatrix} 1 & 0 & 0 & 0 \\ 0 & 0 & 1 & 0 \end{bmatrix} \quad (4.35)$$

The measurement noise covariance matrix (R) is represented as

$$R = \begin{bmatrix} \sigma_x^2 & 0 \\ 0 & \sigma_y^2 \end{bmatrix} \quad (4.36)$$

where,  $\sigma_x$  and  $\sigma_y$  are standard deviations of measurement noise in  $x$  and  $y$  directions respectively. These standard deviations are modeled as the Gaussian distribution with zero mean.

The process noise covariance matrix (Q) is given by

$$Q = a^2 \cdot \Delta T \begin{bmatrix} \Delta T^3/3 & \Delta T^2/2 & 0 & 0 \\ \Delta T^2/2 & \Delta T & 0 & 0 \\ 0 & 0 & \Delta T^3/3 & \Delta T^2/2 \\ 0 & 0 & \Delta T^2/2 & \Delta T \end{bmatrix} \quad (4.37)$$

where,  $a$  is acceleration and briefly about process noise covariance matrix is de-

scribed in (Aziz, 2007; Bar-Shalom et al., 2004).

The population size in PSO is taken as 25 and the learning constants are selected as  $C_1 = C_2 = 1.46$ . The population size in GA is chosen as 25. The crossover and mutation percentage in GA are considered as 0.8 and 0.3 respectively. A Comparison is made between JPDA with Mahalanobis distance, fuzzy clustering means, Fuzzy-PSO and Fuzzy-GA data associations for the following four cases. All the data association algorithms are compared in terms of position and velocity root mean square value (Table 4.2 & Table 4.3). The results are validated for 100 Monte Carlo runs.

#### 4.5.1 Linear crossing targets

In this case, two crossing linear targets are considered. The initial positions of target-1 and target-2 are  $(25000, 210) m$  and  $(5000, 210) m$  respectively. Both travel with a constant velocity of  $50 m/s$ . The detection probability is assumed to be 1 and the sampling interval is considered as  $1 s$ . The standard deviation of noise covariance matrix for target-1 is taken as  $\sigma_{x1} = \sigma_{y1} = 100m$  and while for target-2 is taken as  $\sigma_{x2} = \sigma_{y2} = 105m$ . Figures 4.4, 4.5, 4.6 and 4.7 exhibits the estimates of target in case of JPDA, FCM, Fuzzy-PSO and Fuzzy-GA data association techniques respectively. Figures 4.8 and 4.9 shows the comparison of position and velocity RMSE for different jammer power levels against different data association techniques. Also, Figures 4.8 and 4.9 clearly depicts that there is an increase in position and velocity RMSE values with increase in jammer power levels. Both these RMSE values for Fuzzy-GA is less when compared to other data association techniques. Further, in this case, the average position RMSE for target-1 with Fuzzy-GA approach is 49.13%, 39.30% and 21.85% less when compared to JPDA, FCM and Fuzzy-PSO techniques respectively. Besides that, the average position RMSE for target-2 with Fuzzy-GA approach is 45.71%, 32.33% and 7.976% less, when compared to JPDA, FCM, and Fuzzy-PSO techniques respectively. In addition, The average velocity RMSE for target-1 with Fuzzy-GA approach is 36.79%, 34.47% and 27.62% less when compared to JPDA, FCM, and Fuzzy-PSO techniques respectively. Whereas, the average velocity RMSE

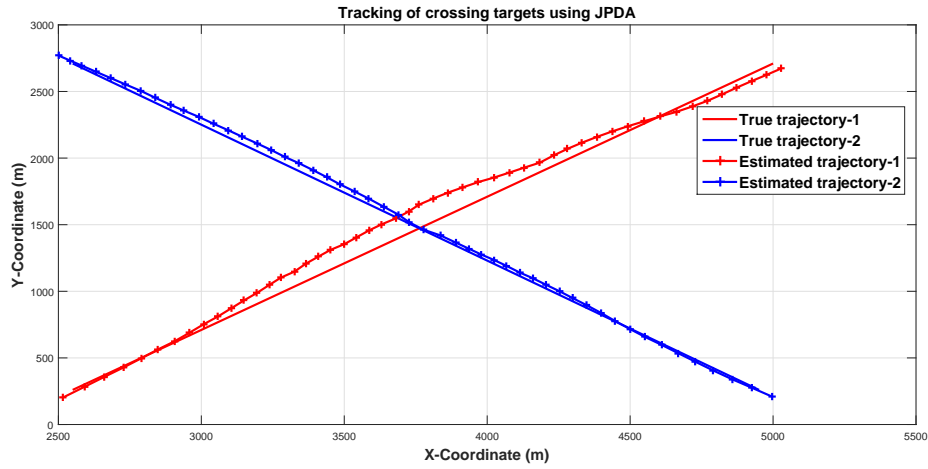


Figure 4.4: True and estimated trajectory by using JPDA

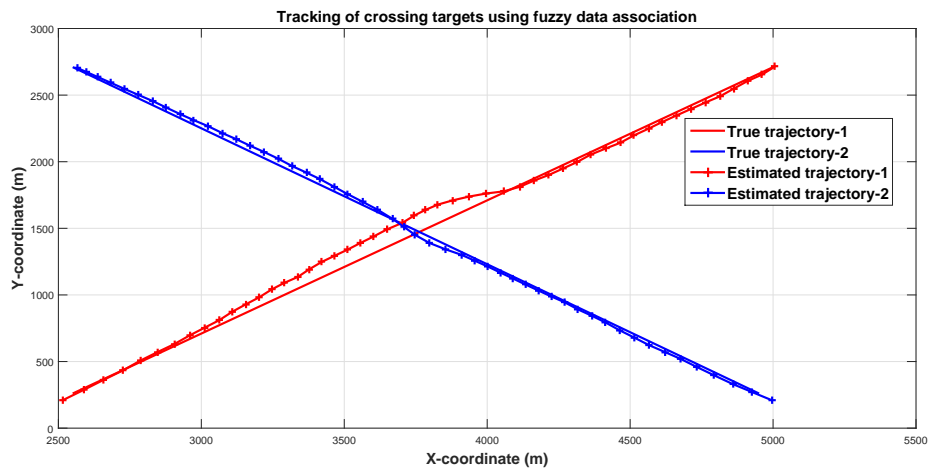


Figure 4.5: True and estimated trajectory by using fuzzy data association

for target-2 with Fuzzy-GA approach is 4.58%, 16.24% and 7.14% less when compared to JPDA, FCM, and Fuzzy-PSO techniques respectively. Therefore, these results indicate that Fuzzy-GA based hybrid data association approach is performing better in terms of both position and velocity RMSE values.

## 4.5.2 Parallel targets

In this scenario, The target-1 position, velocity and sampling interval taken as in Sub-section 4.5.1, the only change, in this case, is target-2 initial position is (3000,210) *m*.

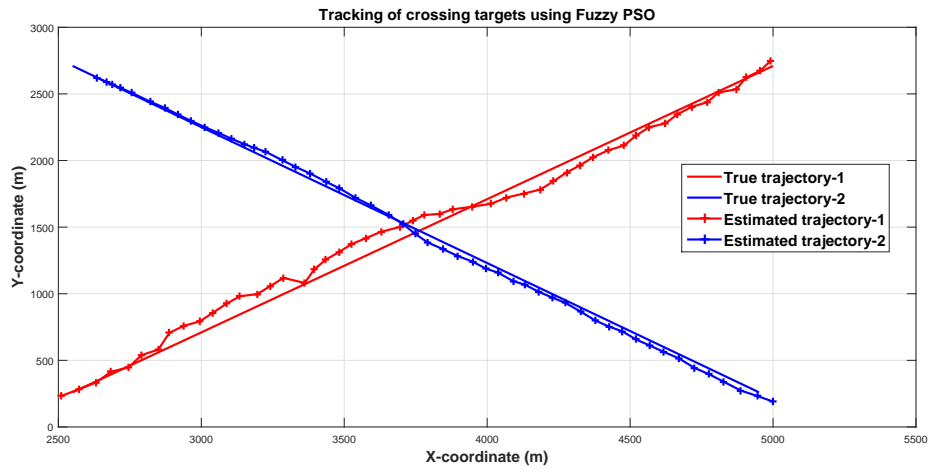


Figure 4.6: True and estimated trajectory by using Fuzzy-PSO

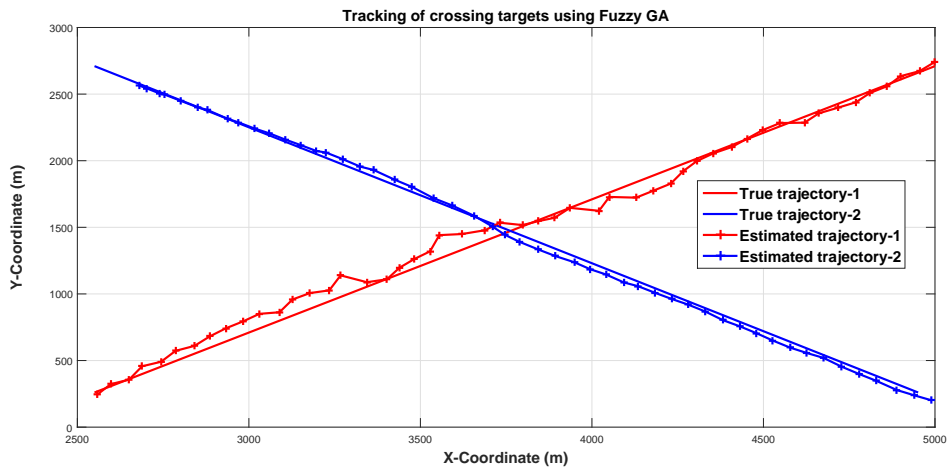


Figure 4.7: True and estimated trajectory by using Fuzzy-GA

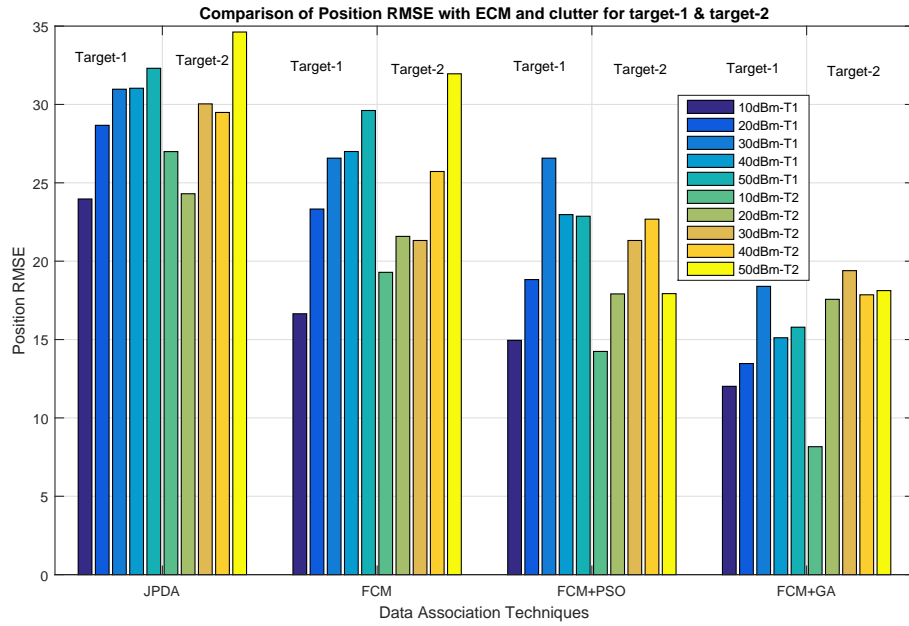


Figure 4.8: Comparison performance of position RMSE of two crossing targets  $T1 \rightarrow Target - 1, T2 \rightarrow Target - 2$

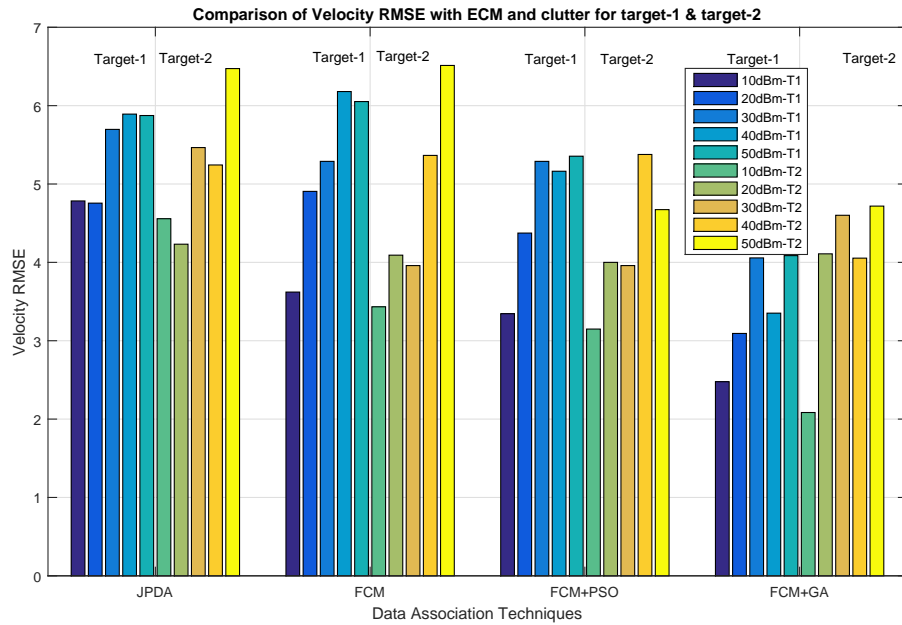


Figure 4.9: Comparison performance of velocity RMSE of two crossing targets  $T1 \rightarrow Target - 1, T2 \rightarrow Target - 2$

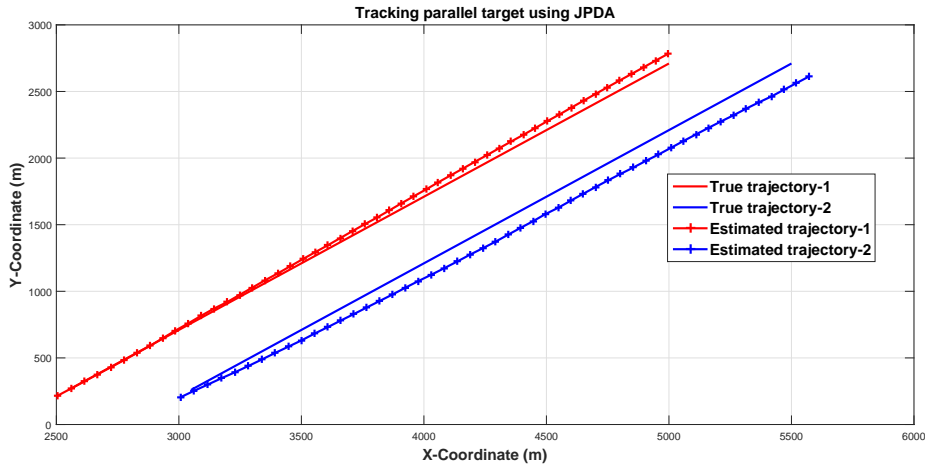


Figure 4.10: True and estimated trajectory by using JPDA

The standard deviation of noise covariance matrix for target-1 is taken as  $\sigma_{x1} = \sigma_{y1} = 100m$  and while for target-2 is taken as  $\sigma_{x2} = \sigma_{y2} = 105m$ . Figures 4.10, 4.11, 4.12 and 4.13 exhibits the estimates of target in case of JPDA, FCM, Fuzzy-PSO and Fuzzy-GA data association techniques respectively. Figures 4.14 and 4.15 shows the comparison of position and velocity RMSE for different jammer power levels against different data association techniques. Figures 4.14 and 4.15 clearly depicts that if the jammer power is increased, then there will also be an increase in position and velocity RMSE values. Both the RMSE values for Fuzzy-GA is less when compared to other data association techniques. For parallel targets, the average position RMSE for target-1 with Fuzzy-GA approach is 27.91%, 19.07% and 7.062% less when compared to JPDA, FCM and Fuzzy-PSO techniques respectively. Whereas, the average position RMSE for target-2 with Fuzzy-GA approach is 27.05%, 12.46% and 6.59% less when compared to JPDA, FCM, and Fuzzy-PSO techniques respectively. The average velocity RMSE for target-1 with Fuzzy-GA approach is 61.47%, 35.61% and 4.93% less when compared to JPDA, FCM and Fuzzy-PSO techniques respectively. Whereas, the average velocity RMSE for target-2 with Fuzzy-GA approach is 58.99%, 51.71% and 9.12% less when compared to JPDA, FCM, and Fuzzy-PSO techniques respectively.

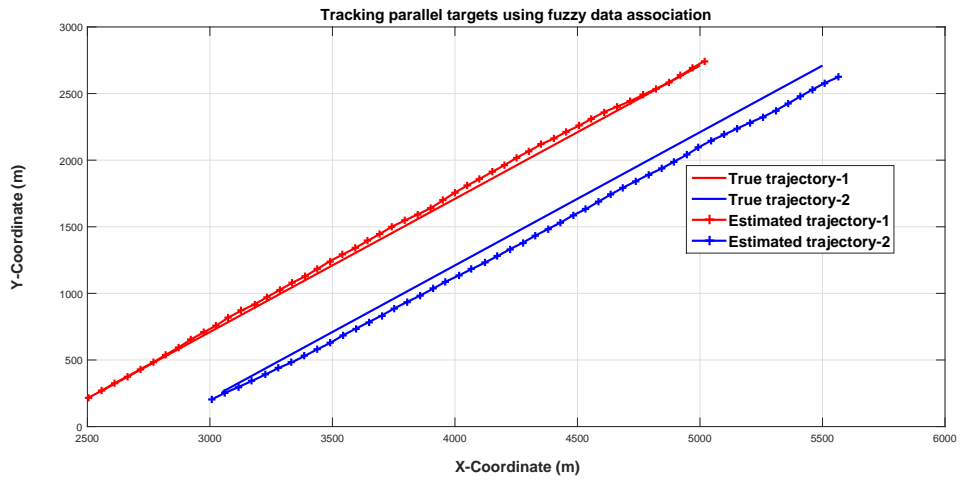


Figure 4.11: True and estimated trajectory by using fuzzy data association

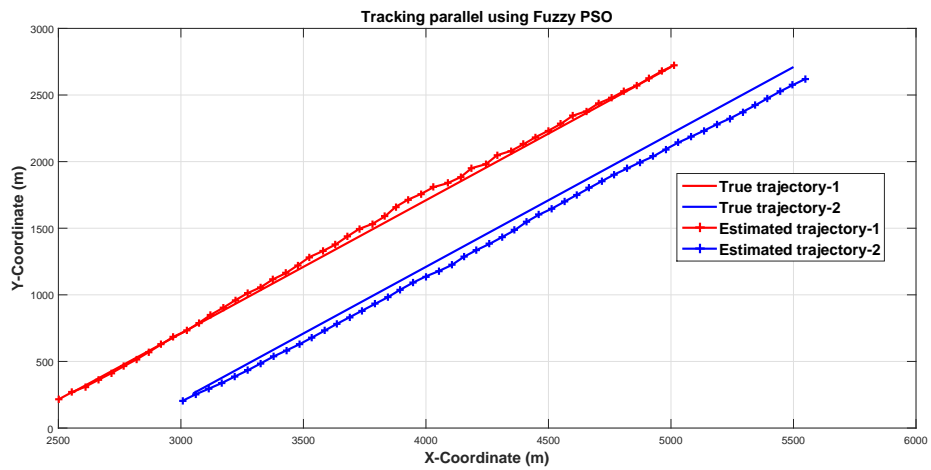


Figure 4.12: True and estimated trajectory by using Fuzzy-PSO

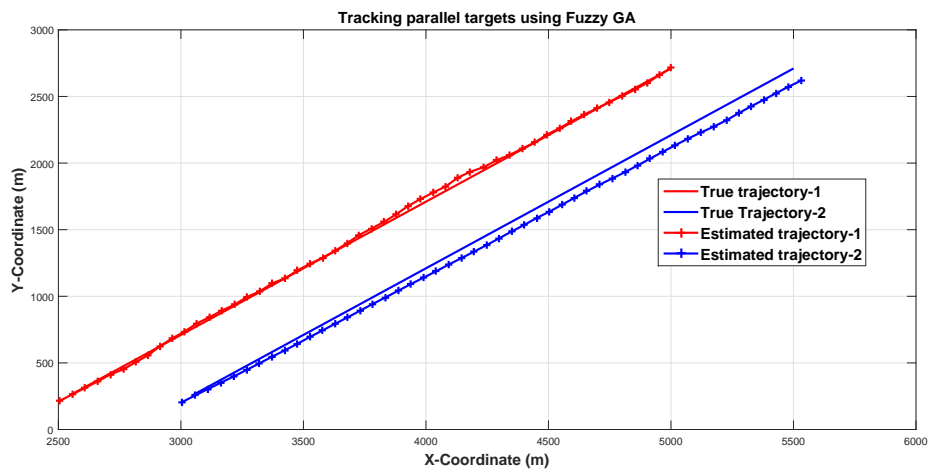


Figure 4.13: True and estimated trajectory by using Fuzzy-GA

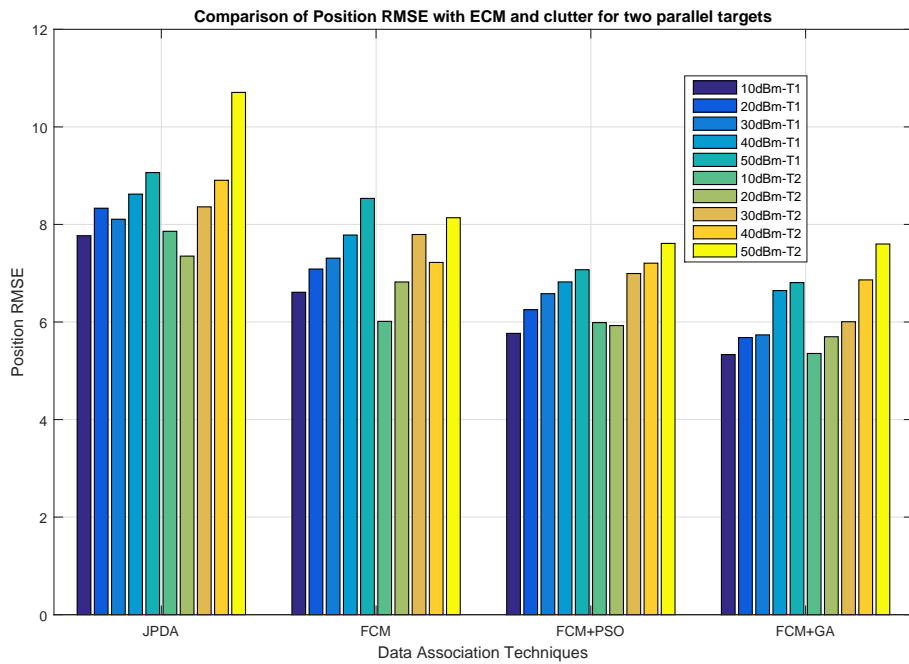


Figure 4.14: Comparison performance of Position RMSE of two Parallel targets  $T1 \rightarrow Target - 1, T2 \rightarrow Target - 2$

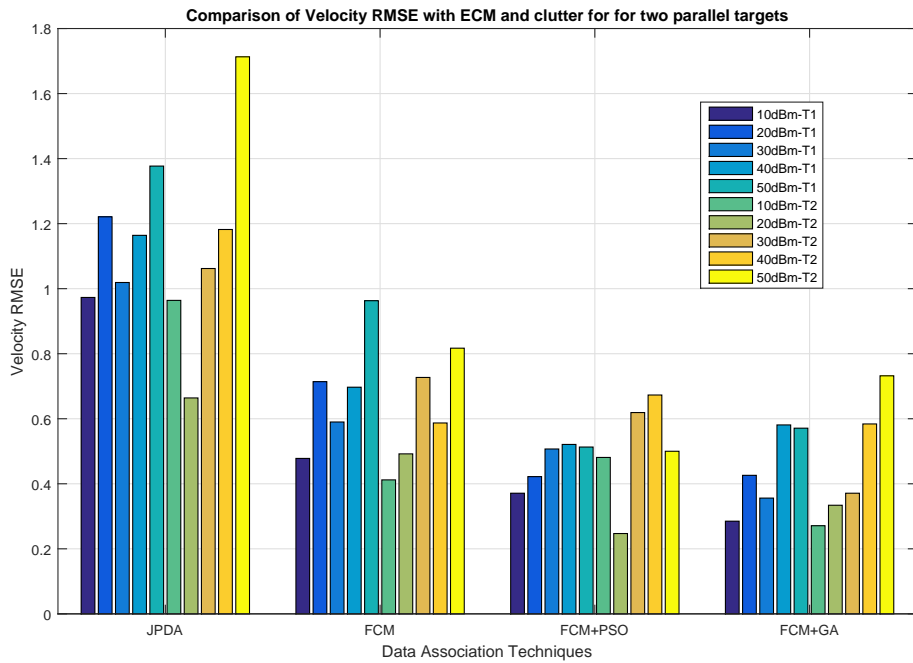


Figure 4.15: Comparison performance of velocity RMSE of two Parallel targets  $T1 \rightarrow Target - 1, T2 \rightarrow Target - 2$

### 4.5.3 Maneuvering and linear crossing targets

A linear and a maneuvering crossing targets are considered for the case-3 study. Benchmark trajectory-2 (Kirubarajan et al., 1998) in two dimensions is considered as maneuvering target. The second target moves in linear trajectory with a velocity of  $70 \text{ m/s}$ . Both the trajectories are simulated for  $150\text{s}$ . The standard deviation of noise covariance matrix for both the targets is taken as  $\sigma_{x1} = \sigma_{y1} = \sigma_{x2} = \sigma_{y2} = 0.1\text{m}$ . Figures 4.16, 4.17, 4.18 and 4.19 exhibits the estimates of target in case of JPDA, FCM, Fuzzy-PSO and Fuzzy-GA data association techniques. Figures 4.20 and 4.21 shows the comparison of position and velocity RMSE for different jammer power levels against different data association techniques. Figures 4.20 and 4.21 clearly depicts that if the jammer power is increased, then there will also be an increase in position and velocity RMSE values. Both the RMSE values for Fuzzy-GA is less when compared to other data association techniques. For case-3, the average position RMSE for target-1 with Fuzzy-GA approach is 0.15%, 1.20% and 2.66% less when compared to JPDA, FCM and Fuzzy-PSO techniques respectively. Whereas, the average position RMSE for target-2 with Fuzzy-GA approach is 2.02%, 1.37% and 0.97% less when compared to JPDA, FCM, and Fuzzy-PSO techniques respectively. The average velocity RMSE for target-1 with Fuzzy-GA approach is 3.71%, 0.904% and 2.457% less when compared to JPDA, FCM and Fuzzy-PSO techniques respectively. Whereas, the average velocity RMSE for target-2 with Fuzzy-GA approach is 1.53%, 0.86% and -2.32% less when compared to JPDA, FCM, and Fuzzy-PSO techniques respectively.

### 4.5.4 Maneuvering crossing targets

Two maneuvering crossing target trajectories are taken for case-4 study. Benchmark trajectory-2 in two dimensions is considered as one of the maneuvering target trajectories. The second trajectory is a random trajectory with  $3g$  and  $-3g$  turn. Both the trajectories are simulated up to  $150\text{s}$ . The standard deviation of noise covariance matrix for both the targets is taken as  $\sigma_{x1} = \sigma_{y1} = \sigma_{x2} = \sigma_{y2} = 3.162\text{m}$ . Figures 4.22, 4.23,

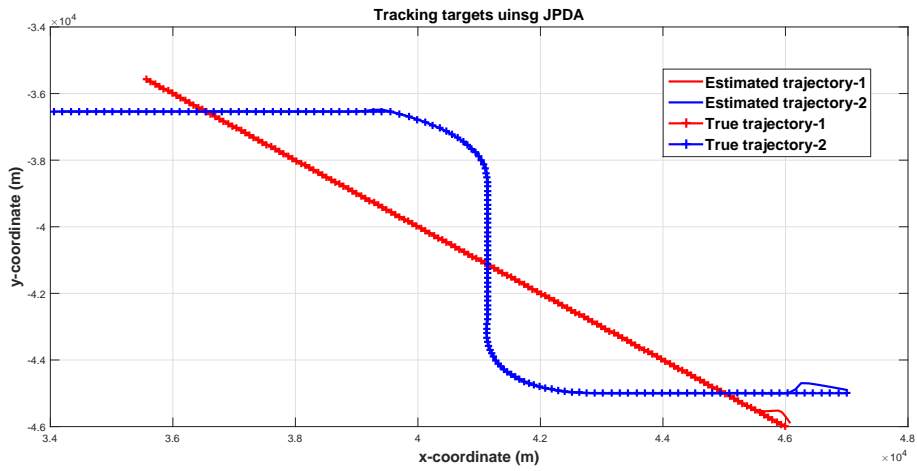


Figure 4.16: True and estimated trajectory by using JPDA

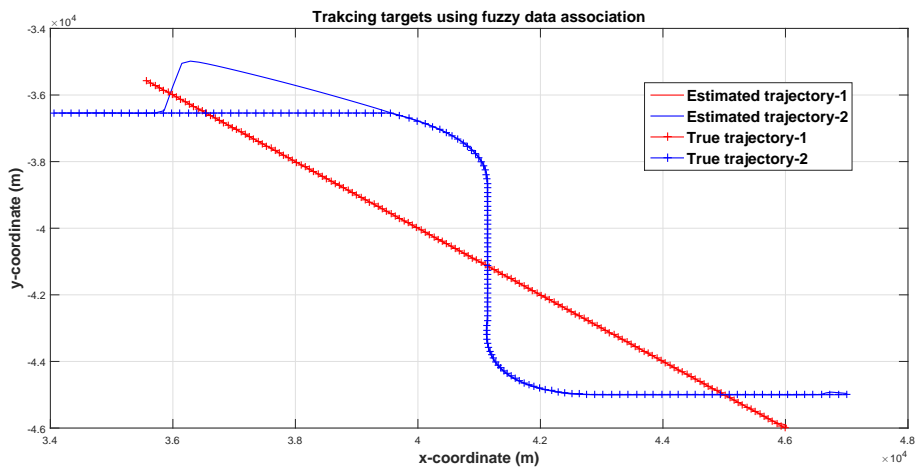


Figure 4.17: True and estimated trajectory by using fuzzy data association

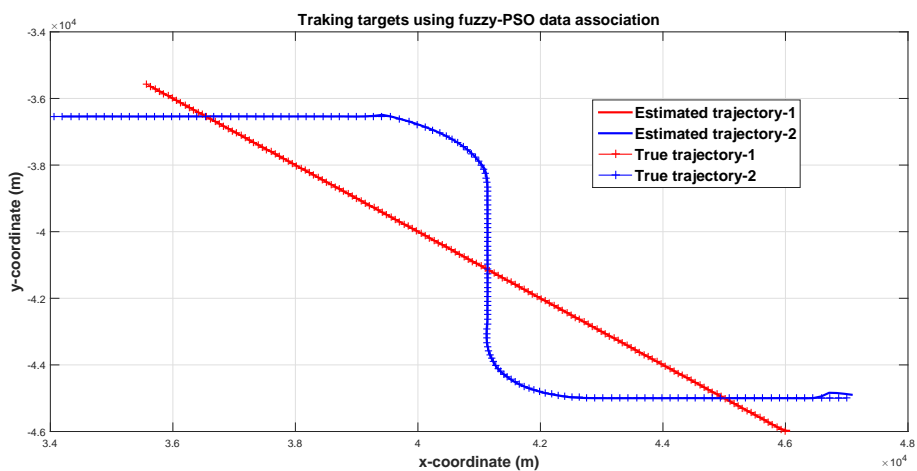


Figure 4.18: True and estimated trajectory by using Fuzzy-PSO data association

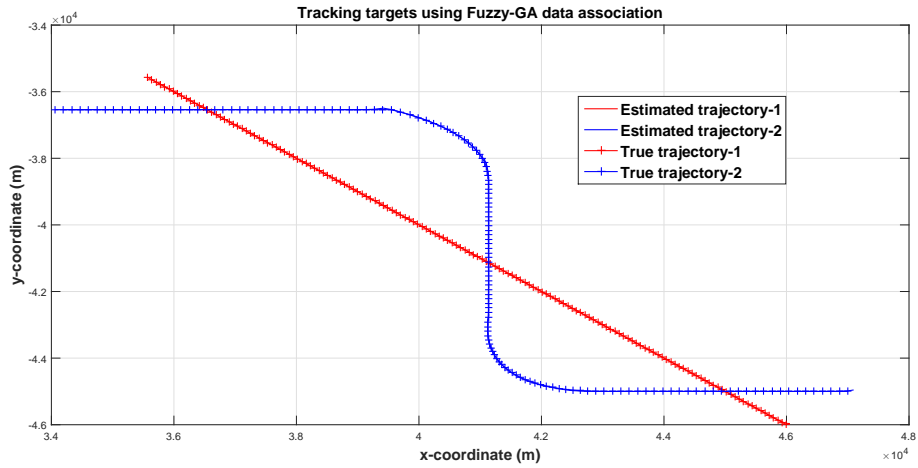


Figure 4.19: True and estimated trajectory by using Fuzzy-GA data association

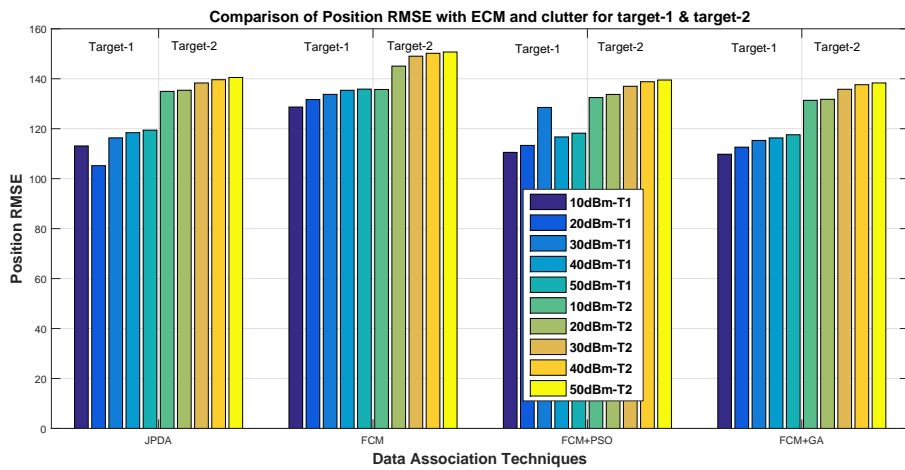


Figure 4.20: Comparison performance of Position RMSE of two targets  $T1 \rightarrow$  Target - 1,  $T2 \rightarrow$  Target - 2

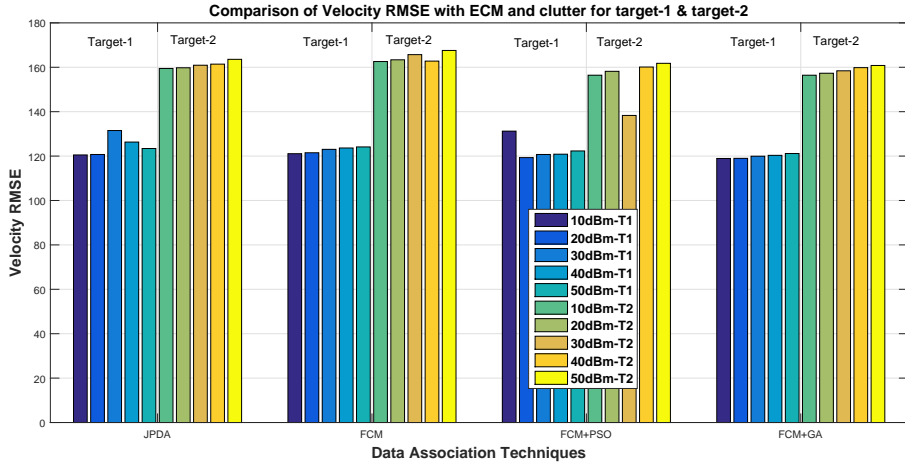


Figure 4.21: Comparison performance of Velocity RMSE of two targets  $T1 \rightarrow Target - 1, T2 \rightarrow Target - 2$

4.24 and 4.25 exhibits the estimates of target in case of JPDA, FCM, Fuzzy-PSO and Fuzzy-GA data association techniques. Figures 4.26 and 4.27 shows the comparison of position and velocity RMSE for different jammer power levels against different data association techniques. Figures 4.26 and 4.27 clearly depicts that if the jammer power is increased, then there will also be an increase in position and velocity RMSE values. Both the RMSE values for Fuzzy-GA is less when compared to other data association techniques. For maneuvering crossing targets, the average position RMSE for target-1 with Fuzzy-GA approach is 1.30%, 0.88% and 0.44% less when compared to JPDA, FCM and Fuzzy-PSO techniques respectively. Whereas, the average position RMSE for target-2 with Fuzzy-GA approach is 1.57%, 0.82% and 0.55% less when compared to JPDA, FCM, and Fuzzy-PSO techniques respectively. The average velocity RMSE for target-1 with Fuzzy-GA approach is 6.34%, 4.22% and 1.488% less when compared to JPDA, FCM and Fuzzy-PSO techniques respectively. Whereas, the average velocity RMSE for target-2 with Fuzzy-GA approach is 4.26%, 3.45% and 1.76% less when compared to JPDA, FCM, and Fuzzy-PSO techniques respectively.

It is evident from the experimental results from all the four cases that proposed methods Fuzzy-GA and Fuzzy-PSO provides improved association, position RMSE, and velocity RMSE compared to all other existing methods. However, the computational complexity of the proposed methods are higher when compared with FCM, but

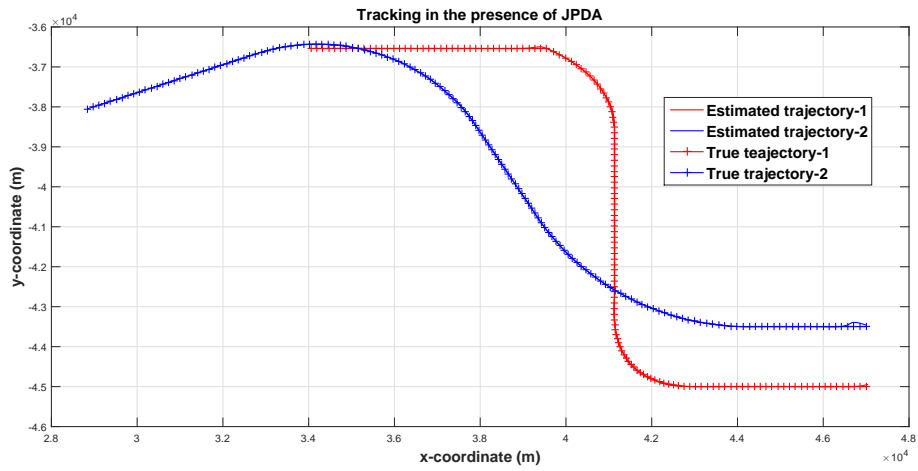


Figure 4.22: True and estimated trajectory by using JPDA

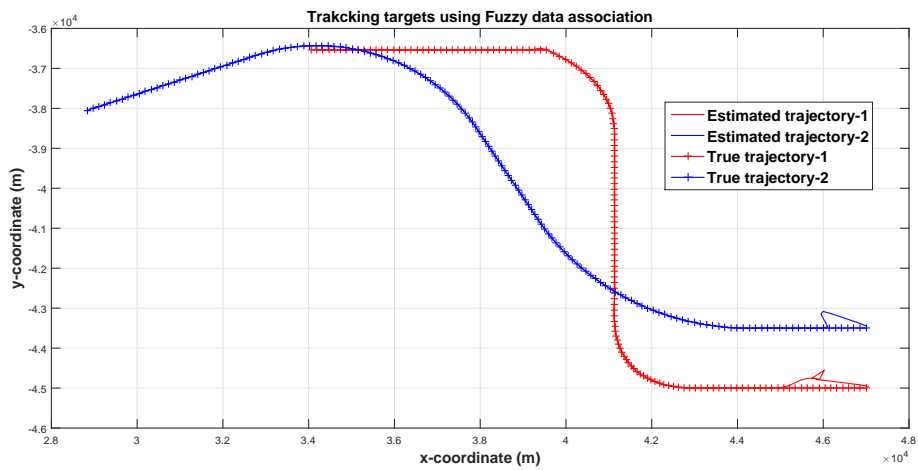


Figure 4.23: True and estimated trajectory by using fuzzy data association

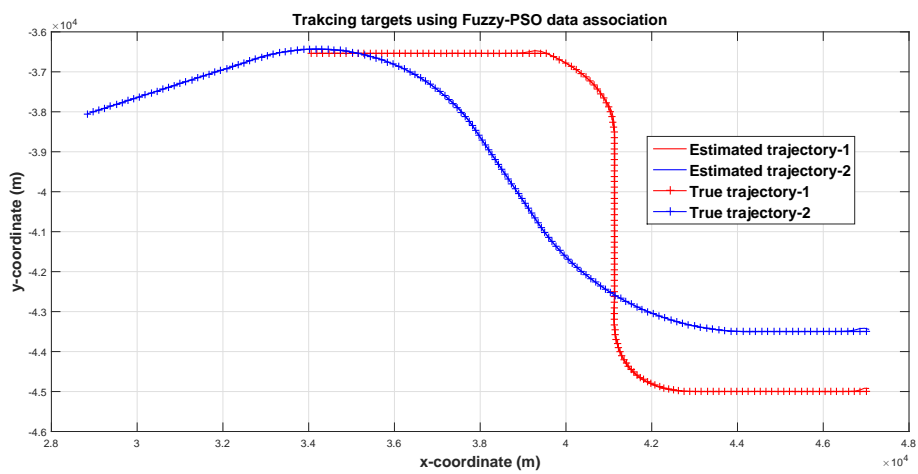


Figure 4.24: True and estimated trajectory by using Fuzzy-PSO data association

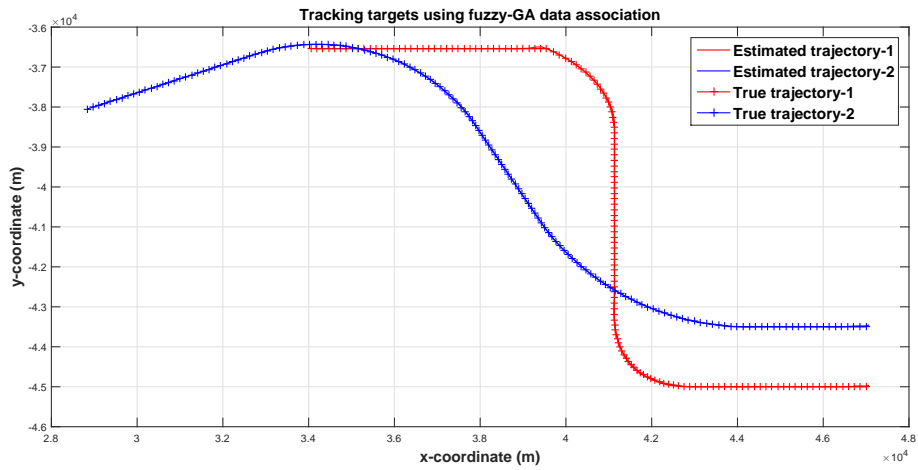


Figure 4.25: True and estimated trajectory by using Fuzzy-GA data association

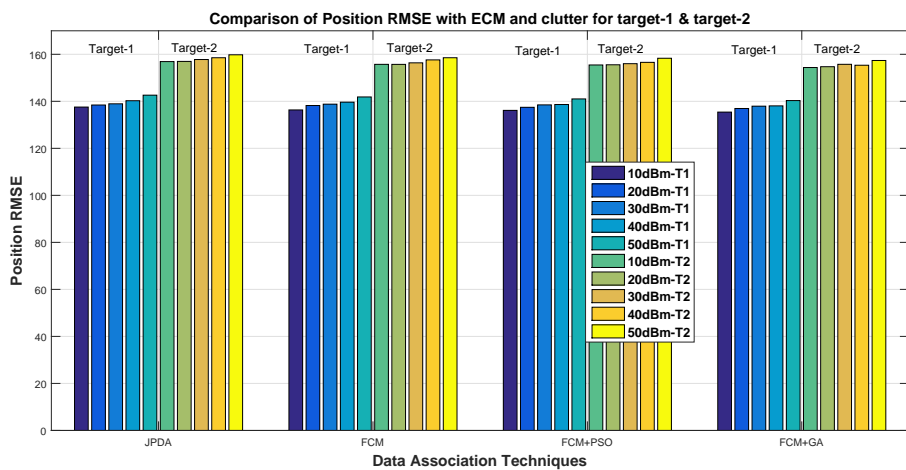


Figure 4.26: Comparison performance of Position RMSE of two targets  $T1 \rightarrow$  Target - 1,  $T2 \rightarrow$  Target - 2

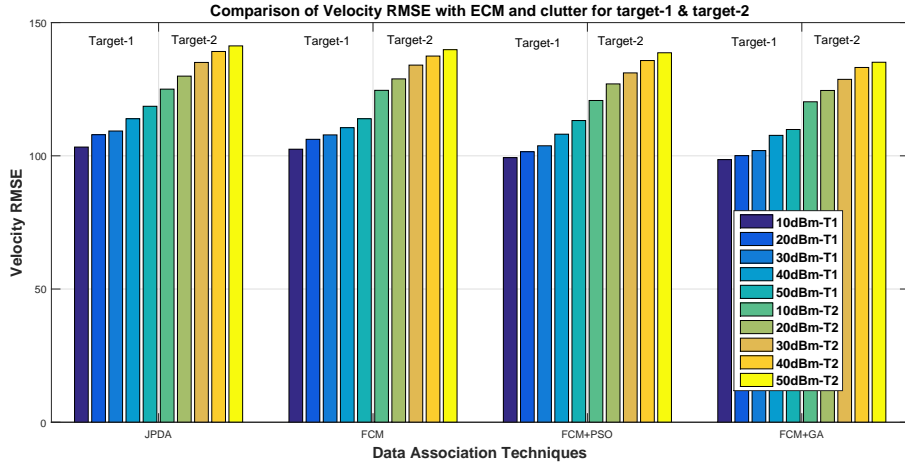


Figure 4.27: Comparison performance of Velocity RMSE of two targets  $T1 \rightarrow Target - 1, T2 \rightarrow Target - 2$

provides enhanced performance when compared to JPDA.

Further, it is observed from Figure 4.17 (for case 3) FCM method is falling into local minima, thus increasing the association error, resulting to large mismatch between the actual and estimated track. On the other hand, it is apparent from Figures 4.18 and 4.19 (for case 3) the proposed methods provides superior performance in terms of association, thus resulting in accurate track performance. Therefore, proposed methods demonstrate enhanced track performance with reasonable computational requirements.

One can carry out future research work in multiple target tracking by deploying multi-objective evolutionary computing techniques such as multi-objective particle swarm optimization (MOPSO), nondominated sorting genetic algorithm II (NSGA-II), etc. to simultaneously optimize track performance and computational complexity. Furthermore, the current research study is carried out by using fixed linear frequency modulated (LFM) waveform. Future researchers can carry out further work by using adaptive waveform selection, waveform agile sensing, adaptive pulse compression, etc. to improve the performance in the presence of ECM.

Besides that, current investigations ignored closely spaced targets and unresolved targets. Hence, one can carry out further research in this domain. Moreover, our study is focused on stand-off jammer (SOJ), clutter and false alarms (FA) but not consid-

ered multipath into account and one can incorporate other jamming scenarios like self-screening jammer (SSJ), range gate pull-off (RGPO), velocity gate pull-off (VGPO) etc. and carry out future work in this direction. In addition, a future research work can be carried out by using space-time adaptive processing (STAP) approach using multi-input and multi-output (MIMO) radar and multi-static radar scenarios.

#### **4.5.5 Computational complexity**

The time taken for execution by four data association approaches for four different case studies is depicted in Table 4.1. Programs were run on Dell Optiplex 9020 with Intel(R) Core(TM) i7-4790 CPU @ 3.60 GHz, 8 GB RAM and 100 Monte Carlo runs. It is clear from Table 4.1 values that as the jamming power increases from 10 dBm to 50 dBm, the run time also increases for all the four data association techniques. This is due to increase in the number of observations for the association. FCM has less execution time and Fuzzy-PSO has higher computational time. Fuzzy-GA has less execution time when compared to Fuzzy-PSO. In JPDA, probability association matrices have to be generated according to validation matrix. But in FCM, only clustering approach is applied to obtain partition matrix. So, the execution time in FCM is less when compared to JPDA.

A group of chromosomes or particles are considered in proposed hybrid data association approach so that every possibility is checked and care is taken not to allow the cluster centers to fall in local minima. In Fuzzy-PSO, position and velocity have to be updated for each particle in the swarm and the fitness evaluation is performed. A number of addition and multiplication operations has to be executed for updating position and velocity. But, in Fuzzy-GA, some interchanging of values and additions are implemented which offers it to take less time when compared to Fuzzy-PSO. Fuzzy-GA consumes average time 5.19s, 22.11s more than JPDA and FCM respectively. But, Fuzzy-GA data association has its own advantages of robustness and efficiency in terms of tracking performance. Next chapter explores two fuzzy based methods to reduce the computational complexity of the existing techniques.

Table 4.1: Comparison of execution time in seconds

Sl.no	Jammer Power	JPDA	FCM	Fuzzy-PSO	Fuzzy-GA
Case-I: Linear crossing targets					
1	10dBm	1.440	0.193	4.824	4.361
2	20dBm	0.846	0.178	4.363	4.081
3	30dBm	0.530	0.179	4.368	4.169
4	40dBm	0.538	0.136	4.40	4.253
5	50dBm	0.566	0.150	4.508	4.315
Case-II: Parallel targets					
6	10dBm	0.622	0.149	4.330	4.059
7	20dBm	0.905	0.142	4.335	4.078
8	30dBm	0.867	0.150	4.335	4.082
9	40dBm	0.906	0.150	4.338	4.084
10	50dBm	1.016	0.152	4.378	4.085
Case-III: Maneuvering and linear crossing targets					
11	10dBm	31.743	7.742	165.67	163.2
12	20dBm	31.936	7.967	165.89	164.32
13	30dBm	32.517	8.71	168.35	167.19
14	40dBm	33.945	9.316	169.124	168.319
15	50dBm	34.654	10.429	169.87	168.214
Case-IV: Maneuvering crossing targets					
16	10dBm	21.731	5.198	108.99	107
17	20dBm	22.543	6.788	109.874	107.945
18	30dBm	23.945	6.978	110.427	108.935
19	40dBm	24.351	7.329	110.934	109.721
20	50dBm	25.698	7.842	111.317	110.112

Table 4.2: Performance comparison in the presence of stand off jamming, clutter and false alarms

Sl.no	Jammer power (dBm)	Performance measure	JPDA		FCM		Fuzzy-PSO		Fuzzy-GA	
			Target-1	Target-2	Target-1	Target-2	Target-1	Target-2	Target-1	Target-2
<b>Case 1: Linear crossing Targets</b>										
1	10	Pos.RMSE ( $m/s$ )	23.969	26.992	16.647	19.289	14.952	14.241	12.016	8.164
2		Vel.RMSE ( $m/s^2$ )	4.784	4.557	3.621	3.433	3.345	3.149	2.477	2.084
3	20	Pos.RMSE ( $m/s$ )	28.669	24.303	23.327	21.583	18.828	17.912	13.468	17.567
4		Vel.RMSE ( $m/s^2$ )	4.756	4.232	4.906	4.092	4.374	4.000	3.093	4.109
5	30	Pos.RMSE ( $m/s$ )	30.973	30.037	26.574	21.321	21.306	15.373	18.395	19.396
6		Vel.RMSE ( $m/s^2$ )	5.697	5.465	5.289	3.959	5.346	3.875	4.057	4.601
7	40	Pos.RMSE ( $m/s$ )	31.035	29.490	26.998	25.723	22.972	22.681	15.115	17.855
8		Vel.RMSE ( $m/s^2$ )	5.892	5.243	6.180	5.365	5.163	5.377	3.352	4.054
9	50	Pos.RMSE ( $m/s$ )	32.308	34.621	29.615	31.956	22.869	17.930	15.788	18.123
10		Vel.RMSE ( $m/s^2$ )	5.874	6.473	6.052	6.513	5.355	4.673	4.086	4.718
<b>Case 2: Parallel Targets</b>										
11	10	Pos.RMSE ( $m/s$ )	7.770	7.860	6.610	6.014	5.767	5.988	5.332	5.355
12		Vel.RMSE ( $m/s^2$ )	0.973	0.964	0.478	0.412	0.371	0.481	0.285	0.271
13	20	Pos.RMSE ( $m/s$ )	8.333	7.351	7.086	6.821	6.253	5.927	5.681	5.698
14		Vel.RMSE ( $m/s^2$ )	1.221	0.664	0.714	0.492	0.422	0.247	0.426	0.334
15	30	Pos.RMSE ( $m/s$ )	8.107	8.361	7.309	7.794	6.581	6.994	5.736	6.006
16		Vel.RMSE ( $m/s^2$ )	1.019	1.062	0.590	0.727	0.507	0.619	0.356	0.371
17	40	Pos.RMSE ( $m/s$ )	8.622	8.906	7.783	7.221	6.822	7.206	6.644	6.863
18		Vel.RMSE ( $m/s^2$ )	1.164	1.182	0.697	0.587	0.521	0.673	0.581	0.584
19	50	Pos.RMSE ( $m/s$ )	9.063	10.707	8.534	8.138	7.072	7.611	6.808	7.599
20		Vel.RMSE ( $m/s^2$ )	1.377	1.713	0.963	0.817	0.513	0.500	0.571	0.732

Table 4.3: Performance comparison in the presence of stand off jamming, clutter and false alarms

Sl.no	Jammer power (dBm)	Performance measure	JPDA		FCM		Fuzzy-PSO		Fuzzy-GA	
			Target-1	Target-2	Target-1	Target-2	Target-1	Target-2	Target-1	Target-2
<b>Case 3: Maneuvering and linear crossing targets</b>										
1	10	Pos.RMSE ( $m/s$ )	113.103	134.947	111.205	133.827	110.524	132.471	109.791	131.369
2		Vel.RMSE ( $m/s^2$ )	120.521	159.463	119.376	157.528	131.239	156.431	118.931	156.426
3	20	Pos.RMSE ( $m/s$ )	105.206	135.398	114.195	134.176	113.316	133.725	112.612	131.781
4		Vel.RMSE ( $m/s^2$ )	120.726	159.781	119.79	158.31	119.321	158.18	118.987	157.32
5	30	Pos.RMSE ( $m/s$ )	116.345	138.312	116.281	137.151	128.517	136.983	115.315	135.791
6		Vel.RMSE ( $m/s^2$ )	131.514	160.925	121.321	160.637	120.731	138.312	119.951	158.416
7	40	Pos.RMSE ( $m/s$ )	118.416	139.615	117.914	139.312	116.712	138.816	116.319	137.615
8		Vel.RMSE ( $m/s^2$ )	126.317	161.417	121.933	160.718	120.856	160.112	120.337	159.837
9	50	Pos.RMSE ( $m/s$ )	119.428	140.513	118.976	139.818	118.216	139.491	117.578	138.317
10		Vel.RMSE ( $m/s^2$ )	123.414	163.58	122.413	162.517	122.314	161.783	121.157	160.814
<b>Case 4: Maneuvering crossing targets</b>										
11	10	Pos.RMSE ( $m/s$ )	137.559	156.905	136.34	155.731	136.15	155.465	135.417	154.379
12		Vel.RMSE ( $m/s^2$ )	103.528	125.028	102.484	124.58	99.316	120.768	98.576	120.284
13	20	Pos.RMSE ( $m/s$ )	138.431	156.982	138.218	155.718	137.457	155.548	136.951	154.731
14		Vel.RMSE ( $m/s^2$ )	107.924	129.912	106.196	128.872	101.536	126.992	100.064	124.528
15	30	Pos.RMSE ( $m/s$ )	138.943	157.781	138.793	156.374	138.49	156.016	137.938	155.743
16		Vel.RMSE ( $m/s^2$ )	109.312	135.048	107.856	134.048	103.772	131.124	101.964	128.7
17	40	Pos.RMSE ( $m/s$ )	140.259	158.541	139.643	157.623	138.641	156.579	138.069	155.351
18		Vel.RMSE ( $m/s^2$ )	113.921	139.164	110.56	137.444	108.12	135.76	107.68	133.16
19	50	Pos.RMSE ( $m/s$ )	142.621	159.794	141.862	158.541	141.021	158.321	140.321	157.37
20		Vel.RMSE ( $m/s^2$ )	118.596	141.26	113.92	139.84	113.24	138.68	109.88	135.12

## 4.6 Conclusion

Two novel hybrid data association techniques (Fuzzy-GA and Fuzzy-PSO) have been demonstrated for tracking multiple targets in the presence of ECM, clutter, and false alarms. Data association matrix has been computed by using Fuzzy-GA and Fuzzy-PSO algorithms between all target tracks and validated measurements for four different cases. The probability data association matrix in JPDA is replaced by optimized fuzzy correlation matrix. The next state of the target is predicted by applying optimized fuzzy correlation matrix, which is evaluated based on proposed Fuzzy-GA and Fuzzy-PSO approaches. Further, a comprehensive research study is carried out with four data association techniques (JPDA, FCM, Fuzzy-PSO, and Fuzzy-GA) for four different cases. It is evident from the simulation results that Fuzzy-GA data association technique provides improved performance compared to all other methods in terms of position and velocity RMSE values (38.69% and 33.19 % average improvement for target-1; 31.17% and 9.68 % average improvement for target-2) respectively for crossing linear targets case. But, FCM technique gives superior performance in terms of execution time (94.88% less average execution time) in comparison with other three techniques (JPDA, Fuzzy-GA, and Fuzzy-PSO) despite having a local minima problem. Thus concludes two novel soft and evolutionary computing based hybrid data association techniques for tracking multiple targets in the presence of strong interference.

## **CHAPTER 5**

# **FUZZY BASED DATA ASSOCIATION APPROACHES FOR TRACKING MULTIPLE TARGETS IN THE PRESENCE OF ECM**

### **5.1 Introduction**

The previous chapter presented soft and evolutionary computation based techniques to overcome local minima problem in fuzzy clustering means based approach. This chapter addresses multi target tracking problem using two novel fuzzy data association techniques. The aim of this chapter is to decrease the computational complexity by retaining comparable performance in terms of RMSE compared to association techniques that are discussed in chapter 4. These data association approaches are based on rough fuzzy and all neighbor fuzzy relational (ANFR) clustering techniques. Further, the data association matrix is evaluated for all tracks using validated measurements obtained by phased array radar for four different cases by applying five data association methods (JPDA, FCM, Fuzzy-GA, Rough-Fuzzy and ANFR). The literature survey related to these fuzzy based data association techniques have been presented in section 4.2. The following subsections gives detailed explanation of these data association approaches.

### **5.2 Proposed data association techniques**

This subsection briefly explains about the proposed novel data association approaches rough fuzzy and all neighbor fuzzy relational (ANFR). The two main steps involved in the proposed methods are given below:

- i. Calculating posterior possibility weights.

- ii. Updating the predicted state and covariance matrix.

### 5.2.1 Rough fuzzy data association

The computing of posterior possibility weights based on Rough fuzzy clustering means algorithm is briefly described below.

Let  $N_T$  be the number of multiple targets that intended at each scan in the presence of ECM, clutter, and false alarms. The number of measurements obtained from radar at each scan be  $N$ . Out of these  $N$  measurements only  $N_V$  number of measurements are validated by using validation gate criterion (Bar-Shalom, 1990; Aziz, 2014). These validated measurements have a high probability to be considered as true measurements, and the remaining measurements are occurred due to interference. Then, the validation matrix between targets ( $N_T$ ) and validated measurements ( $N_V$ ) is defined as

$$\omega = \omega^{qr}; \quad q = 1, 2, \dots, N_T; r = 0, 1, \dots, N_V \quad (5.1)$$

and

$$\omega^{qr} = \begin{cases} 1, & \text{If } r^{th} \text{ measurement lies in the gate of } q^{th} \text{ target} \\ 0, & \text{Otherwise} \end{cases}$$

Index  $r=0$  represents that at-least a single measurement is not valid. The distance between  $r^{th}$  validated measurement and  $q^{th}$  target is calculated as

$$(d^{qr})^2 = \tilde{z}^{qr'} (S^q)^{-1} \tilde{z}^{qr} \quad (5.2)$$

Where,  $\tilde{z}^{qr} = z^r - \hat{z}^q$  represents the difference between observed and predicted measurements.

Using the rules described in (Aziz, 2013, 2014), the distance matrix between  $r^{th}$  measurement and  $q^{th}$  target is determined by gate probability ( $P_G$ ), distance, detection probability ( $P_D$ ) and clutter density ( $\lambda$ ).

$$\delta^{qr} = \begin{cases} P_G P_D \lambda^{n_q - 1} (d^{qr})^2; & \text{if } \omega^{qr} = 1; q = 1, \dots, N_T; \\ & r = 1, 2, \dots, N_V \\ (1 - P_G P_D) \lambda^{n_q} & \text{if } \omega^{qr} = 0; r = 0; q = 1, 2, \dots, N_T \end{cases} \quad (5.3)$$

and the partition matrix is given as

$$\mu^{qr} = \delta^{qr} = (1 - P_D P_G) \lambda^{n_q}, q = 1, 2, \dots, N_T, r = 0 \quad (5.4)$$

and follows below rules

$$\mu^{qr} \in [0, 1]; 1 \leq q \leq N_T, 1 \leq r \leq N_V \quad (5.5a)$$

$$\sum_{q=1}^{N_T} \mu^{qr} = 1; \forall r \neq 0 \quad (5.5b)$$

$$0 \leq \sum_{r=1}^{N_V} \mu^{qr} \leq N_T; q = 1, 2, 3, \dots, N_T \quad (5.5c)$$

The distribution of partition matrix in rough fuzzy clustering becomes more appropriate due to upper and lower approximations in the rough set. Let  $V^q$  be the centroid and  $\alpha^q$  be the threshold value for  $q^{th}$  target and obeys the following set of rules. Then the lower approximation is given as

$$\underline{\mathcal{R}}q = \{Z_{i,g} | Z_{i,g} \in q\} \quad (5.6a)$$

and the upper approximation is defined as

$$\overline{\mathcal{R}}q = \{Z_{i,g} | \|Z_{i,g} - v_q\| \leq \alpha_q; \alpha_q > 0\} \quad (5.6b)$$

Where  $i = 1, 2, \dots, N_V$  and  $q = 1, 2, \dots, N_T$ . Then,

- i. If  $Z_{i,g} \in \underline{\mathcal{R}}q$ , then  $\forall l \in \{1, 2, \dots, N_T\}, l \neq q, Z_{i,g} \in \overline{\mathcal{R}}q, Z_{i,g} \notin \overline{\mathcal{R}}l$ .

ii. If  $Z_{i,g} \in \overline{R}q$ , then at least  $l \in \{1, 2, 3, \dots, N_T\}$ , and  $Z_{i,g} \in \overline{R}l$

The upper approximation limit  $\alpha^q$  defines the border for all possibilities of measurements that belong to a particular target. If the distance between the cluster and measurement is more than the threshold for a particular target, then that measurement belongs to other targets.

Based on the above rules of rough sets, the objective function that has to be minimized to obtain possibility weight matrix ( $\mu^{qr}$  and  $r \neq 0$ ) is given as

$$J_p = \sum_{r=1}^{N_V} \sum_{q=1}^{N_T} (\mu^{qr})^p \delta^{qr}; q = 1, 2, \dots, N_T; r = 1, 2, \dots, N_V \quad (5.7)$$

and the constraint conditions are

$$\mu^{qr} \in [0, 1] \quad (5.8a)$$

$$0 \leq \sum_{r=1}^{N_V} \mu^{qr} \leq N_T \quad (5.8b)$$

and

$$\sum_{q=1; Z_{i,g} \in \overline{R}q}^{N_T} \mu^{qr} = 1 \quad (5.8c)$$

Equation 5.7 can be minimized by using rough fuzzy clustering algorithm. The possibility weights are calculated by using Equation 5.9.

$$\mu^{qr} = \frac{1}{\sum_{n=1; Z_{i,g} \in \overline{R}q}^{N_T} \left(\frac{\delta^{qr}}{\delta^{nr}}\right)^{2/(p-1)}} \quad (5.9)$$

Where,  $q = 1, 2, \dots, N_T$  and  $r = 1, 2, \dots, N_V$ .

The centroid is updated by using Equation 5.10

$$V^q = \frac{\sum_{r=1}^{N_V} (\mu^{qr})^m Z^r}{\sum_{r=1}^{N_V} (\mu^{qr})^m} \quad (5.10)$$

If,  $\delta^{qr} = \infty$ , then the corresponding possibility value  $\mu^{qr}$  will be zero. The possibility matrix is normalized, so that the contribution of all measurements for a particular

target must be equal to 1. *i.e.*,

$$\sum_{r=0}^{N_V} \mu^{qr} = 1; q = 1, 2, \dots, N_T \quad (5.11)$$

The possibility matrix obtained from Equation 5.9 is the updated rough fuzzy data association matrix relating validated observations and the number of targets present.

### 5.2.2 All neighbor fuzzy relational data association(ANFRDA)

The computing of posterior possibility weights is based on all neighbor fuzzy relational clustering <sup>1</sup> algorithm is briefly described below.

Let  $N$  be the number of observations received from radar.  $N_v$  be the number of observations which are validated from all the  $N$  observations by using gating technique (Blair et al., 1998). The validated observations have a high probability of belonging to true observations. Consider the number of targets be  $N_t$  then the validation matrix is defined as

$$\Phi = \Phi^{jk} \quad j = 1, 2, \dots, N_t, k = 0, 1, 2, \dots, N_v \quad (5.12)$$

and

$$\Phi^{jk} = \begin{cases} 1 & \text{If } k^{th} \text{ observation lies in the gate of } j^{th} \text{ target} \\ 0 & \text{Otherwise} \end{cases}$$

Index  $k = 0$  represents that no observation is valid.  $(d^{jk})^2$  is the mahalanobis distance which is calculated between  $j^{th}$  target and  $k^{th}$  observation and is given as

$$(d^{jk})^2 = \tilde{z}^{jk'} (S^j)^{-1} \tilde{z}^{jk} \quad (5.13)$$

---

<sup>1</sup>Basic code of fuzzy relational clustering is available at [www.mathworks.com/matlabcentral/fileexchange/47825-frecca-zip](http://www.mathworks.com/matlabcentral/fileexchange/47825-frecca-zip)

Based on rules described in Aziz (2014, 2013) distance matrix between  $j^{th}$  target and  $k^{th}$  measurement is calculated by considering distance, gate probability ( $P_g$ ), clutter density ( $\lambda$ ) and detection probability ( $P_d$ ).

$$\delta^{jk} = \begin{cases} \lambda^{n_j-1} P_g P_d (d^{jk})^2 & \text{if } \Phi^{jk} = 1; j = 1, \dots, N_t; \\ & k = 1, 2, \dots, N_v \\ (\lambda^{n_j} (1 - p_g p_d)) & k = 0; j = 1, 2, \dots, N_t \end{cases} \quad (5.14)$$

Pairwise similarity matrix is computed using the norm of the distance matrix.

$$S_{jm} = e^{-\delta^{jm}/2\sigma^2}, \quad j = m = 1, 2, \dots, N_v \quad (5.15)$$

A random partition matrix  $\beta^{jk}$  where  $j = 1, 2, \dots, N_t$  and  $k = 1, 2, \dots, N_v$  is considered and normalized to satisfy the below condition.

$$\beta^{jk} \in [0, 1]; 1 \leq j \leq N_t; 1 \leq k \leq N_v$$

and

$$0 \leq \sum_{k=1}^{N_v} \beta^{jk} \leq N_t, j = 1, 2, \dots, N_t$$

Equal prior value of each target is considered as

$$\psi^j = \frac{1}{N_t}; j = 1, 2, \dots, N_t \quad (5.16)$$

The affinity weight matrix for a particular target  $j$  is calculated as

$$\omega_{mk}^j = s_{mk}^j \times \beta_m^j \times \beta_k^j \quad (5.17)$$

where  $j = 1, 2, \dots, N_t; k = m = 1, 2, \dots, N_v$

The affinity matrix contains the contribution of both similarity matrix and partition values. The rank for observations is evaluated for particular target and is given as

$$TR^j(m) = (1 - \zeta) + \zeta \sum_{k=1}^{N_v} \omega_{km}^j \frac{TR_k^j}{\sum_{l=1}^{N_v} \omega_{kl}^j} \quad (5.18)$$

$\zeta$  is the damping factor and value ranges between 0.8 to 0.9. Observation rank determines how much the value of observation belongs to a particular target and it is assigned as likelihood.

$$\Lambda^{jk} = TR^{jk} \quad (5.19)$$

$$j = 1, 2, \dots, N_t, k = 1, 2, \dots, N_v$$

The likelihood value is important to update the partition matrix and new partition matrix depending on likelihood and prior value is given as

$$\beta_{new}^{jk} = \frac{\psi^j \Lambda^{jk}}{\sum_{j=1}^{N_t} \psi^j \Lambda^{jk}} \quad (5.20)$$

$$j = 1, 2, \dots, N_t, k = 1, 2, \dots, N_v$$

The new prior of the target  $j$  is updated as

$$\psi^j = \frac{1}{N_v} \sum_{k=1}^{N_v} \beta^{jk} \quad (5.21)$$

$$j = 1, 2, \dots, N_t, k = 1, 2, \dots, N_v$$

The partition matrix in Equation 5.20 is the new data association matrix between valid measurements and the targets.

Partition matrix obtained by both the data association matrix is replaced in Equation 4.9 to further estimate the next state of the target. Updating of state and covariance matrix of a tracking algorithm is briefly described in subsection 4.4.2.

### 5.3 Result and discussion

This section furnishes results and discussions obtained by considering four case studies (linear crossing targets, parallel targets, linear and non-linear crossing targets, and

non-linear crossing targets) to evaluate the performance of the proposed hybrid data association techniques. The results achieved in each case study are compared with existing techniques, such as JPDA, FCM and Fuzzy-GA. The entire details of environment, target trajectories, state vector equations, radar specifications etc., that are required for simulation is explained in detailed in subsection 4.5. The comparison of position and velocity RMSE for different case studies with proposed data association techniques are depicted in Tables 5.2 and 5.3 respectively.

### 5.3.1 Linear crossing targets

Two linear crossing targets traveling with constant velocity of  $50 \text{ m/sec}$  are considered with initial positions  $(25000,201)m$  and  $(5000,201)m$ . The targets are simulated for  $50s$  duration with a sampling interval of  $1s$ . The result of tracking linear crossing target using RF-JPDA and ANFRDA is portrayed in Figure 5.1 and Figure 5.2 respectively. Figures 5.3 and 5.4 shows the comparison of position and velocity RMSE for different jammer power levels against different data association techniques. Also, Figures 5.3 and 5.4 clearly depict that there is an increase in position and velocity RMSE values with increase in jammer power levels. In this case, initialization is done very near to measurement value, hence the tracking error is insignificant at initial points. The average position RMSE for target-1 with ANFR based data association approach is  $47.35\%$ ,  $37.18\%$ , and  $0.611\%$  less when compared to conventional JPDA, Fuzzy-JPDA, and Rough-Fuzzy data association techniques respectively. Whereas, The average position RMSE for target-2 with ANFR based data association approach is  $35.629\%$  and  $21.434\%$  less when compared to conventional JPDA, Fuzzy-JPDA based approaches respectively. However, average position RMSE for target-2 with ANFR based data association approach is  $15.434\%$ ,  $2.845\%$  more when compared to Fuzzy-GA and Rough-Fuzzy based data association approaches. Similarly, the average velocity for target-1 with ANFR based data association approach is  $20.42\%$  and  $17.502\%$  less when compared to conventional JPDA and Fuzzy-JPDA respectively. But, the RMSE velocity of target-1 obtained with ANFR based data association is  $25.924\%$  and  $6.502\%$  more when

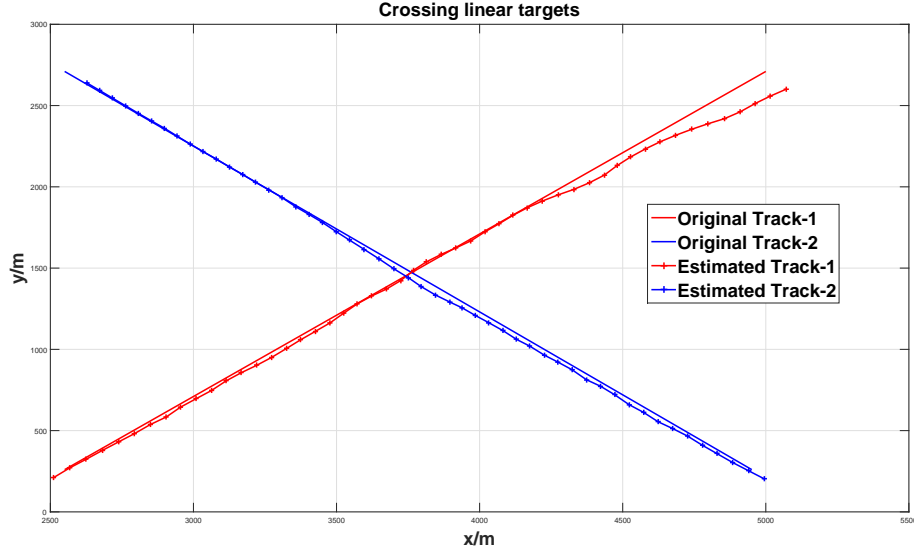


Figure 5.1: Tracking linear crossing targets using RF-JPDA technique

compared to Fuzzy-GA and Rough-Fuzzy based approaches respectively. Further, the velocity RMSE of target-2 with ANFR based data association is 9.177%, 30.358%, and 7.407% more when compared to conventional Fuzzy-JPDA, Fuzzy-GA, and Rough-Fuzzy data association approaches respectively. These results show that the proposed ANFR and Rough-Fuzzy based data association technique is comparable with Fuzzy-GA based data association approach.

### 5.3.2 Parallel targets

Two parallel targets are examined for case study-2. The initial position of the target-1 is at  $(2550, 260)m$  and target-2 is at  $(3050, 260)m$ . The trajectory is simulated for 50s duration with a sampling interval of 1s. The detection probability is taken as 0.95. RF-JPDA and ANFRDA are used for tracking the parallel targets and the results are depicted in Figure 5.5 and Figure 5.6 respectively. Figures 5.7 and 5.8 exhibits the comparison of position and velocity RMSE for different stand-off-jammer power levels with different data association techniques. Both Figures 5.7 and 5.8 clearly illustrates that position and velocity RMSE values increase with the increase in jammer power levels. The average position RMSE for target-1 with ANFR based data asso-

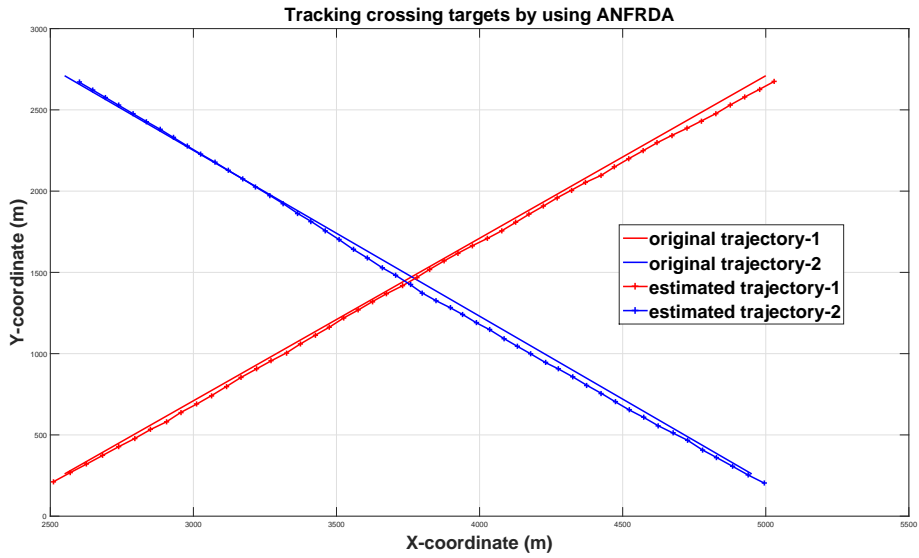


Figure 5.2: Tracking linear crossing targets using ANFRDA technique

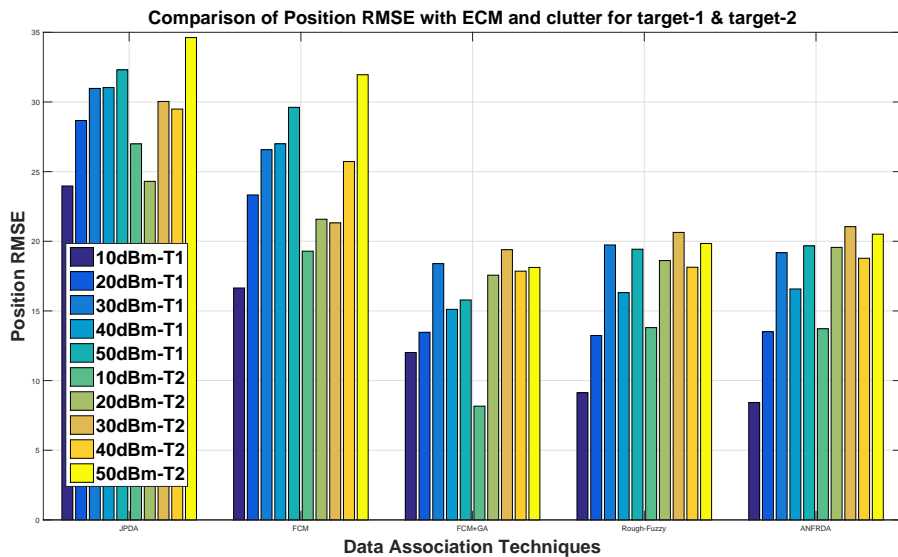


Figure 5.3: Comparison performance of position RMSE of two crossing targets  $T1 \rightarrow Target - 1, T2 \rightarrow Target - 2$

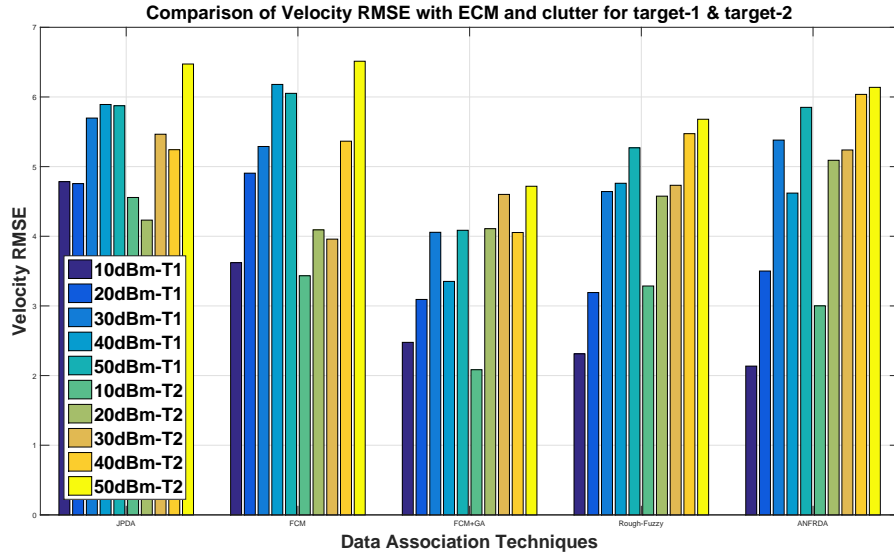


Figure 5.4: Comparison performance of velocity RMSE of two crossing targets  $T1 \rightarrow Target - 1$ ,  $T2 \rightarrow Target - 2$

ciation approach is 24.146%, 14.851%, and 4.234% less when compared to conventional JPDA, Fuzzy-JPDA, and Rough-Fuzzy data association techniques respectively. Whereas, The average position RMSE for target-2 with ANFR based data association approach is 17.251% and 0.703% less when compared to conventional JPDA, Fuzzy-JPDA based approaches respectively. However, average position RMSE for target-2 with ANFR based data association approach is 13.368%, 6.557% more when compared to Fuzzy-GA and Rough-Fuzzy based data association approaches. Similarly, the average velocity for target-1 with ANFR based data association approach is 47.775% and 12.696% less when compared to conventional JPDA and Fuzzy-JPDA respectively. But, the RMSE velocity of target-1 obtained with ANFR based data association is 35.421% and 21.120% more when compared to Fuzzy-GA and Rough-Fuzzy based approaches respectively. Further, the velocity RMSE of target-2 with ANFR based data association is 48.995%, 97.294%, and 51.541% more when compared to Fuzzy-JPDA, Fuzzy-GA and Rough-Fuzzy data association approaches respectively. These results show that the proposed ANFR and Rough-Fuzzy based data association technique is comparable with Fuzzy-GA based data association approach.

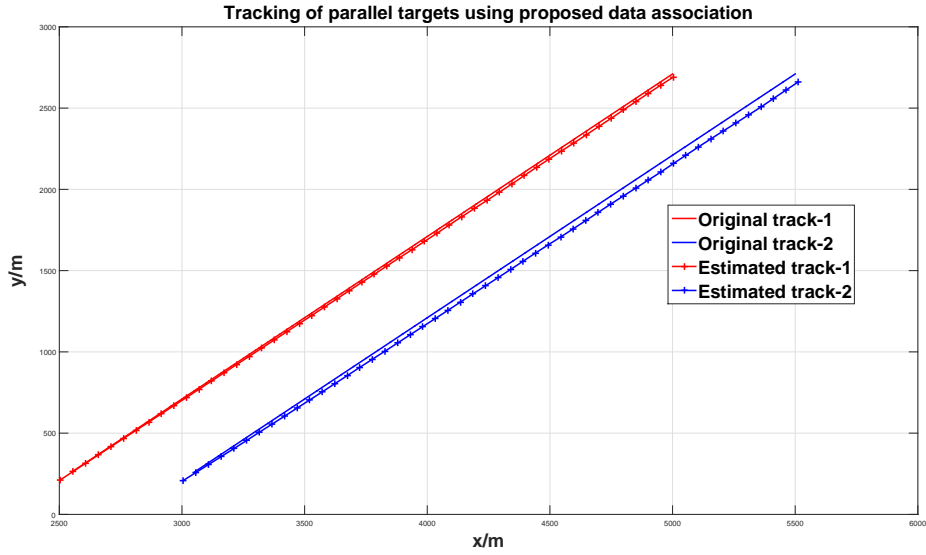


Figure 5.5: Tracking of parallel targets using RF-JPDA technique

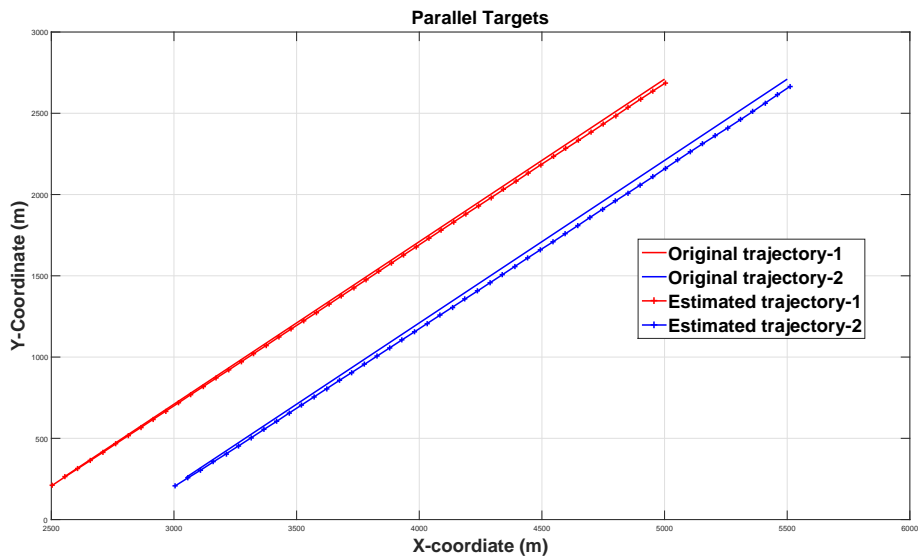


Figure 5.6: Tracking linear parallel targets using ANFRDA technique

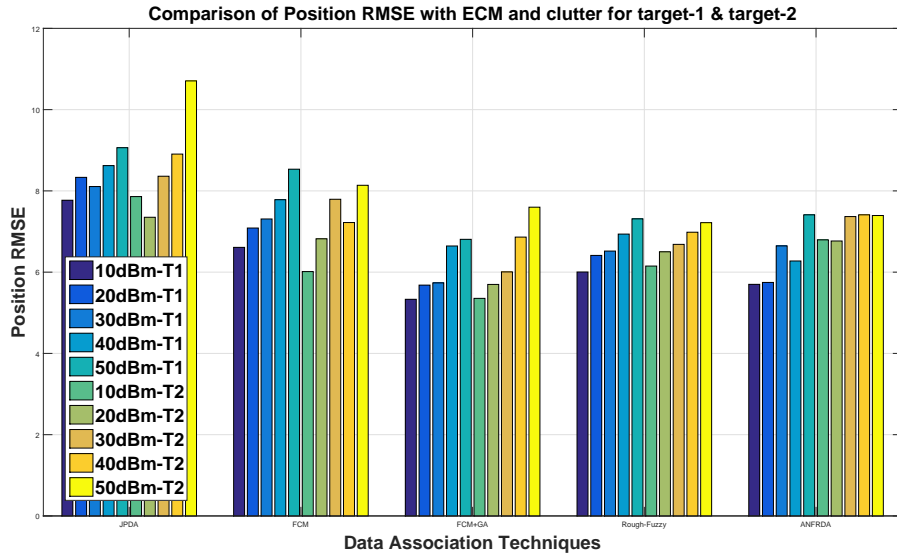


Figure 5.7: Comparison performance of position RMSE of two crossing targets  $T1 \rightarrow Target - 1, T2 \rightarrow Target - 2$

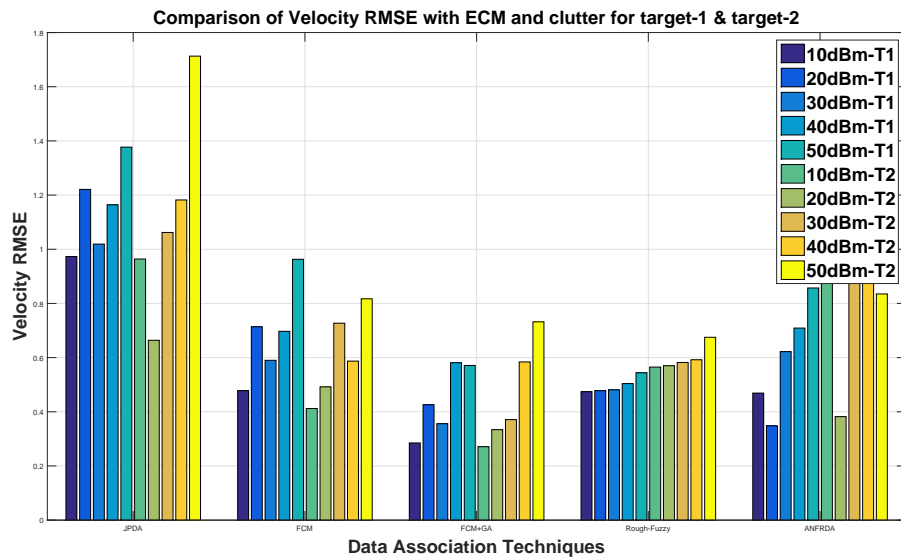


Figure 5.8: Comparison performance of velocity RMSE of two crossing targets  $T1 \rightarrow Target - 1, T2 \rightarrow Target - 2$

### 5.3.3 Maneuvering and linear crossing targets

In this scenario, two targets (one linear and the other maneuvering bench mark trajectory (Kirubarajan et al., 1998)) are considered. Both trajectories are simulated for 150s with a sample period of 0.46s. The result of tracking maneuvering and linear crossing targets for both RF-JPDA and ANFDA are portrayed in Figures 5.9 and 5.10 respectively. Figures 5.11 and 5.12 exhibits the comparison of position and velocity RMSE for different stand-off-jammer power levels with different data association techniques. Both Figures 5.11 and 5.12 clearly illustrates that position and velocity RMSE values increase with the increase in jammer power levels. The average position RMSE for target-1 with ANFR based data association approach is 17.264% and 0.076% less when compared to Fuzzy-JPDA, and Rough-Fuzzy data association techniques respectively. Whereas, The average position RMSE for target-2 with ANFR based data association approach is 1.247% and 1.123% less when compared to conventional JPDA, Fuzzy-JPDA based approaches respectively. However, average position RMSE for target-2 with ANFR based data association approach is 0.788%, 0.447% more when compared to Fuzzy-GA and Rough-Fuzzy based data association approaches. Similarly, the average velocity for target-1 with ANFR based data association approach is 0.098% and 3.9641% less when compared to conventional JPDA and Fuzzy-JPDA respectively. But, the RMSE velocity of target-1 obtained with ANFR based data association is 3.756% and 3.231% more when compared to Fuzzy-GA and Rough-Fuzzy based approaches respectively. Further, the velocity RMSE of target-2 with ANFR based data association is 1.826%, 2.661%, 3.413% and 2.695% more when compared to conventional JPDA, Fuzzy-JPDA, Fuzzy-GA and Rough-Fuzzy data association approaches respectively. These results show that the proposed ANFR and Rough-Fuzzy based data association technique is comparable with Fuzzy-GA based data association approach.

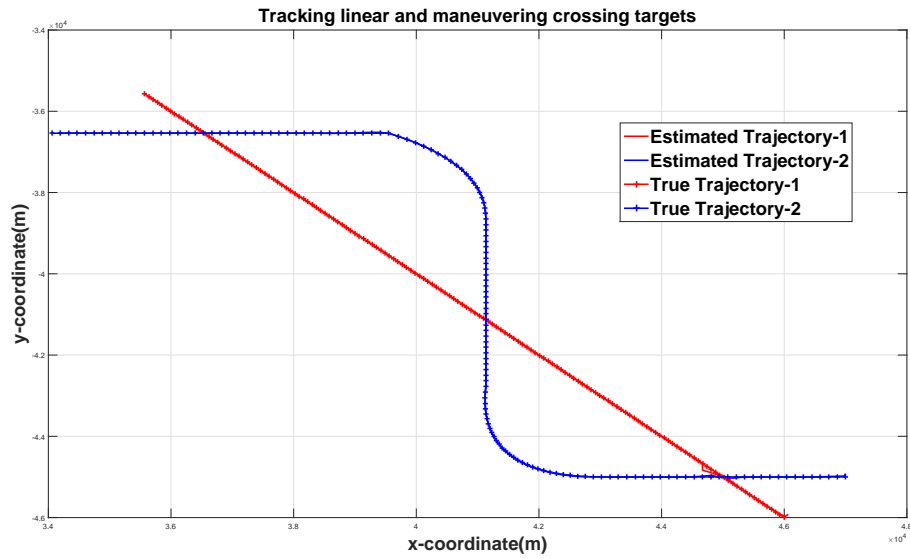


Figure 5.9: Tracking of maneuvering and linear crossing targets using RF-JPDA technique

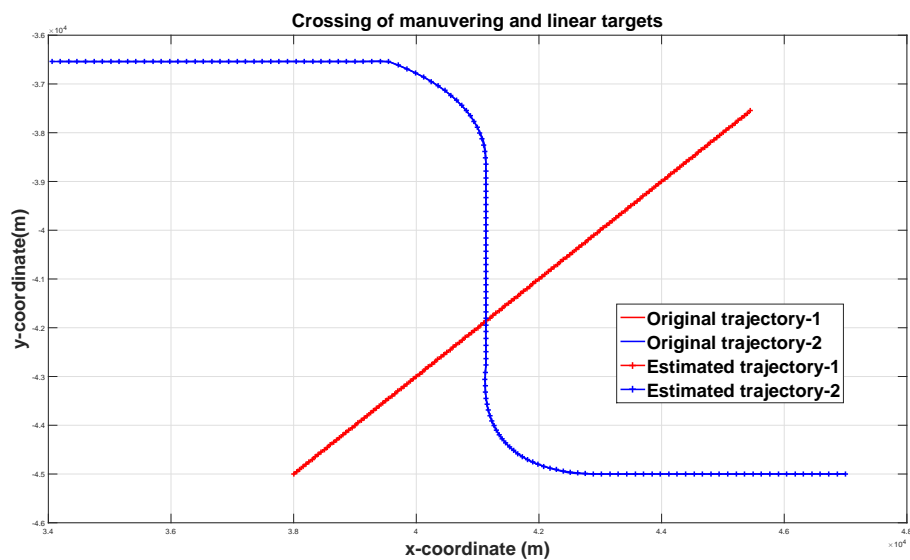


Figure 5.10: Tracking of maneuvering and linear crossing targets using ANFRDA technique

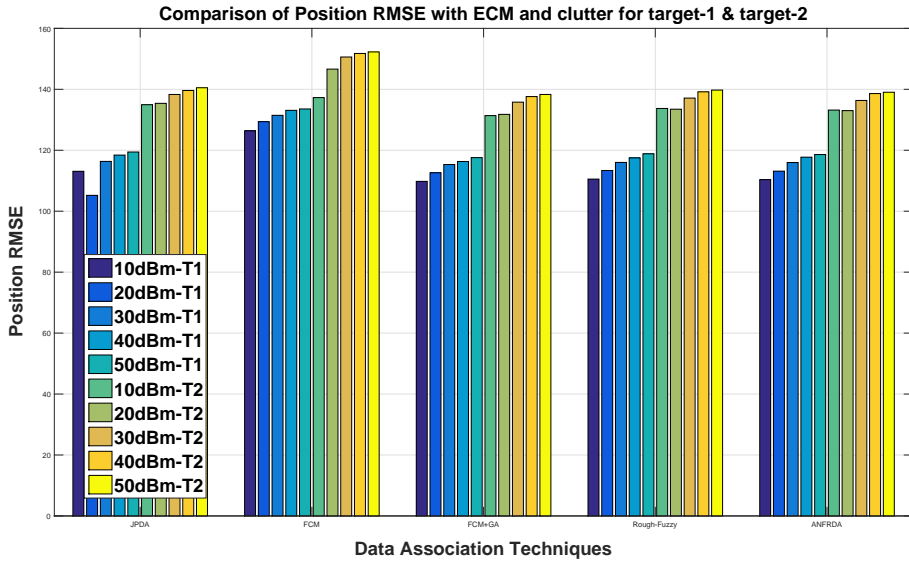


Figure 5.11: Comparison performance of position RMSE of two crossing targets  $T1 \rightarrow Target - 1, T2 \rightarrow Target - 2$

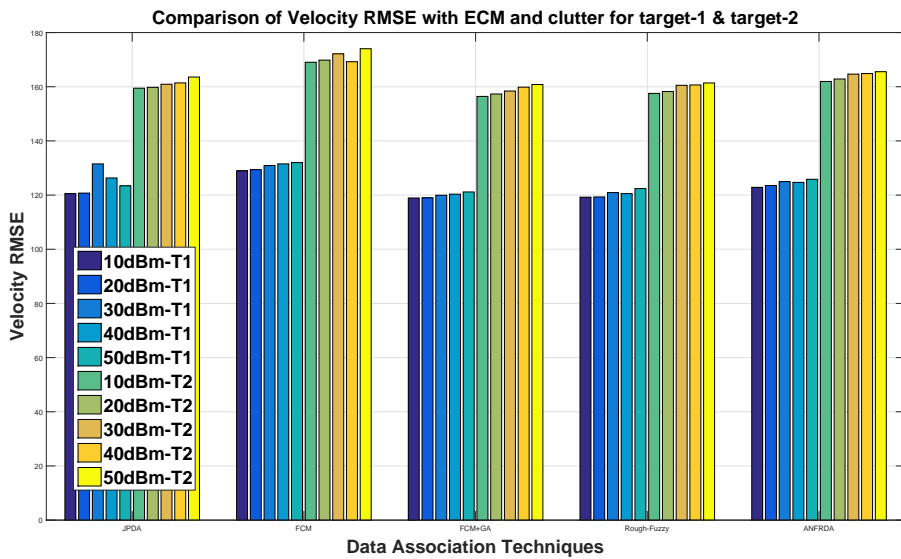


Figure 5.12: Comparison performance of velocity RMSE of two crossing targets  $T1 \rightarrow Target - 1, T2 \rightarrow Target - 2$

### 5.3.4 Maneuvering crossing targets

This case deals with two maneuvering crossing targets. Benchmark trajectory in (Kirubaran et al., 1998) is taken as target-1 and a random trajectory with  $+3g$  and  $-3g$  turns is considered for target-2. Both the trajectories are simulated for 150 s with a sampling period of 0.46 s. Figures 5.13 and 5.14 shows the tracking of maneuvering crossing targets with RF-JPDA and ANFRDA based approaches respectively. Figures 5.15 and 5.16 exhibits the comparison of position and velocity RMSE for different stand-off-jammer power levels with different data association techniques. Both Figures 5.15 and 5.16 clearly illustrates that position and velocity RMSE values increase with the increase in jammer power levels. The average position RMSE for target-1 with ANFR based data association approach is 0.897% and 0.475% less when compared to conventional JPDA, Fuzzy-JPDA, and Rough-Fuzzy data association techniques respectively. But, the average position RMSE for target-1 with ANFR based data association approach is 0.414% and 0.098% more when compared to Fuzzy-GA and RF-JPDA techniques respectively. Whereas, The average position RMSE for target-2 with ANFR based data association approach is 2.522% , 1.774%, 0.964% and 0.177% less when compared to conventional JPDA, Fuzzy-JPDA, Fuzzy-GA and RF-JPDA based approaches respectively. Similarly, the average velocity for target-1 with ANFR based data association approach is 4.832%, 7.163%, 11.889% and 3.585% more when compared to conventional JPDA, Fuzzy-JPDA, Fuzzy-GA and RF-JPDA respectively. Further, the velocity RMSE of target-2 with ANFR based data association is 2.809%, 3.680%, 7.394% and 2.962% more when compared to conventional JPDA, Fuzzy-JPDA, Fuzzy-GA and Rough-Fuzzy data association approaches respectively. These results show that the proposed ANFR and Rough-Fuzzy based data association technique is comparable with Fuzzy-GA based data association approach.

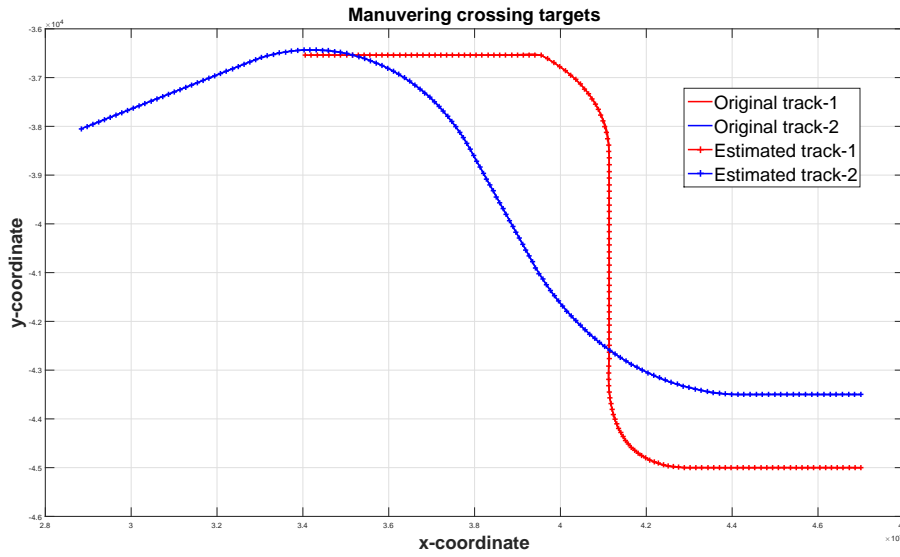


Figure 5.13: Tracking maneuvering crossing targets using RF-JPDA technique

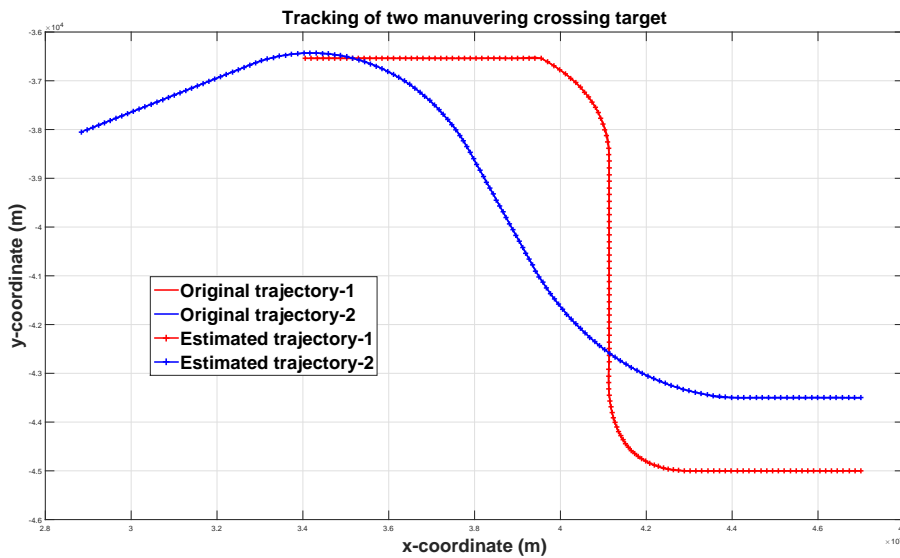


Figure 5.14: Tracking maneuvering crossing targets using ANFRDA technique

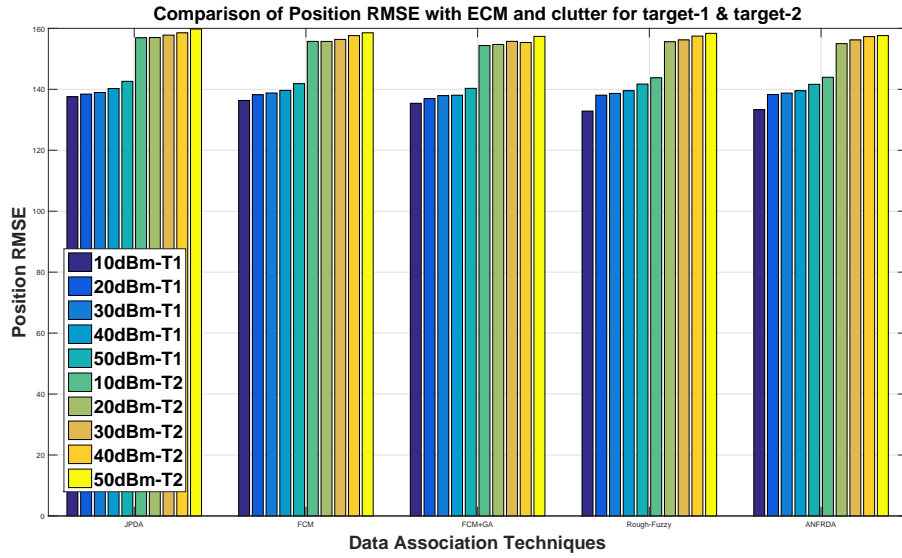


Figure 5.15: Comparison performance of position RMSE of two crossing targets  $T1 \rightarrow Target - 1, T2 \rightarrow Target - 2$

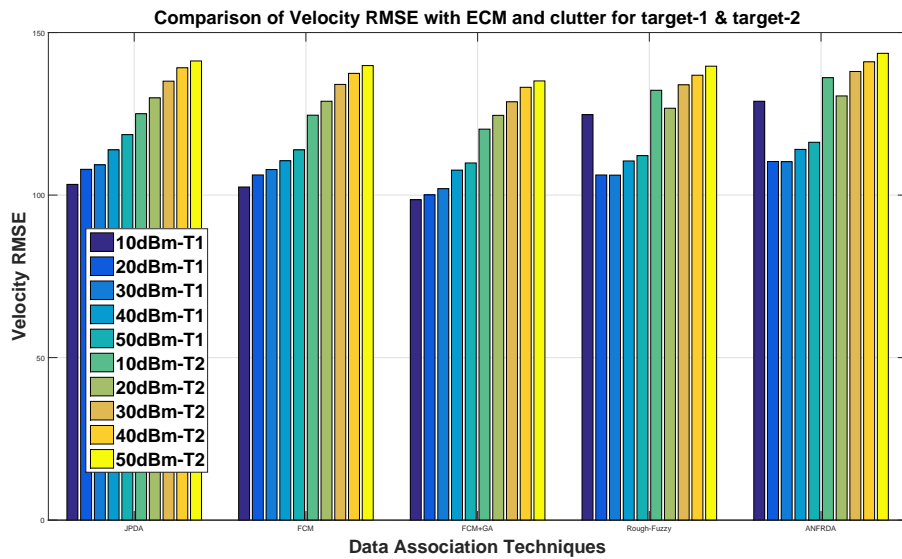


Figure 5.16: Comparison performance of velocity RMSE of two crossing targets  $T1 \rightarrow Target - 1, T2 \rightarrow Target - 2$

Table 5.1: Comparison of execution time in seconds

Sl.no	Jammer Power	JPDA	FCM	Fuzzy-GA	Rough-Fuzzy	ANFRDA
Case-I: Linear crossing targets						
1	10dBm	1.440	0.193	4.361	0.058	0.312
2	20dBm	0.846	0.178	4.081	0.0625	0.385
3	30dBm	0.530	0.179	4.169	0.0648	0.391
4	40dBm	0.538	0.136	4.253	0.0654	0.397
5	50dBm	0.566	0.150	4.315	0.0693	0.402
Case-II: Parallel targets						
6	10dBm	0.622	0.149	4.059	0.052	0.290
7	20dBm	0.905	0.142	4.078	0.0517	0.297
8	30dBm	0.867	0.150	4.082	0.0523	0.292
9	40dBm	0.906	0.150	4.084	0.0535	0.296
10	50dBm	1.016	0.152	4.085	0.0556	0.304
Case-III: Maneuvering and linear crossing targets						
11	10dBm	31.743	7.742	163.2	0.7243	8.943
12	20dBm	31.936	7.967	164.32	0.7359	9.004
13	30dBm	32.517	8.71	167.19	0.7571	9.162
14	40dBm	33.945	9.316	168.319	0.8143	9.223
15	50dBm	34.654	10.429	168.214	0.8062	9.218
Case-IV: Maneuvering crossing targets						
16	10dBm	21.731	5.198	107	0.6942	5.867
17	20dBm	22.543	6.788	107.945	0.6678	5.915
18	30dBm	23.945	6.978	108.935	0.7107	5.969
19	40dBm	24.351	7.329	109.721	0.7276	6.012
20	50dBm	25.698	7.842	110.112	0.7477	6.034

Table 5.2: Performance comparison in the presence of stand off jamming, clutter and false alarms

Sl.no	Jammer power (dBm)	Performance measure	JPDA		FCM		Fuzzy-GA		Rough-Fuzzy		ANFRDA	
			Target-1	Target-2	Target-1	Target-2	Target-1	Target-2	Target-1	Target-2	Target-1	Target-2
<b>Case 1: Linear crossing Targets</b>												
1	10	Pos.RMSE (m/s)	23.969	26.992	16.647	19.289	12.016	8.164	9.125	13.802	8.429	13.721
2		Vel.RMSE (m/s <sup>2</sup> )	4.784	4.557	3.621	3.433	2.477	2.084	2.312	3.286	2.136	3.001
3	20	Pos.RMSE (m/s)	28.669	24.303	23.327	21.583	13.468	17.567	13.237	18.614	13.511	19.561
4		Vel.RMSE (m/s <sup>2</sup> )	4.756	4.232	4.906	4.092	3.093	4.109	3.192	4.576	3.501	5.091
5	30	Pos.RMSE (m/s)	30.973	30.037	26.574	21.321	18.395	19.396	19.735	20.638	19.180	21.049
6		Vel.RMSE (m/s <sup>2</sup> )	5.697	5.465	5.289	3.959	4.057	4.601	4.642	4.732	5.381	5.239
7	40	Pos.RMSE (m/s)	31.035	29.490	26.998	25.723	15.115	17.855	16.314	18.137	16.577	18.782
8		Vel.RMSE (m/s <sup>2</sup> )	5.892	5.243	6.180	5.365	3.352	4.054	4.761	5.473	4.620	6.037
9	50	Pos.RMSE (m/s)	32.308	34.621	29.615	31.956	15.788	18.123	19.431	19.842	19.669	20.510
10		Vel.RMSE (m/s <sup>2</sup> )	5.874	6.473	6.052	6.513	4.086	4.718	5.27	5.68	5.851	6.138
<b>Case 2: Parallel Targets</b>												
11	10	Pos.RMSE (m/s)	7.770	7.860	6.610	6.014	5.332	5.355	6.004	6.150	5.700	6.795
12		Vel.RMSE (m/s <sup>2</sup> )	0.973	0.964	0.478	0.412	0.285	0.271	0.474	0.565	0.469	0.986
13	20	Pos.RMSE (m/s)	8.333	7.351	7.086	6.821	5.681	5.698	6.412	6.501	5.747	6.767
14		Vel.RMSE (m/s <sup>2</sup> )	1.221	0.664	0.714	0.492	0.426	0.334	0.478	0.570	0.348	0.382
15	30	Pos.RMSE (m/s)	8.107	8.361	7.309	7.794	5.736	6.006	6.519	6.684	6.646	7.368
16		Vel.RMSE (m/s <sup>2</sup> )	1.019	1.062	0.590	0.727	0.356	0.371	0.481	0.582	0.622	1.247
17	40	Pos.RMSE (m/s)	8.622	8.906	7.783	7.221	6.644	6.863	6.937	6.983	6.275	7.411
18		Vel.RMSE (m/s <sup>2</sup> )	1.164	1.182	0.697	0.587	0.581	0.584	0.504	0.592	0.709	1.072
19	50	Pos.RMSE (m/s)	9.063	10.707	8.534	8.138	6.808	7.599	7.312	7.218	7.411	7.394
20		Vel.RMSE (m/s <sup>2</sup> )	1.377	1.713	0.963	0.817	0.571	0.732	0.544	0.675	0.857	0.835

Table 5.3: Performance comparison in the presence of stand off jamming, clutter and false alarms

Sl.no	Jammer power (dBm)	Performance measure	JPDA		FCM		Fuzzy-GA		Rough-Fuzzy		ANFRDA	
			Target-1	Target-2	Target-1	Target-2	Target-1	Target-2	Target-1	Target-2	Target-1	Target-2
<b>Case 3: Maneuvering and linear crossing targets</b>												
1	10	Pos.RMSE ( $m/s$ )	113.103	134.947	111.205	133.827	109.791	131.369	110.541	133.719	110.356	133.192
2		Vel.RMSE ( $m/s^2$ )	120.521	159.463	119.376	157.528	118.931	156.426	119.227	157.538	122.860	161.974
3	20	Pos.RMSE ( $m/s$ )	105.206	135.398	114.195	134.176	112.612	131.781	113.362	133.479	113.144	133.006
4		Vel.RMSE ( $m/s^2$ )	120.726	159.781	119.79	158.31	118.987	157.32	119.315	158.264	123.540	162.857
5	30	Pos.RMSE ( $m/s$ )	116.345	138.312	116.281	137.151	115.315	135.791	116.013	137.124	115.976	136.347
6		Vel.RMSE ( $m/s^2$ )	131.514	160.925	121.321	160.637	119.951	158.416	120.917	160.532	124.964	164.658
7	40	Pos.RMSE ( $m/s$ )	118.416	139.615	117.914	139.312	116.319	137.615	117.496	139.174	117.734	138.605
8		Vel.RMSE ( $m/s^2$ )	126.317	161.417	121.933	160.718	120.337	159.837	120.548	160.657	124.680	164.863
9	50	Pos.RMSE ( $m/s$ )	119.428	140.513	118.976	139.818	117.578	138.317	118.831	139.752	118.593	139.044
10		Vel.RMSE ( $m/s^2$ )	123.414	163.58	122.413	162.517	121.157	160.814	122.407	161.383	125.835	165.547
<b>Case 4: Maneuvering crossing targets</b>												
11	10	Pos.RMSE ( $m/s$ )	137.559	156.905	136.34	155.731	135.417	154.379	132.858	143.777	133.32	143.960
12		Vel.RMSE ( $m/s^2$ )	103.528	125.028	102.484	124.58	98.576	120.284	124.740	132.248	128.870	136.119
13	20	Pos.RMSE ( $m/s$ )	138.431	156.982	138.218	155.718	136.951	154.731	138.086	155.612	138.293	154.980
14		Vel.RMSE ( $m/s^2$ )	107.924	129.912	106.196	128.872	100.064	124.528	106.183	126.719	110.327	130.501
15	30	Pos.RMSE ( $m/s$ )	138.943	157.781	138.793	156.374	137.938	155.743	138.654	156.218	138.766	156.204
16		Vel.RMSE ( $m/s^2$ )	109.312	135.048	107.856	134.048	101.964	128.7	106.136	133.927	110.272	138.023
17	40	Pos.RMSE ( $m/s$ )	140.259	158.541	139.643	157.623	138.069	155.351	139.538	157.465	139.526	157.296
18		Vel.RMSE ( $m/s^2$ )	113.921	139.164	110.56	137.444	107.68	133.16	110.499	136.874	114.056	141.000
19	50	Pos.RMSE ( $m/s$ )	142.621	159.794	141.862	158.541	140.321	157.37	141.733	158.367	141.645	157.632
20		Vel.RMSE ( $m/s^2$ )	118.596	141.26	113.92	139.84	109.88	135.12	112.142	139.653	116.244	143.607

### 5.3.5 Computational Complexity

The tracking of a target should be computationally efficient with the acceptable precision. The execution time of the proposed RF-JPDA and ANFRDA along with other data association techniques with variations in jamming power is illustrated in Table 5.1. It is clearly observable that the execution time for all the cases is increased with increase in jamming level from  $10dBm$  to  $50dBm$ . The reason is due to raise in the number of false alarms measurements. It is clear from Table 5.1 that the execution time for RF-JPDA is less when compared to all other data association. In JPDA all the possibilities are applied to compute the association matrix. While in Fuzzy-GA approach a number of multiplication and addition operations along with fitness evaluation is performed for all the chromosomes. Whereas, in ANFRDA each validated measurement is assigned equal prior value and by performing expectation maximization operation the association weights are calculated. But in FCM, only clustering mechanism is done besides that in RF-JPDA, upper and lower boundary approximations are calculated and the uncertainty of associating measurements is cleared at very first level and then clustering mechanism is applied. So, the computational complexity is less for RF-JPDA. The average simulation of RF-JPDA is increased by 89.05%, 60.07%, 97.75% and 89.85% when compared to JPDA, FCM, Fuzzy-GA and ANFRDA respectively for all the case studies. The entire simulation is carried out in Dell Optiplex 9020 with Intel(R) Core(TM) i7-4790 CPU 3.60 GHz, 8 GB RAM and 100 Monte-Carlo runs.

## 5.4 Conclusion

Two new rough fuzzy joint probabilistic data association filter (RF-JPDA) and all neighbor fuzzy relational data association filter (ANFRDA) for multi-target tracking in the presence of ECM has been proposed in this chapter. A through study is done by considering five jamming power levels with five data association approaches. The proposed techniques are similar to conventional JPDA, in which the probability partition matrix is replaced with the partition matrix obtained by the proposed algorithms. In RF-JPDA

the association of uncertain measurements obtained from radar becomes a simple problem due to lower and upper approximation values in the rough set. Further, it reduces the computational complexity. Simulation results show that the proposed approaches has comparable performance in terms of position RMSE, velocity RMSE when compared to Fuzzy-GA data association mechanism. It is also noticed that the over all computational complexity of RF-JPDA is improved by 84.18% with other three data association techniques (JPDA, FCM, Fuzzzy-GA and ANFRDA). The chapter-4 and chapter-5 described about novel data association approaches for multiple target tracking in the presence of strong interference. The next chapter presents direction of arrival estimation for closely spaced targets using Stockwell transform based MUSIC algorithm in the presence of ECM.

## **CHAPTER 6**

# **DIRECTION OF ARRIVAL ESTIMATION FOR CLOSELY SPACED TARGETS USING STOCKWELL TRANSFORM BASED MUSIC ALGORITHM IN THE PRESENCE OF ECM**

### **6.1 Introduction**

Till this chapter, tracking closely spaced targets have been ignored in the current research investigation. This chapter proposes direction of arrival estimation for closely spaced targets using Stockwell transform based MUSIC algorithm in the presence of ECM. The direction of arrival (DOA) estimation algorithms possess numerous applications in the area of radar and sonar. One of the resilient tasks in DOA is estimating angles of closely spaced targets. The multiple returns of the targets fall in a single resolution cell if the targets are closely spaced. In this scenario, sensor (radar/sonar) determines the multiple targets as a single target. To overcome this problem, many works have been reported in the literature (Mosca, 1969; Bar-Shalom and Li, 1995; George, 1990; Blackman, 1986). A typical closely spaced scenario is illustrated in Figure 6.1.

### **6.2 Literature survey**

To extract the angle of the targets in a single resolution cell, the monopulse ratio which yielded large errors is proposed in (Sherman, 1988). The in-phase and quadrature-phase of complex monopulse ratio is used to compute generalized likelihood ratio test (GLRT) for detecting unresolved targets (Blair and Brandt-Pearce, 1998b). Later, the work is

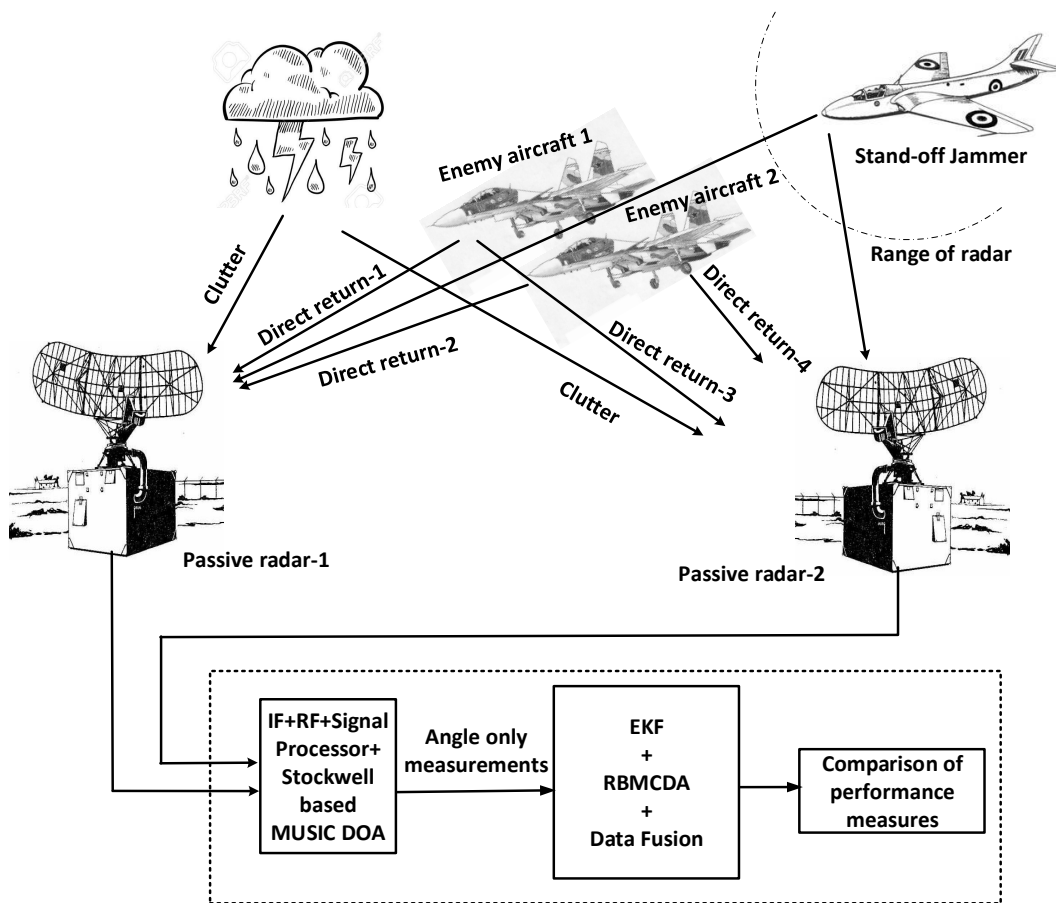


Figure 6.1: Block diagram of closely spaced tracking scenario using bi-static passive radars

extended to develop conditional probability density function (pdf) of the sum signals to complex monopulse ratio. The conditional pdf is employed to calculate Crammer-Rao lower bound (CRLB) of the DOA estimator (Blair and Brandt-Pearce, 2001). Furthermore, an improved angle estimator is proposed to observe the signal strength of the two targets using in-phase and quadrature-phase of complex monopulse ratio (Blair and Brandt-Pearce, 1998a).

The following contributions are based on non-Bayesian estimation techniques. Maximum likelihood (ML) estimator to extract the angle of closely spaced targets with Swerling-I and Swerling-III models is presented in (Sinha et al., 2002). The closed form solution to ML estimator of (Sinha et al., 2002) is suggested in (Wang et al., 2004). A search radar with ML estimator to detect the closely spaced targets by changing the pattern of antenna main beam has been proposed in (Farina et al., 2002). The results in this technique were promising that the estimated values are comparable to CRLB. In (Gini et al., 2003, 2004) asymptotic maximum likelihood (AML) estimator and sequential hypothesis testing approach is suggested to solve the global maximization of ML approach. All the above mentioned techniques utilized a single matched filter for pulse compression.

In general, the radar target returns of single/multiple targets leaks to minimum of one adjoint range cell. With this knowledge, a correlated consecutive matched filter is developed to detect maximum of five closely spaced targets (Zhang et al., 2005). Based on Gibbs sampling with ML approach and particle filtering, closely spaced targets are detected and tracked in (Isaac et al., 2007). All the above algorithms used monopulse based signal processing to detect the closely spaced targets.

Besides monopulse DOA and other DOA estimators like multiple signal classification (MUSIC) (Bruckstein et al., 1985), estimation of signal parameters via rotational invariance technique (ESPRIT), etc are proposed to detect the closely spaced targets (Baig and Malik, 2013). In recent years, a new short time Fourier transform (STFT) based MUSIC algorithm is proposed to detect closely spaced sources (Zhang et al., 2016). The STFT has single constant window length and due to this, STFT based

MUSIC algorithm provides poor frequency resolution either at low or high frequency signals.

To overcome this problem, this chapter presents Stockwell transform based MUSIC DOA estimator to resolve closely spaced targets in the presence of strong interference (ECM, clutter and FA) using bi-static passive radars. The Stockwell transform has a variable window size, which varies according to the frequency of the signal. This variable window size helps to resolve the two different frequency signals which are closely spaced. Further, the angles are used to estimate the future state of the closely spaced targets by using RBMCDA based EKF tracker.

### 6.3 Proposed Stockwell transform based MUSIC DOA algorithm

In the proposed Stockwell transform based MUSIC DOA algorithm, two N-element equally spaced uniform circular arrays (UCA) are used to acquire the angle of the targets in the presence of ECM as illustrated in Figure 6.1. Let  $u_i(k)$ ,  $i = 1, 2, \dots, M$ , be the number of known signals that impinges on N-element UCA at  $k^{th}$  observation snapshot. Then the output at N-dimensional sensor array is given as

$$Z(k) = s(\theta)u(k) + n(k) \quad (6.1)$$

Where,  $s(\theta) = [s(\theta_1), s(\theta_2), \dots, s(\theta_M)]$  represents the array complex valued manifold matrix and  $s(\theta_m)$  denotes the steering vector of source  $m$ . The output signals from the sensor array are defined as  $Z(k) = [Z_1(k), Z_2(k), \dots, Z_N(k)]^T$  and  $n(k)$  is Gaussian white noise with zero mean.

The Stockwell transform ( $\mathcal{T}$ ) (Stockwell et al., 1996) of the signals at the sensor output in a noise free environment is given as

$$\begin{aligned}
\mathcal{T}_z(t, f) &= s(\theta)\mathcal{T}_u(t, f) \\
&= [s(\theta_1) \quad s(\theta_2) \quad \dots \quad s(\theta_M)] \begin{bmatrix} \mathcal{T}_{u1}(t, f) \\ \mathcal{T}_{u2}(t, f) \\ \vdots \\ \mathcal{T}_{uM}(t, f) \end{bmatrix}
\end{aligned} \tag{6.2}$$

Where,  $\mathcal{T}_{ui}(t, f)$  represents the Stockwell transform of the signal from source  $i$ .

The steering vector from source  $i$  is denoted as  $s(\theta_i) = [s_{i1}, s_{i2}, \dots, s_{iN}]^T$ ;  $i = 1, 2, \dots, M$  and its  $N^{th}$  element value is given by

$$s_{iN} = \frac{1}{\sqrt{N}} e^{-j\frac{2\pi}{\lambda} d(n-1)\sin(\theta_i)}; \quad n \in \{1, 2, \dots, N\} \tag{6.3}$$

Where,  $\lambda$  is the wavelength,  $d$  is the inter element spacing between arrays and  $\theta_i$  indicates the direction of arrival from source  $i$  which has to be estimated.

Let,  $\mathcal{W}_{uu}(t, f)$  describe the Stockwell transform matrix of the input signal and it is given below:

$$\mathcal{W}_{uu}(t, f) = \begin{bmatrix} \mathcal{T}_{u1}(t, f)\mathcal{T}_{u1}^*(t, f) & \dots & \mathcal{T}_{u1}(t, f)\mathcal{T}_{uM}^*(t, f) \\ \vdots & \vdots & \vdots \\ \mathcal{T}_{uM}(t, f)\mathcal{T}_{u1}^*(t, f) & \dots & \mathcal{T}_{uM}(t, f)\mathcal{T}_{uM}^*(t, f) \end{bmatrix} \tag{6.4}$$

The DOA is estimated by choosing the peaks of the spatial spectrum derived using Stockwell transform based MUSIC DOA algorithm which is determined as

$$\mathcal{P}(\theta) = \frac{s^H(\theta)s(\theta)}{s^H(\theta)e_n e_n^H s(\theta)} \tag{6.5}$$

Where,  $e_n$  is the noise eigen values of Stockwell transform matrix which is computed from Equation 6.4.

The measurements (in terms of angles) of targets which are obtained from Equation 6.5 are given as input to Rao-Blackwellized Monte Carlo data association (RBMCD) based extended Kalman filter (EKF) to further estimate the next state of the target. This technique is briefly described in the following section.

## 6.4 Rao-Blackwellized Monte Carlo data association based extended Kalman filter (EKF)

This section presents bearing only tracking for multiple targets using EKF based on RBMCDA approach. A brief explanation of RBMCDA based EKF tracker is described in (Särkkä et al., 2004; Hartikainen and Särkkä, 2008; Beard and Arulampalam, 2007).

### 6.4.1 Extended Kalman filter

In general, EKF is a non linear target tracking algorithm used for single target tracking with angle only measurements. The mean and covariance of the target is updated by using the measurements obtained from sensors. Let  $x_l^j$  and  $P_l^j$  be the state and covariance of target  $j$  at  $l^{th}$  time instant. Then the dynamic model of target  $j$  is given as

$$x_l^j = F x_{l-1}^j + v_l^j \quad (6.6)$$

Where,  $F$  is the state transition matrix and  $v_l^j$  is the process noise of  $j^{th}$  target at  $l^{th}$  instant. Let the number of sensors be  $m$ . Then the single target tracking equations for EKF are as follows.

The predicted state ( $\hat{x}_{l|l-1}^j$ ) and covariance ( $\hat{P}_{l|l-1}^j$ ) equations are given as

$$\hat{x}_{l|l-1}^j = F \hat{x}_{l-1|l-1}^j \quad (6.7)$$

$$\hat{P}_{l|l-1}^j = F P_{l-1|l-1}^j F^T + Q \quad (6.8)$$

Where  $Q$  is the covariance of process noise.

The updated state and covariance equations are described as

$$\hat{x}_{l|l}^j = \hat{x}_{l|l-1}^j + G_l^j \tilde{Z}_l^j \quad (6.9)$$

$$\hat{P}_{l|l}^j = [I - G_l^j H_l] P_{l|l-1}^j \quad (6.10)$$

Where  $G_l^j$ ,  $H_l$  and  $\tilde{Z}_l^j$  are gain, measurement and innovation matrix respectively which are calculated as

$$G_l^j = P_{l|l-1} H_l^T [H_l P_{l|l-1} H_l^T + R]^{-1} \quad (6.11)$$

$$H_l^j = \frac{\partial h(x, s^m)}{\partial x} \Big|_{x=\hat{x}_{l|l-1}^j} \quad (6.12)$$

and

$$\tilde{Z}_l^j = Z_l - Z_{l|l-1} \quad (6.13)$$

Where,  $Z_l$  is the measurement obtained from sensors and  $Z_{l|l-1}$  is measurement prediction which is given as

$$Z_{l|l-1} = h(\hat{x}_{l|l-1}^j, s^m) \quad (6.14)$$

where,  $h$  is a nonlinear term. The above Equations represent EKF tracker for single target tracking. If the targets are more than one in the environment then RBMCDA data association is used, so that multi-target tracking problem is solved into single target tracking problem. Flow chart of the entire process is illustrated in Figure 6.2.

## 6.4.2 Rao-Blackwellized Monte Carlo data association

RBMCDA is used to assign the correct measurements to the right targets in multi-target tracking scenario. The number of targets and the distribution of measurements are assumed to be known a priori. RBMCDA consists of group of particles and each particle comprises particle weight along the state and covariance of a particular target. Both the state and covariance are updated by using EKF.

The issue of multi-target tracking is divided into two subproblems i.e, single target tracking and data association. Particle filter is used to solve the problem of data association and tracking problem is solved by EKF, once the measurements are associated properly to the target. A concise description of RBMCDA is given in (Hartikainen and Särkkä, 2008).

An example for two sensors and two targets is considered for simplicity. Let, the

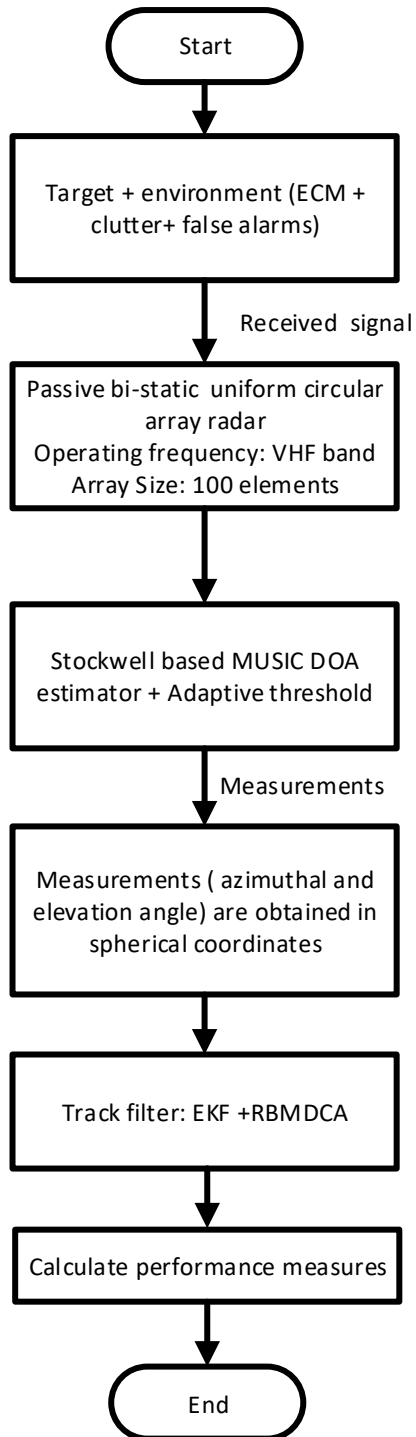


Figure 6.2: Flowchart of entire process

number of particles be  $O$ , then particle preserves the state, covariance and particle weight of both the targets. The  $b^{th}$  particle at  $l^{th}$  instant of time is represented as

$$\mathcal{P} = \{x_l^{1,b}, P_l^{1,b}, x_l^{2,b}, P_l^{2,b}, \omega_l^b\} \quad (6.15)$$

Where,  $x_l^{t,b}$  and  $p_l^{t,b}$  are state and covariance of the  $t$  at  $l^{th}$  time instant.  $\omega_l^b$  is the associated particle weight value. Bearing intersection criterion is used to initialize the particles. The association weight of all particles is initialized to  $\frac{1}{O}$  i.e, each particle is given equal prior. Sequential importance resampling (SIR) is used to update the particles by using the measurements. The algorithm of SIR is described in the following steps.

- i. The state and covariance of the targets are predicted.
- ii. Normalized association value is calculated by using prior association probability and measurement likelihood function.

$$p(c_l^b | Z_{1:l}, c_{1:l-1}^b) \propto p(Z_l | c_l, Z_{1:l-1}, c_{1:l-1}^b) p(c_l) \quad (6.16)$$

Where  $c_l^b$  is association event to a particular target.

- iii. The association value is sampled using optimal importance distribution to obtain new measurements

$$c_l^b \sim p(c_l^b | Z_{1:l}, c_{1:l-1}^b) \quad (6.17)$$

- iv. State and covariance values of a particular target are updated using the new measurement.
- v. New particle weight is calculated by using

$$\omega_l^b \sim \omega_{l-1}^b \times \frac{p(Z_l | c_l^b, Z_{1:l-1}, c_{1:l-1}^b) p(c_l^b | c_{1:l-1}^b)}{p(c_l^b | Z_{1:l-1}, c_{1:l-1}^b)} \quad (6.18)$$

The new updated particle weight is normalized and the effective number of particles is computed as

$$O_{eff} = \frac{1}{\sum_{i=1}^O (\omega_i^b)^2} \quad (6.19)$$

The process of resampling is repeated if the  $O_{eff}$  is less than the threshold value and the particle weights are assigned to  $\frac{1}{O_{eff}}$ . The next section describes the simulation

results and associated discussion.

## 6.5 Results and discussion

Closely spaced benchmark target trajectories from (Sinha et al., 2002, 2006) are considered to validate the proposed algorithm. The Stockwell transform based MUSIC DOA algorithm results are compared with existing algorithms (MUSIC (Bruckstein et al., 1985) and STFT based MUSIC (Zhang et al., 2016)). Two 100 elements equally spaced UCAs with radius 80m (approx) are considered to receive the signal. The UCAs are passive radars operating at very high frequency band (VHF). The environment is considered to be effected by ECM, clutter and FAs. Barrage jammer (Mahafza and Elsherbeni, 2003) is taken to induce ECM in the radar side lobes along with gamma clutter (Barton, 1985) influences the environment. Adaptive thresholding (Dersan and Tanik, 2002) for angle of arrival is used to suppress the jamming and clutter. A constant signal to noise ratio of 20dB is considered at any instant of time. The entire process is illustrated in Figure 6.2. The parameters such as state transition matrix, process and noise covariance values are considered from (Sinha et al., 2002; Hartikainen and Särkkä, 2008; Sinha et al., 2006; Isaac et al., 2007).

### 6.5.1 Case 1

Trajectories of scenario 8 in (Sinha et al., 2006) is considered for case study 1. The two trajectories are parallel traveling with zero acceleration. The initial position of the target-1 is  $(10e3, -250, 3e3)m$ , while the initial position of target-2 is  $(10e3, 250, 3e3)m$ . The trajectory is executed for 220s. The first UCA radar is placed at  $(40e3, 300, 20)m$  and the second UCA radar is placed at  $(40e3, 300, 20)m$ . Direction of arrival angles are taken using MUSIC, STFT based MUSIC and Stockwell transform based MUSIC DOA algorithms. Using these angles, tracking is performed by using EKF which is illustrated in Figure 6.3. The tracking parameters for EKF are considered from (Isaac et al., 2007). Position root mean square error (RMSE) of target-1 and target-2 are shown in Figure

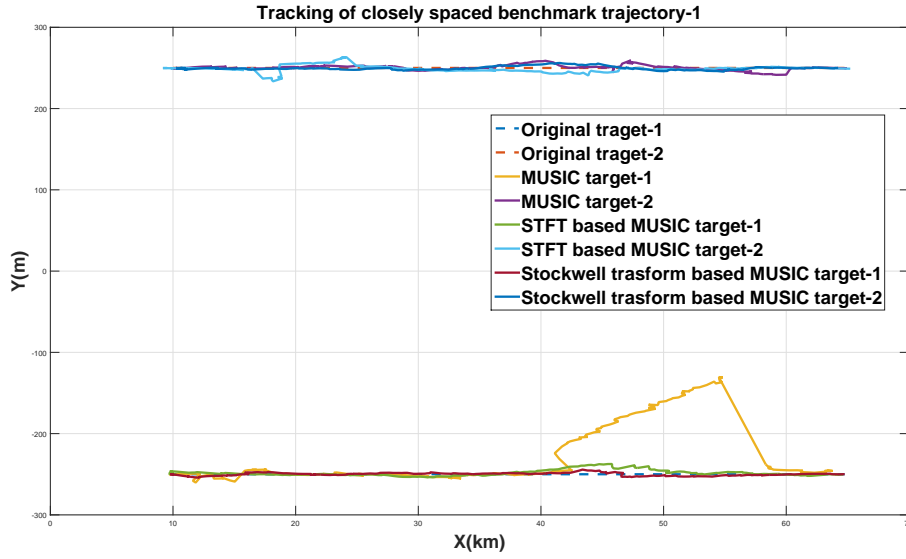


Figure 6.3: Tracking of closely spaced benchmark scenario-1

6.4 and 6.5 respectively.

### 6.5.2 Case 2

Trajectories of scenario 9 in (Sinha et al., 2006) are examined for second case study. The initial range, velocity and height of the targets are considered to be  $68km$ ,  $290m/s$  and  $3.5km$  respectively. The entire simulation time of trajectory is  $215s$ . The targets makes a  $2g$  turn after  $100s$  for a period of  $20s$ . The first UCA radar is placed at  $(6e4, 1.5e4, 20)m$  and the second UCA radar is placed at  $(30e3, 0, 20)m$ . Direction of arrival angles are taken using MUSIC, STFT based MUSIC and Stockwell transform based MUSIC DOA algorithms. However, the targets are unresolved by MUSIC DOA algorithm. The tracking of closely spaced benchmark scenario-2 using STFT based MUSIC and Stockwell transform based MUSIC DOA is depicted in Figure 6.6 and 6.7 respectively. The tracking parameters for EKF are considered from (Sinha et al., 2002). Position RMSE of target-1 and target-2 are depicted in Figure 6.8 and 6.9 respectively.

Comparison of results for closely spaced benchmark target scenario is shown in Table6.1. From Table6.1 it is can be noticed that Stockwell transform based MUSIC DOA performance is superior compared to other two existing algorithms. The Stock-

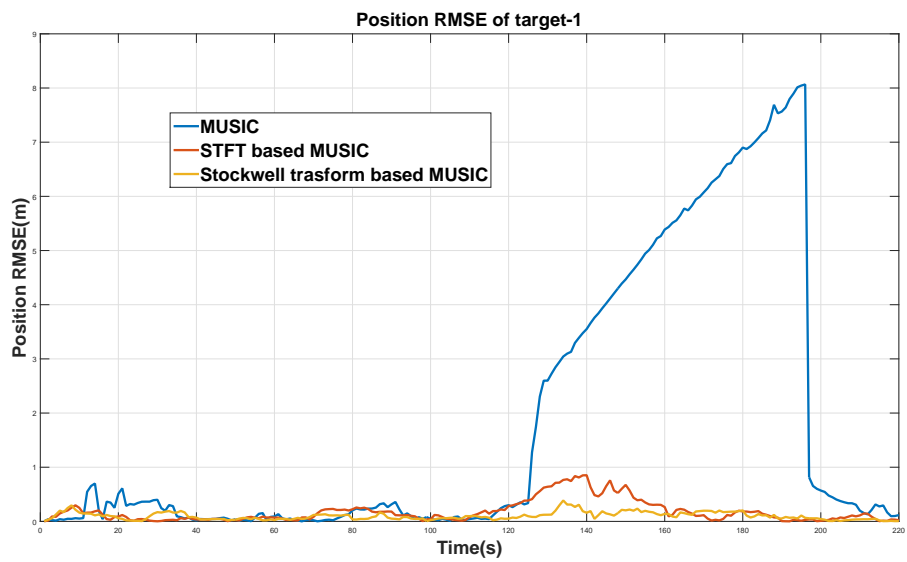


Figure 6.4: Position RMSE of target-1 from closely spaced benchmark scenario-1

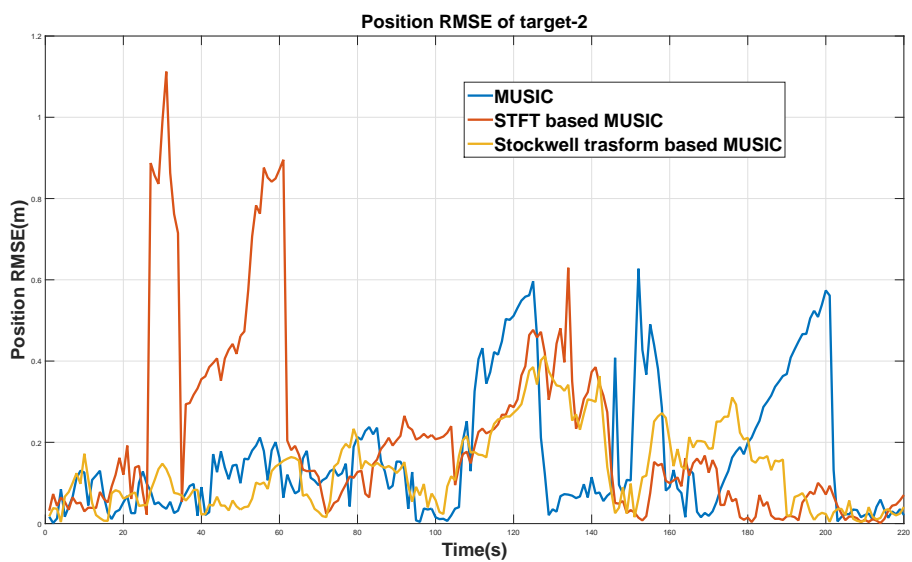


Figure 6.5: Position RMSE of target-2 from closely spaced benchmark scenario-1

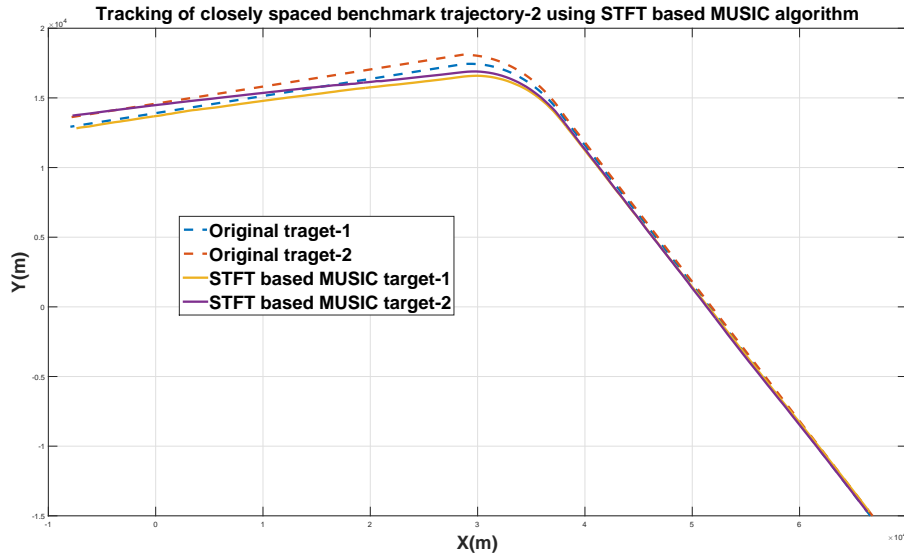


Figure 6.6: Tracking of closely spaced benchmark scenario-2 using STFT based MUSIC

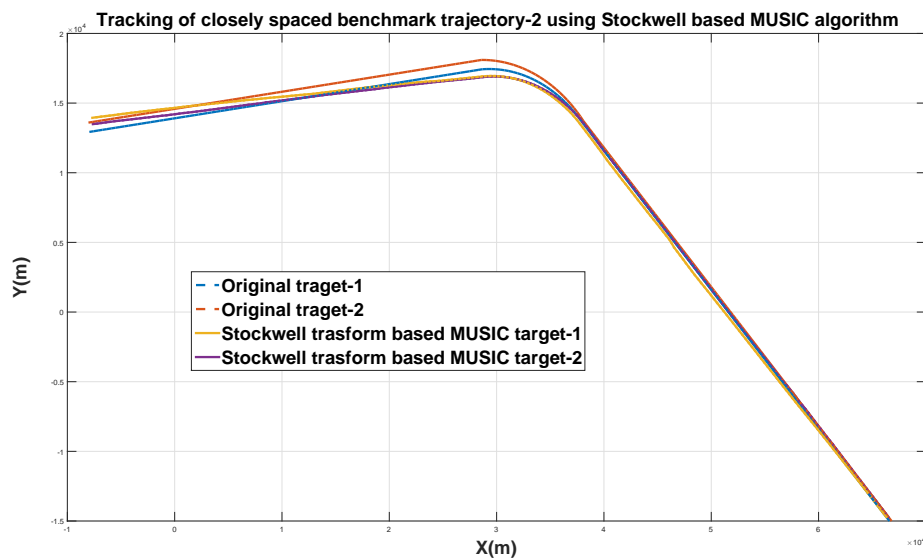


Figure 6.7: Tracking of closely spaced benchmark scenario-2 using Stockwell transform based MUSIC

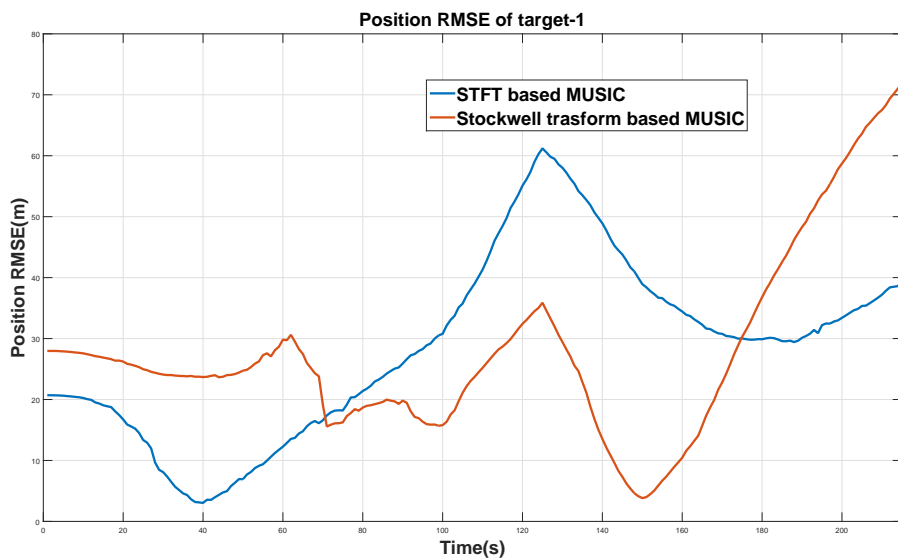


Figure 6.8: Position RMSE of target-1 from closely spaced benchmark scenario-2

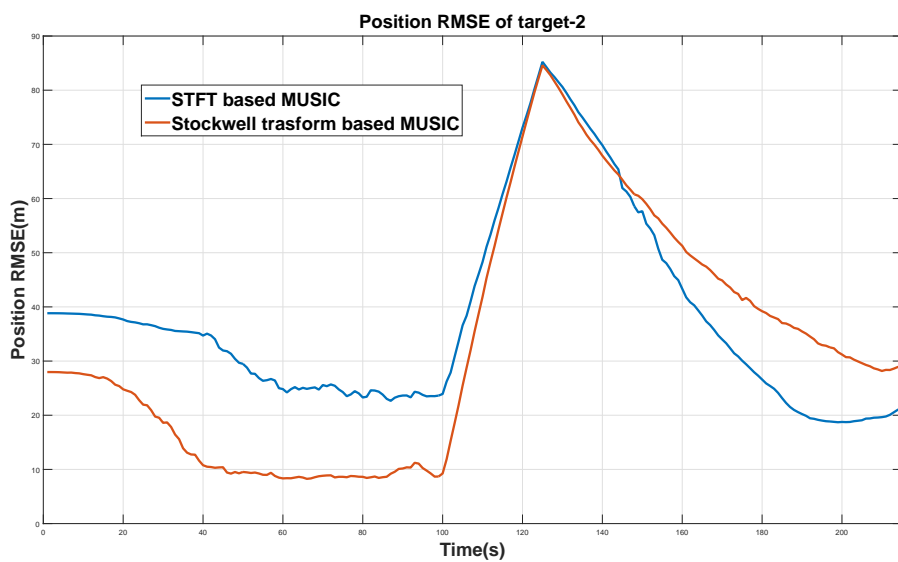


Figure 6.9: Position RMSE of target-2 from closely spaced benchmark scenario-2

Table 6.1: Comparison of results for closely spaced benchmark target scenario

Sl.no	Target number	Time length (s)	Max .Acc. ( $m/s^2$ )	MUSIC		STFT-MUSIC		Stockwell-MUSIC	
				Pos. RMSE ( $m$ )	Vel. RMSE ( $m/s$ )	Pos. RMSE ( $m$ )	Vel. RMSE ( $m/s$ )	Pos. RMSE ( $m$ )	Vel. RMSE ( $m/s$ )
Benchmark Scenario-1									
1	1	220	0	46.96	0.78	3.96	0.14	1.80	0.11
2	2			3.33	0.19	4.63	0.16	2.42	0.09
Benchmark Scenario-2									
3	1	215	21	*	*	471.35	9.42	461.19	11.14
4	2			*	*	611.12	15.7	579.24	14.79

\* represents unresolved targets.

well transform based MUSIC DOA algorithm possess an improved position RMSE ( 91.56% and 96.16% when compared to MUSIC and STFT based MUSIC DOA algorithms respectively) for benchmark scenario 1. But, there is a decrease in position RMSE of STFT based MUSIC DOA when compared to MUSIC DOA by 28.03% for target-2. However, the position RMSE of target-2 is increased by 27.21% for Stockwell transform based MUSIC DOA algorithm when compared to MUSIC DOA technique. Similarly, the velocity RMSE of Stockwell transform based MUSIC and STFT based MUSIC DOA algorithms has an average increment of (69.26% and 48.91% for target-1 and target-2 respectively) when compared to MUSIC DOA algorithm.

The MUSIC DOA algorithm fails to resolve the targets for closely spaced benchmark scenario-2. The Stockwell transform based MUSIC position RMSE for target-1 and target-2 is increased by 2.15% and 5.21% respectively, compared to STFT based MUSIC DOA algorithm. However, there is a decrease in velocity RMSE for target-1 of Stockwell transform based MUSIC DOA algorithm by 15.43% as compared to STFT based MUSIC DOA technique. The velocity RMSE of target-2 using Stockwell transform based MUSIC DOA algorithm has an improvement by 5.79% as compared to STFT based MUSIC DOA technique.

This work is carried out using bi-static passive radars. One can carry out future research by considering multi-static passive radar scenario. Further, performance improvement can be accomplished by using interacting multiple model based track filters. Besides that, the present study ignores other ECM techniques such as self screening jammer (SSJ), velocity gate pull off (VGPO) and range gate pull off (RGPO). Future research work may be carried out by incorporating these ECM techniques.

## **6.6 Conclusion**

Stockwell transform based multiple signal classification (MUSIC) direction of arrival (DOA) estimator for closely spaced targets has been demonstrated in the presence of strong interference. Bi-static passive radars have been considered to resolve closely

spaced maneuvering targets. Rao-Blackwellized Monte Carlo data association (RBM-CDA) based extended Kalman filter (EKF) was successfully deployed to track closely spaced benchmark target trajectories. The proposed Stockwell transformed based MUSIC DOA algorithm is compared with MUSIC and STFT based MUSIC DOA approaches. Simulation results show that Stockwell transform based MUSIC algorithm has an average improvement of (61.68% and 69.26%; 51.11% and 32.58% ) compared to (MUSIC based DOA; STFT based MUSIC DOA) in terms of position and velocity RMSEs respectively for tracking benchmark trajectory-1. Furthermore, the proposed Stockwell transform based approach resolved closely spaced targets which were unresolved in existing MUSIC based DOA algorithm.



# CHAPTER 7

## CONCLUSIONS AND FUTURE WORK

This chapter concludes the thesis with a summary of the contributions of research work along with some suggestions for future work to be carried out.

### 7.1 Conclusions

In this thesis alternative solutions to three major challenging problems of target tracking in the presence of ECM is addressed. Improved performance for tracking benchmark trajectories has been demonstrated using waveform agile sensing technique in the presence of strong interference (ECM, FAs, clutter and multipath). Further, space time adaptive processing (STAP) combined with WAS was suggested to improve the performance in terms of RMSE. The track performance is improved by applying 5 to 50 frequency coded waveforms from the waveform bank. IMM-PDAF estimator is employed to track highly maneuvering benchmark target trajectories with ECM (SSJ/SOJ), multipath and background clutter. It can also be noticeable that there is a decrease in both position and velocity RMSE with increase in number of waveforms in waveform bank from 5 to 50. However, there is an increase in position and velocity RMSEs when compared to earlier fixed waveform studies. Results obtained reveals that there is a decrease in position and velocity RMSE values with slight increase in radar cost functions while using WAS with space time adaptive processing.

Secondly, two novel hybrid data association techniques (Fuzzy-GA and Fuzzy-PSO) have been successfully applied for tracking multiple targets in the presence of strong interference. The probability data association matrix in JPDA is replaced by optimized fuzzy correlation matrix. The next state of the target is predicted by applying optimized fuzzy correlation matrix, which is evaluated based on proposed Fuzzy-GA and Fuzzy-PSO approaches. Additionally, a comprehensive research study was carried out with

four data association techniques (JPDA, FCM, Fuzzy-PSO, and Fuzzy-GA) for four different cases. It can be noticed from the results that there is a reduction in RMSE values with increase in computational complexity especially for Fuzzy-GA association technique. Besides this, two computationally efficient data association algorithms (all neighbor fuzzy- relational and rough fuzzy) have been accomplished. A through study is done by considering five jamming power levels with five data association approaches. Furthermore, the computational complexity was reduced with comparable RMSEs when compared to soft and evolutionary computation based hybrid data association techniques. Rough fuzzy based data association approach has accomplished comparable RMSE performance with reduced computational complexity.

Finally, Stockwell transform based MUSIC direction of arrival algorithm (DOA) was proposed to address the problem of closely spaced targets in the presence of strong interference. Bi-static passive radars have been considered to resolve closely spaced maneuvering targets. Rao-Blackwellized Monte Carlo data association (RBMCD) based extended Kalman filter (EKF) was successfully deployed to track closely spaced benchmark target trajectories. The proposed Stockwell transform based MUSIC DOA obtained better results compared with MUSIC and STFT based MUSIC algorithms. Furthermore, the proposed Stockwell transform based approach resolved closely spaced targets which were unresolved in existing MUSIC based DOA algorithms.

The chapters two and three of the thesis deal with waveform agile sensing approach with phased array antenna radar in the presence of strong interference. In particular, the chapter three presents spatio-temporal adaptive processing (STAP) based technique to mitigate the strong interference. The research results indicate these techniques can be deployed in practical scenarios with phased array radar which will enhance the performance of surveillance system.

Further, the novel soft and evolutionary based data association approaches presented in chapter four and five will improve the performance of the surveillance system as these techniques have given enhanced performance in terms of position and velocity RMSE values in the presence of strong interference. Furthermore, the computational efficiency

Fuzzy based approaches presented in chapter five will be a candidate algorithm for real-time practical applications in various types of ground-based and airborne surveillance systems. Finally, Chapter six presents a novel approach based on Stockwell transform-MUSIC to track closely spaced targets in the presence of a strong interface.

Therefore, all the contributed chapters presented in the thesis will have significant impact on phased array radar based surveillance systems which generally operates in the presence of a combination of clutter, ECM, and false alarms.

## **7.2 Future work**

Even though some of the tracking issues in the presence of ECM scenario are addressed in this thesis, there is a strong need to carryout further research in this area to improve the results. In the case of waveform agile sensing, only point targets have been assumed in our research study, one can carryout future research with extended targets. Besides this, only frequency coded waveforms were used for waveform agile sensing and phase coded waveforms have not been explored. Furthermore, ECM techniques such as; range gate pull off (RGPO) and velocity gate pull off (VGPO) were not examined.

Whereas in the area of data association one can carry out future research work in multiple target tracking by deploying multi-objective evolutionary computing techniques such as multi-objective particle swarm optimization (MOPSO), nondominated sorting genetic algorithm II (NSGA-II), etc. to simultaneously optimize track performance and computational complexity. Furthermore, the current research study in multiple target tracking is carried out by using fixed linear frequency modulated (LFM) waveform. Future researchers can carry out further work by using adaptive waveform selection, waveform agile sensing, adaptive pulse compression, etc. to improve the performance in the presence of ECM for data association problems.

Besides that, current investigation of data association ignored closely spaced targets and unresolved targets. Hence, one can carry out further research in this domain. Moreover, our data association study is focused using stand-off jammer (SOJ), clutter and

false alarms (FA) but not considered multipath into account and one can incorporate other ECM techniques like self-screening jammer (SSJ), range gate pull-off (RGPO), velocity gate pull-off (VGPO) etc. and carry out future work in this direction. In addition, a future research work can be carried out by using space-time adaptive processing (STAP) approach using multi-input and multi-output (MIMO) radar and multi-static radar scenarios.

In our research study for tracking benchmark closely spaced targets, only passive bi-static radar framework was considered to resolve closely spaced targets. Future research may be aimed at using active and multi-static radar scenarios. Performance improvement can further be accomplished by using interacting multiple model based track filters.

## REFERENCES

- Angelova, D., Semerdjiev, E., Mihaylova, L., and Li, X. R. (1999). “An IMMPPDAF Solution to Benchmark Problem for Tracking in Clutter and Standoff Jammer.” In *Proceedings of the International Conference on EuroFusion*, 99, 123–128.
- Aziz, A. M. (2007). “Fuzzy track-to-track association and track fusion approach in distributed multisensor–multitarget multiple-attribute environment.” *Signal Processing*, 87(6), 1474–1492.
- Aziz, A. M. (2008). “A simple and efficient suboptimal multilevel quantization approach in geographically distributed sensor systems.” *Signal Processing*, 88(7), 1698–1714.
- Aziz, A. M. (2011). “A novel all-neighbor fuzzy association approach for multitarget tracking in a cluttered environment.” *Signal Processing*, 91(8), 2001–2015.
- Aziz, A. M. (2013). “A new nearest-neighbor association approach based on fuzzy clustering.” *Aerospace Science and Technology*, 26(1), 87–97.
- Aziz, A. M. (2014). “A joint possibilistic data association technique for tracking multiple targets in a cluttered environment.” *Information Sciences*, 280, 239–260.
- Aziz, A. M. (2015). “A new multitarget tracking approach based on a non-iterative fuzzy clustering means algorithm.” In *2015 IEEE Aerospace Conference*, 1–10. IEEE.
- Aziz, A. M., Tummala, M., and Cristi, R. (1999). “Fuzzy logic data correlation approach in multisensor–multitarget tracking systems.” *Signal Processing*, 76(2), 195–209.
- Baig, N. A. and Malik, M. B. (2013). “Comparison of direction of arrival (DOA) estimation techniques for closely spaced targets.” *International Journal of Future Computer and Communication*, 2(6), 654.
- Balleri, A., Nehorai, A., and Wang, J. (2007). “Maximum likelihood estimation for compound-Gaussian clutter with inverse gamma texture.” *Aerospace and Electronic Systems, IEEE Transactions on*, 43(2), 775–779.
- Bar-Shalom, Y. (1987). “Tracking and data association.” Academic Press Professional, Inc.
- Bar-Shalom, Y. (1990). “Multitarget-multisensor tracking: advanced applications.” *Norwood, MA, Artech House, 1990, 391 p.*, 1.
- Bar-Shalom, Y. (2000). “Multitarget-multisensor tracking: Applications and advances. Volume III.” *Norwood, MA, Artech House, Inc., 2000.*

- Bar-Shalom, Y., Chang, K., and Blom, H. A. (1989). "Tracking a maneuvering target using input estimation versus the interacting multiple model algorithm." *Aerospace and Electronic Systems, IEEE Transactions on*, 25(2), 296–300.
- Bar-Shalom, Y. and Fortmann, T. (1988). "Tracking and Data Association." Mathematics in Science and Engineering Series. Academic Press.
- Bar-Shalom, Y. and Li, X.-R. (1995). "Multitarget-multisensor tracking: principles and techniques," 19. YBs London, UK:.
- Bar-Shalom, Y., Li, X. R., and Kirubarajan, T. (2004). "Estimation with applications to tracking and navigation: theory algorithms and software." John Wiley & Sons.
- Barton, D. K. (1985). "Land clutter models for radar design and analysis." *Proceedings of the IEEE*, 73(2), 198–204.
- Beard, M. and Arulampalam, S. (2007). "Comparison of data association algorithms for bearings-only multi-sensor multi-target tracking." In *Information Fusion, 2007 10th International Conference on*, 1–7. IEEE.
- Behar, V., Angelova, D., Vassileva, B., Kabakchiev, C., and Semerdjiev, E. (2001). "A Set of Algorithms for Radar Management and Target Tracking in the Presence of SOJ." *Comptes Rendus de l'Academie Bulgare des Sciences*, 54(7), 17.
- Behar, V. and Kabakchiev, C. (2002). "Radar waveform allocation by using post detection integration." *Comptes Rendus de l'Academie Bulgare des Sciences*, 55(1), 63.
- Blackman, S., Dempster, R., Busch, M., and Popoli, R. (1999). "IMM/MHT solution to radar benchmark tracking problem." *Aerospace and Electronic Systems, IEEE Transactions on*, 35(2), 730–738.
- Blackman, S. S. (1986). "Multiple-target tracking with radar applications." *Dedham, MA, Artech House, Inc., 1986, 463 p.*, 1.
- Blair, W. and Brandt-Pearce, M. (1998a). "Statistical description of monopulse parameters for tracking Rayleigh targets." *IEEE Transactions on Aerospace and Electronic Systems*, 34(2), 597–611.
- Blair, W., Watson, G., Gentry, G., and Hoffman, S. (1995). "Benchmark problem for beam pointing control of phased array radar against maneuvering targets in the presence of ECM and false alarms." In *American Control Conference, Proceedings of the 1995*, 4, 2601–2605. IEEE.
- Blair, W., Watson, G., and Hoffman, S. (1994). "Benchmark problem for beam pointing control of phased array radar against maneuvering targets." In *American Control Conference, 1994*, 2, 2071–2075. IEEE.
- Blair, W., Watson, G., Kirubarajan, T., and Bar-Shalom, Y. (1998). "Benchmark for radar allocation and tracking in ECM." *Aerospace and Electronic Systems, IEEE Transactions on*, 34(4), 1097–1114.

- Blair, W. D. and Brandt-Pearce, M. (1998b). “Unresolved Rayleigh target detection using monopulse measurements.” *IEEE Transactions on Aerospace and Electronic Systems*, 34(2), 543–552.
- Blair, W. D. and Brandt-Pearce, M. (2001). “Monopulse DOA estimation of two unresolved Rayleigh targets.” *IEEE Transactions on Aerospace and Electronic Systems*, 37(2), 452–469.
- Bruckstein, A., Shan, T.-J., and Kailath, T. (1985). “The resolution of overlapping echos.” *IEEE Transactions on Acoustics, Speech, and Signal Processing*, 33(6), 1357–1367.
- Chung, Y.-N., Chou, P.-H., and Yang, M.-R. (2007). “Multiple-target tracking with competitive hopfield neural network based data association.” *Aerospace and Electronic Systems, IEEE Transactions on*, 43(3), 1180–1188.
- Clark, D. E. and Bell, J. (2007). “Multi-target state estimation and track continuity for the particle PHD filter.” *Aerospace and Electronic Systems, IEEE Transactions on*, 43(4), 1441–1453.
- Daeipour, E., Bar-Shalom, Y., and Li, X. (1994). “Adaptive beam pointing control of a phased array radar using an IMM estimator.” In *American Control Conference, 1994*, 2, 2093–2097. IEEE.
- Dersan, A. and Tanik, Y. (2002). “Passive radar localization by time difference of arrival.” In *MILCOM 2002. Proceedings*, 2, 1251–1257. IEEE.
- Dubois, D., Prade, H., and Sudkamp, T. (2005). “On the representation, measurement, and discovery of fuzzy associations.” *Fuzzy Systems, IEEE Transactions on*, 13(2), 250–262.
- Farina, A., Gini, F., and Greco, M. (2002). “DOA estimation by exploiting the amplitude modulation induced by antenna scanning.” *IEEE Transactions on Aerospace and Electronic Systems*, 38(4), 1276–1286.
- Fisher, J. L. and Casasent, D. P. (1989). “Fast JPDA multitarget tracking algorithm.” *Applied optics*, 28(2), 371–376.
- Gad, A. S., Farooq, M., and Midwood, S. (2001). “Application of fuzzy logic to target tracking in a cluttered environment.” In *Aerospace/Defense Sensing, Simulation, and Controls*, 91–104. International Society for Optics and Photonics.
- Gan, G., Wu, J., and Yang, Z. (2009). “A genetic fuzzy k-Modes algorithm for clustering categorical data.” *Expert Systems with Applications*, 36(2), 1615–1620.
- George, B. (1990). Optimal radar tracking systems.
- Gini, F., Bordonni, F., and Farina, A. (2004). “Multiple radar targets detection by exploiting induced amplitude modulation.” *IEEE Transactions on Signal Processing*, 52(4), 903–913.

- Gini, F., Greco, M., and Farina, A. (2003). “Multiple radar targets estimation by exploiting induced amplitude modulation.” *IEEE Transactions on Aerospace and Electronic Systems*, 39(4), 1316–1332.
- Golberg, D. E. (1989). “Genetic algorithms in search, optimization, and machine learning.” *Addion wesley*, 1989, 102.
- Gorji, A. A., Tharmarasa, R., and Kirubarajan, T. (2011). “Performance measures for multiple target tracking problems.” In *Information Fusion (FUSION), 2011 Proceedings of the 14th International Conference on*, 1–8. IEEE.
- Hartikainen, J. and Särkkä, S. (2008). “RBMCDABox-Matlab toolbox of Rao-Blackwellized data association particle filters.” *documentation of RBMCDA Toolbox for Matlab V, 2008*.
- Hong, S.-M., Evans, R. J., and Shin, H.-S. (2005). “Optimization of waveform and detection threshold for range and range-rate tracking in clutter.” *Aerospace and Electronic Systems, IEEE Transactions on*, 41(1), 17–33.
- Isaac, A., Willett, P., and Bar-Shalom, Y. (2007). “MCMC methods for tracking two closely spaced targets using monopulse radar channel signals.” *IET Radar, Sonar & Navigation*, 1(3), 221–229.
- Izakian, H. and Abraham, A. (2011). “Fuzzy C-means and fuzzy swarm for fuzzy clustering problem.” *Expert Systems with Applications*, 38(3), 1835–1838.
- Kalman, R. E. et al. (1960). “A new approach to linear filtering and prediction problems.” *Journal of basic Engineering*, 82(1), 35–45.
- Kennedy, J., Kennedy, J. F., Eberhart, R. C., and Shi, Y. (2001). “Swarm intelligence.” Morgan Kaufmann.
- Kershaw, D. J. and Evans, R. (1997). “Waveform selective probabilistic data association.” *Aerospace and Electronic Systems, IEEE Transactions on*, 33(4), 1180–1188.
- Kershaw, D. J. and Evans, R. J. (1994). “Optimal waveform selection for tracking systems.” *Information Theory, IEEE Transactions on*, 40(5), 1536–1550.
- Kirubarajan, T., Bar-Shalom, Y., Blair, W., and Watson, G. (1998). “IMMPDAF for radar management and tracking benchmark with ECM.” *IEEE Transactions on Aerospace and Electronic Systems*, 34(4), 1115–1134.
- Kirubarajan, T., Bar-Shalom, Y., and Daeipour, E. (1995). “Adaptive beam pointing control of a phased array radar in the presence of ECM and false alarms using IMM-PDAF.” In *American Control Conference, Proceedings of the 1995*, 4, 2616–2620. IEEE.
- Kosko, B. (1992). “Neural networks and fuzzy systems: a dynamical systems approach to machine intelligence/book and disk.” *Vol. 1 Prentice hall*.

- Liang-Qun, L. and Wei-Xin, X. (2014). “Intuitionistic fuzzy joint probabilistic data association filter and its application to multitarget tracking.” *Signal Processing*, 96, 433–444.
- Magdalena, L. and Monasterio, F. (1995). “Evolutionary-based learning applied to fuzzy controllers.” In *Fuzzy Systems, 1995. International Joint Conference of the Fourth IEEE International Conference on Fuzzy Systems and The Second International Fuzzy Engineering Symposium., Proceedings of 1995 IEEE Int*, 3, 1111–1118. IEEE.
- Mahafza, B. R. (2008). “Radar signal analysis and processing using MATLAB.” CRC Press.
- Mahafza, B. R. and Elsherbeni, A. (2003). “MATLAB simulations for radar systems design.” CRC press.
- Mazor, E., Averbuch, A., Bar-Shalom, Y., and Dayan, J. (1998). “Interacting multiple model methods in target tracking: a survey.” *Aerospace and Electronic Systems, IEEE Transactions on*, 34(1), 103–123.
- Miao, L., Zhang, J. J., Chakrabarti, C., and Papandreou-Suppappola, A. (2011). “Algorithm and parallel implementation of particle filtering and its use in waveform-agile sensing.” *Journal of Signal Processing Systems*, 65(2), 211.
- Molnar, K. J. and Modestino, J. W. (1998). “Application of the EM algorithm for the multitarget/multisensor tracking problem.” *Signal Processing, IEEE Transactions on*, 46(1), 115–129.
- Mosca, E. (1969). “Angle estimation in amplitude comparison monopulse systems.” *IEEE Transactions on Aerospace and Electronic Systems*, (2), 205–212.
- Nguyen, N., Dogancay, K., and Davis, L. (2015). “Adaptive waveform selection for multistatic target tracking.” *Aerospace and Electronic Systems, IEEE Transactions on*, 51(1), 688–701.
- Niu, R., Willett, P., and Bar-Shalom, Y. (2002). “Tracking considerations in selection of radar waveform for range and range-rate measurements.” *Aerospace and Electronic Systems, IEEE Transactions on*, 38(2), 467–487.
- Osman, H. M., Farooq, M., and Quach, T. (1996). “Fuzzy logic approach to data association.” In *Aerospace/Defense Sensing and Controls*, 313–322. International Society for Optics and Photonics.
- Pang, W., Wang, K.-p., Zhou, C.-g., and Dong, L.-j. (2004). “Fuzzy discrete particle swarm optimization for solving traveling salesman problem.” In *Computer and Information Technology, 2004. CIT'04. The Fourth International Conference on*, 796–800. IEEE.
- Panta, K., Vo, B.-N., and Singh, S. (2007). “Novel data association schemes for the probability hypothesis density filter.” *IEEE Transactions on Aerospace and Electronic Systems*, 43(2), 556–570.

- Perlovsky, L. I. and Deming, R. W. (2007). “Neural networks for improved tracking.” *IEEE Transactions on Neural Networks*, 18(6), 1854–1857.
- Poli, R., Kennedy, J., and Blackwell, T. (2007). “Particle swarm optimization.” *Swarm intelligence*, 1(1), 33–57.
- Rabideau, D. J. (2000). “Clutter and jammer multipath cancellation in airborne adaptive radar.” *IEEE Transactions on Aerospace and Electronic Systems*, 36(2), 565–583.
- Rago, C. and Mahra, R. (1997). “Target tracking in the presence of ECM: a filter design tool.” In *System Theory, 1997., Proceedings of the Twenty-Ninth Southeastern Symposium on*, 514–518. IEEE.
- Rago, C., Willett, P., and Bar-Shalom, Y. (1998). “Detection-tracking performance with combined waveforms.” *Aerospace and Electronic Systems, IEEE Transactions on*, 34(2), 612–624.
- Särkkä, S., Vehtari, A., and Lampinen, J. (2004). “Rao-Blackwellized Monte Carlo data association for multiple target tracking.” In *Proceedings of the seventh international conference on information fusion*, 1, 583–590.
- Satapathi, G. S. and Pathipati, S. (2017). “Waveform Agile Sensing Approach for Tracking Benchmark in the Presence of ECM using IMM-PDAF.” *Radioengineering*, 26(1), 227.
- Savage, C. O. and Moran, B. (2007). “Waveform selection for maneuvering targets within an IMM framework.” *Aerospace and Electronic Systems, IEEE Transactions on*, 43(3), 1205–1214.
- Sengupta, D. and Iltis, R. A. (1989). “Neural solution to the multitarget tracking data association problem.” *Aerospace and Electronic Systems, IEEE Transactions on*, 25(1), 96–108.
- Sherman, S. M. (1988). “Monopulse principles and techniques.” *Aspects of Modern Radar*, 297–335.
- Silva Filho, T. M., Pimentel, B. A., Souza, R. M., and Oliveira, A. L. (2015). “Hybrid methods for fuzzy clustering based on fuzzy c-means and improved particle swarm optimization.” *Expert Systems with Applications*, 42(17), 6315–6328.
- Singh, R.-N. P. and Bailey, W. H. (1997). “Fuzzy logic applications to multisensor-multitarget correlation.” *Aerospace and Electronic Systems, IEEE Transactions on*, 33(3), 752–769.
- Sinha, A., Kirubarajan, T., and Bar-Shalom, Y. (2002). “Maximum likelihood angle extractor for two closely spaced targets.” *IEEE Transactions on Aerospace and Electronic Systems*, 38(1), 183–203.
- Sinha, A., Kirubarajan, T., and Bar-Shalom, Y. (2006). “Tracker and signal processing for the benchmark problem with unresolved targets.” *IEEE Transactions on Aerospace and Electronic Systems*, 42(1), 279–300.

- Sinha, A., Kirubarajan, T., and Bar-Shalom, Y. (2007). “Application of the Kalman-Levy filter for tracking maneuvering targets.” *Aerospace and Electronic Systems, IEEE Transactions on*, 43(3), 1099–1107.
- Sira, Sandeep P, P.-S. A. and Morrell, D. (2007). “Dynamic configuration of time-varying waveforms for agile sensing and tracking in clutter.” *Signal Processing, IEEE Transactions on*, 55(7), 3207–3217.
- Sira, S. P., Li, Y., Papandreou-Suppappola, A., Morrell, D., Cochran, D., and Rangaswamy, M. (2009). “Waveform-agile sensing for tracking.” *IEEE Signal Processing Magazine*, 26(1), 53–64.
- Sira, S. P., Papandreou-Suppappola, A., and Morrell, D. (2006). “Characterization of waveform performance in clutter for dynamically configured sensor systems.” In *Waveform Diversity and Design Conference*.
- Skolnik, M. I. (1970). “Radar handbook.”
- Slocumb, B., West, P., Shirey, T., and Kamen, E. (1995). “Tracking a maneuvering target in the presence of false returns and ECM using a variable state dimension Kalman filter.” In *American Control Conference, Proceedings of the 1995*, 4, 2611–2615. IEEE.
- Smith III, J. F. (1997). “Fuzzy logic multisensor association algorithm.” In *AeroSense’97*, 76–87. International Society for Optics and Photonics.
- Stockwell, R. G., Mansinha, L., and Lowe, R. (1996). “Localization of the complex spectrum: the S transform.” *IEEE transactions on signal processing*, 44(4), 998–1001.
- Stubberud, S. C. and Kramer, K. A. (2006). “Data association for multiple sensor types using fuzzy logic.” *Instrumentation and Measurement, IEEE Transactions on*, 55(6), 2292–2303.
- Tummala, M. and Midwood, S. A. (1998). “A fuzzy associative data fusion algorithm for VTS.” Technical report, Monterey, California. Naval Postgraduate School.
- Wang, Z., Sinha, A., Willett, P., and Bar-Shalom, Y. (2004). “Angle estimation for two unresolved targets with monopulse radar.” *IEEE Transactions on Aerospace and Electronic Systems*, 40(3), 998–1019.
- Yang, F., Sun, T., and Zhang, C. (2009). “An efficient hybrid data clustering method based on K-harmonic means and Particle Swarm Optimization.” *Expert Systems with Applications*, 36(6), 9847–9852.
- Zhang, H., Bi, G., Cai, Y., Razul, S. G., and See, C. M. S. (2016). “DOA estimation of closely-spaced and spectrally-overlapped sources using a STFT-based MUSIC algorithm.” *Digital Signal Processing*, 52, 25–34.
- Zhang, X., Willett, P. K., and Bar-Shalom, Y. (2005). “Monopulse radar detection and localization of multiple unresolved targets via joint bin processing.” *IEEE Transactions on Signal Processing*, 53(4), 1225–1236.

Zhou, B. and Bose, N. (1993). "Multitarget tracking in clutter: fast algorithms for data association." *Aerospace and Electronic Systems, IEEE Transactions on*, 29(2), 352–363.

Zhou, B. and Bose, N. (1995). "An efficient algorithm for data association in multitarget tracking." *Aerospace and Electronic Systems, IEEE Transactions on*, 31(1), 458–468.

## LIST OF PAPERS BASED ON THESIS

### Journal Papers:

- i. Gnane Swarnadh Satapathi, Pathipati Srihari, “Waveform Agile Sensing Approach for Tracking Benchmark in the Presence of ECM using IMMPPDAF”. *Radioengineering*. 2017 Apr 1;26(1):227. **(SCI Indexed)**
- ii. Gnane Swarnadh Satapathi, Pathipati Srihari, “Soft and evolutionary computation based data association approaches for tracking multiple targets in the presence of ECM”. *Expert Systems with Applications*, Elsevier. 2017 Jul 1;77:83-104. **(SCI Indexed)**
- iii. Gnane Swarnadh Satapathi, Pathipati Srihari, “ STAP Based Approach for Target Tracking Using Waveform Agile Sensing in the Presence of ECM”. *Arabian Journal for Science and Engineering*, Springer. 2017 Aug 11; 1-9. **(SCI Indexed)**
- iv. Gnane Swarnadh Satapathi, Pathipati Srihari, “Rough Fuzzy Joint Probabilistic Association for Tracking Multiple Targets in the Presence of ECM”. (Communicated to *Expert Systems with Applications*, Elsevier) **(SCI Indexed)**
- v. Gnane Swarnadh Satapathi, Pathipati Srihari, “Direction of Arrival Estimation for Closely Spaced Targets using Stockwell Transform based MUSIC algorithm in the Presence of ECM”. (Communicated to *Digital Signal Processing*, Elsevier) **(SCI Indexed)**

### Conference Papers:

- i. Gnane Swarnadh Satapathi, Pathipati Srihari, “All neighbor fuzzy relational data association for multitarget tracking in the presence of ECM”. In *India Conference (INDICON)*, 2016 IEEE Annual 2016 Dec 16 (pp. 1-5). IEEE.



# CURRICULUM VITAE

## **Gnane Swarnadh Satapathi**

1-178, Saptagirinagar,

Chinnamushidiwada, Pendurthi, Visakhapatnam - 531 173

Andhra Pradesh, India.

Email: gnaneswarnadh@gmail.com

### **Academic records:**

1. M.Tech (Systems and Signal Processing) from Department of Electronics and Communication Engineering, Jawaharlal Nehru Technological University, Kakinada in 2012.
2. B.Tech (Electronics and Communication Engineering) from Jawaharlal Nehru Technological University, Kakinada in 2010.

### **Research Interests:**

Radar Signal Processing, Radar Target Tracking.

### **Publications:**

No.of Journal Publications: 03

No.of International Conference Proceedings / Publications: 02

